Establishing and application
of a syngeneic cerebral metastasis mouse model

Doctoral thesis

In partial fulfillment of the requirements for the degree

"Doctor rerum naturalium (Dr. rer. nat.)"

in the Molecular Medicine Study Program

at the Georg-August University Göttingen

submitted by

Britta Wenske

born in Hannover

Göttingen 2015

Members of the Thesis committee

Supervisor:

Prof. Dr. Uwe-Karsten Hanisch

Paul-Flechsig-Institute for Brain Research

University of Leipzig

Second member of the thesis committee:

Prof. Dr. Tobias Pukrop

Department of Internal Medicine III/Haematology and Internal Oncology

University Hospital Regensburg

Third member of the thesis committee:

Prof. Dr. Heidi Hahn

Department of Human Genetics/ Section of Developmental Genetics

University Medical Centre Göttingen

AFFIDAVIT

I hereby declare that I wrote my doctoral thesis entitled "Establishing and application of a syngeneic cerebral metastasis mouse model" independently and with no other sources and aids than quoted.

Göttingen, March 2015

(Signature)

List of contents

Acknowledgments

The completion of my dissertation has been a long journey. At any rate, I have finished, but not alone. I could not have succeeded without the invaluable support of several people. Without these supporters, especially the select few I am about to mention, I may not have got to where I am today, at least not sanely. To this select group, I would like to give special thanks, beginning with my supervisor Prof. Tobias Pukrop for giving me the tremendous opportunity of working with him. It was an absolute pleasure and unforgettable experience. Thank you for the excellent supervision, patience, and the around-the-clock support you have provided. Your ongoing support and encouragement meant a lot to me. I also sincerely thank my co-supervisor Prof. Uwe Karsten Hanisch. Thanks for all of the scientific supports, keen supervision, helpful ideas, and warm encouragements. A heartfelt thanks to Prof. Heidi Hahn for her suggestions and ideas during scientific discussions. This work would not be possible without each one of you.

I gratefully acknowledge Prof. Claudia Binder for the constructive scientific discussions as well as the chance to be part of her group. Moreover, I thank Dr. Annalen Bleckmann for her support.

A grateful thanks to my labmates Anke, Raquel, Eugenia and Eva. Thank you for the great help you have been. Thank you to Matthias, Meike and Lena for technical assistance. A special thanks goes to my "Megaoffice" colleagues Julia, Maria, Kristina, Rose and Katharina for amazing support on a daily basis.

A very special thanks goes out to Thomas Weber. Thomas I can't say thank you enough for your tremendous support and help on so many occasions and in so many different ways.

I want to express my sincere thanks to Marco Becker and Emily Cappas for helping me in the last steps of my thesis.

My sincere thanks go to everyone, who was involved in the running of the animal facilities, also a big thanks to all people who are behind the scenes that helped me with daily things.

I also have to say thanks to my mice, as without them it would not have been possible to conduct the experiments.

I extend especially warm thanks to my family. Thanks so much to my parents Renate and Jürgen, my brother Malte, my sister-in-law Özlem, my nephew Can and my grandparents

Abstract

Metastases are a major cause of morbidity and mortality in breast cancer patients. However, current treatments are of limited efficiency because so far very little is known about the colonisation of breast cancer cells into the metastatic organs, in particular the brain. It has been demonstrated that epithelial to mesenchymal transition (EMT) facilitates tumour metastasis with poor prognosis. Moreover, the tumour cell progression might properly be dynamic: EMT during invasion and a reversal (MET) during growth of metastasis. Consequently, EMT and MET might be a promising target as a possible therapeutic cancer treatment. Therefore, the aim of this study was to establish a syngeneic mouse model to investigate the colonization at the distant organs, in this case the brain, of metastatic breast cancer cells and the impact of EMT and MET on this part during the metastasis process.

Furthermore, it has been demonstrated that dysregulation of Wnt signalling is associated with metastasis and also plays an important role in tumour genesis. Furthermore, the Wnt signalling pathway is known to induce EMT and MET and is dysregulated in several cancers, with different Wnt molecules being up regulated. If the Wnt pathway is important in cancer proliferation and metastasis, inhibitors of Wnts may be valuable for a therapeutic strategy. However, because of the multiple receptor combinations and no-central kinase activity the inhibition of the Wnt pathway is not trivial. Therefore, to inhibit the secretion of the Wnt-molecules seemed a very promising strategy. One of the key enzymes during secretion is the membrane bound O-acetyltransferase Porcupine. Inhibition of Porcupine leads to the inhibition of Wnt palmitoylation and Wnt secretion, and therefore, indirect inhibition of receptor binding and activation of the pathway. One Porcupine inhibitor, LGK974, is believed to block initiation of tumours through this mechanism suggesting LGK974 is a good treatment approach for cancer patients. The second aim of this study was now to investigate the inhibitory effects of LGK974, not in tumour initiation, we wanted to study the effect during cerebral colonization *in vitro* and *in vivo*.

Finally, we wanted to investigate the role of the immune system, microglia and astrocytes, during the invasion of breast cancer in the brain. The established immune-competed mouse model provides an opportunity to address this question. Here, the response of microglia and astrocytes to lipopolysaccharide (LPS) was used to trigger an immune response.

In conclusion, a syngeneic cerebral metastasis mouse model was established and different treatment strategies were proved on this. Moreover, the process of colonization of the brain, and the impact of the immune systems on in this progress were investigated.

List of Figures

List of Tables

Abbreviations

APS   Ammonium Persulfate

BBB   Blood-Brain Barrier

BSA   bovine serum albumin

dsDNA   double strained DNA

CAM   Chorioallantoic Membran Assay

cDNA   complementary DNA

CK8/19   Cytokeratin8/19

CNS   Central nervous system

CSF-1(R)   colony stimulation factor-1 (receptor)

CTL   Control

DAB   3,3'-diaminobenzidine

DMSO   dimenthyl sulfoxide

DVL   dishevelled

Ecad   E-cadherin

ECM   extracellular matrix

e.g.   for example

EGF (R)   epidermal growth factor (receptor)

EMT   epithelial mesenchymal transition

EtOH   Ethanol

FCS   fetal calf serum

Fig   figure

fw   forward

fz   Frizzeled

GFAP   Glia fibrillary acidic protein

HE   Haematoxylin and eosin

Her2   human epidermal growth factor 2

H_2O_2 hydrogen peroxide

HRP   horseradish peroxidase

i.	injected side
IBA	Ionized calcium binding adaptor molecule
IHC	Immunohistochemistry
IP	intra peritoneal
IWP	inhibitors of Wnt production
Ki67	Kiel 67
LEF	lymphocyte enhance factor
LPS	lipopolysaccharide
LRP	low-density lipoprotein receptor related protein
mRNA	messenger RNAolig
mm	mus musculus
MPO	Myeloperoxidase
MTT	3-(4,5-Dimethylthiazol-2-yl)-2,5-diphenyltetrazolium bromide
MyD88	myeloid differentiation primary response gene 88
NaCl	Sodium chloride (Natriumchlorid)
n.i.	non- injected side
oligo(dT)	oligonucleotides
PAGE	polyacrylamide gel electrophoresis
PBS	phosphate-buffered saline
PFA	Paraformaldehyde
P/S	penicillin/streptomycon
qRT-PCR	quantitative real-time polymerase chain reaction
RIPA	radioummunoprecipitation assay
RNA	ribonucleic acid
rv	reverse
SD	standard deviation
SDS	sodium dodecyl sulfate
SEM	standard error of the mean
SPF	specific pathogen free

Tab	table
TAM	tumour associated macrophages
TBS	Tris-Buffered Saline
TCF	T-cell factor
TLR	Toll-like receptor
TRIF	TIR-domain-containing adaptor-inducing IFNβ
Tris	tris (hydroxymethyl) aminomethane
vs	versus
WB	Western Blot
WST	water soluble tetrazolium
wt	wild type

Measurements units

% (v/v)	% volume per volume
% (w/v)	% weight per volume
°C	degree Celsius
g	gram
h	hours
l	liter
lx	lux
m	meter
min	minutes
M	Molar
rpm	rounds per minute
Sec	seconds
V	Volt

Metric prefixes

h   hecto; 10^2

k   kilo; 10^3

M   mega; 10^6

c   centi; 10^{-2}

m   milli 10^{-3}

μ   micro; 10^{-6}

n   nano; 10^{-9}

1 Introduction

1.1 Breast cancer and prognosis

The World Health Organisation (WHO) documented that worldwide over 500.000 women die of breast cancer every year (http://www.who.int/cancer/detection/breastcancer/en/2015), thus it is the most common type of cancer. But not only women, men also suffer from breast cancer. Metastases of breast cancer cells are the main cause of death among patients with breast cancer related deaths. 10–15% of patients with breast cancer developed metastases within 3 years after the first diagnosis (Weigelt et al., 2005). During this time, cancer cells are already disseminating and are under dormancy conditions, which mean that pre-metastatic cells have already seeded the distant organs and are not active proliferating (Karrison et al., 1999). In fact, migration of tumour cells away from the primary tumour is generally regarded as the first step in metastatic dissemination of breast cancer. Therefore, the basic steps of metastasis are - local invasion, intravasation, survival in the circulation, extravasation and colonization, which will be described later.

1.2 The role of the environment

However, the complex process of metastasis formation is not fully understood as of today. It is believed that this process is unidirectional, disseminating from the primary tumour cancer cell to the distant organ. The English surgeon Stephen Paget proposed first in 1889 the important role of the microenvironment in metastasis formation. His idea was the "seed and soil" theory where cancer cells (=the seed) have an affinity for certain organs (=the soil), which offer a compatible microenvironment for tumour growth (Paget, 1989). Consequently, metastasis development is not possible when an incompatible "seed and soil" exist. This theory was supported and confirmed in several publications (Ribatti et al., 2006) and believed until today. It was shown that a specific infiltration function of metastatic cells is required after disseminating from the primary tumour to make the cells organ specific. Furthermore, after the infiltration of a new tissue, cancer cells outcompete other cells of this tissue because of a more aggressive form of these cells. Moreover, general steps of metastasis might be the same in all types of tumours, however metastasis

to other tissues might be more specific and requires different sets of infiltration and colonization functions. Also, time periods of metastasis are variable depending on the new microenvironment (Nguyen et al., 2009). Therefore, the role of the tumour microenvironment for cancer progression and the organ-specific colonization should be considered for further investigations. Furthermore, tumour cells are able to create a niche by influencing the surrounding stroma cells during metastasis. The function of the stroma microenvironment in order to contribute to the breast cancer development needs to be addressed both *in vivo* and *in vitro* to better understand breast cancer metastasis (Bhowmick et al., 2004).

1.3 The special situation of brain metastasis

Metastasis of the central nervous system (CNS) was demonstrated as a late event with limitations for treatment therefore it is an indicator for poor prognosis in diagnosed patients (Bos et al., 2009) (Weil et al., 2005). Very little is known about the interactions between the brain and the metastatic cells. Moreover, the reason for brain metastasis being a late event might be the unusual environment of the brain for cancer cells. Additionally, the brain is protected by the Blood-Brain Barrier, which is tighter than the Blood-Organ Barrier (BBB). Therefore, extravasation takes longer into the brain than to other organs. Both, the unique brain microenvironment and the BBB were hypothesised to influence metastatic colonization. Furthermore, the parenchyma of the brain has non-vascular stromal basement membrane components. Without these components, cancer cells cannot bond to epithelial cells, which is a necessary step for their survival (Carbonell et al., 2009). Therefore, neurovasculature was identified as an important partner for metastasis in the brain.

The organ specific immune response of the brain plays an important role in this process. Metastasis into the brain induces a neuro-inflammatory response which involves activated microglia and astrocytes, similar to what happens during mechanical lesions to the brain (Fitzgerald et al., 2008a). Metastatic tumour cells themselves could potentially alter the microglia, resulting in a unique interaction. Recently the initial steps of brain colonization were studied *in vitro*, however, when data were compared to the *in vivo* situation, the colonization of breast cancer cells into the brain was different to the *in vitro* situation.

Therefore, investigations of animal models are necessary to understand the complex mechanisms how cancer cells colonize the brain (Lorger et al., 2011).

1.4 Available animal models in cancer research

Fidler et al. showed that cancer cells with a high metastatic potential could be injected intravenously leading to spontaneous metastases to distant organs (Fidler and Kripke, 1977). Another spontaneous mouse model was established from Kamino et al. (Kamino and Mohr, 1993). They injected lung carcinoma cells in the artery carotids, which lead to brain metastases. However, from the literature we know that not all cell lines are able to generate spontaneous metastases. If not depending on a spontaneous metastases model, intracranial injection of cancer cells is useful to study the role of the brain microenvironment and tumour dissemination. Intracranial Xenograft models were established in late 1980 (Kaye et al., 1986), when for the first time glioma cell lines were injected intracranially into mice. Over the years, also nude mice and severe combined immunodeficient (SCID) mice were compared and tested for intracranial injection of cancer cells (Taghian et al., 1993). However, only an immune-competent model is applicable for studies of immune-based therapeutic strategies. Moreover syngeneic BALB/C mouse models where 4T1 cancer cells were injected in the mammary fatpad, 4T1-cells showed spontaneous metastatic outgrowth (Aslakson and Miller, 1992a). Nevertheless, not all cancer cell lines are able to metastize spontaneously, especially not into the brain. Therefore, investigation of a syngeneic mouse model for cerebral metastasis is necessary.

1.5 Metastasis of cancer

The metastatic cascade was investigated over the last decade: Tumour cells spread to distant organs and form a new tumour mass, which is described as organ-metastasis. Several steps of organ-metastasis make a therapy complex, however, when one of these steps is not completed, metastases cannot occur.

The initial step is that cancer cells manage to enter the circulation were they would taken to a specific organ, which depends on the blood flow pattern (Chambers et al., 2000).

Cancer cells are able to leave the primary tumour and enter into the body circulation blood system. All cancer cells need the ability to survive in the circulation before they can extravasate into surrounding tissue of the distant organ. Once cancer cells have been seeded their colonization will depend on molecular interaction between cancer cells and the environment of the new organ, e.g. the brain.
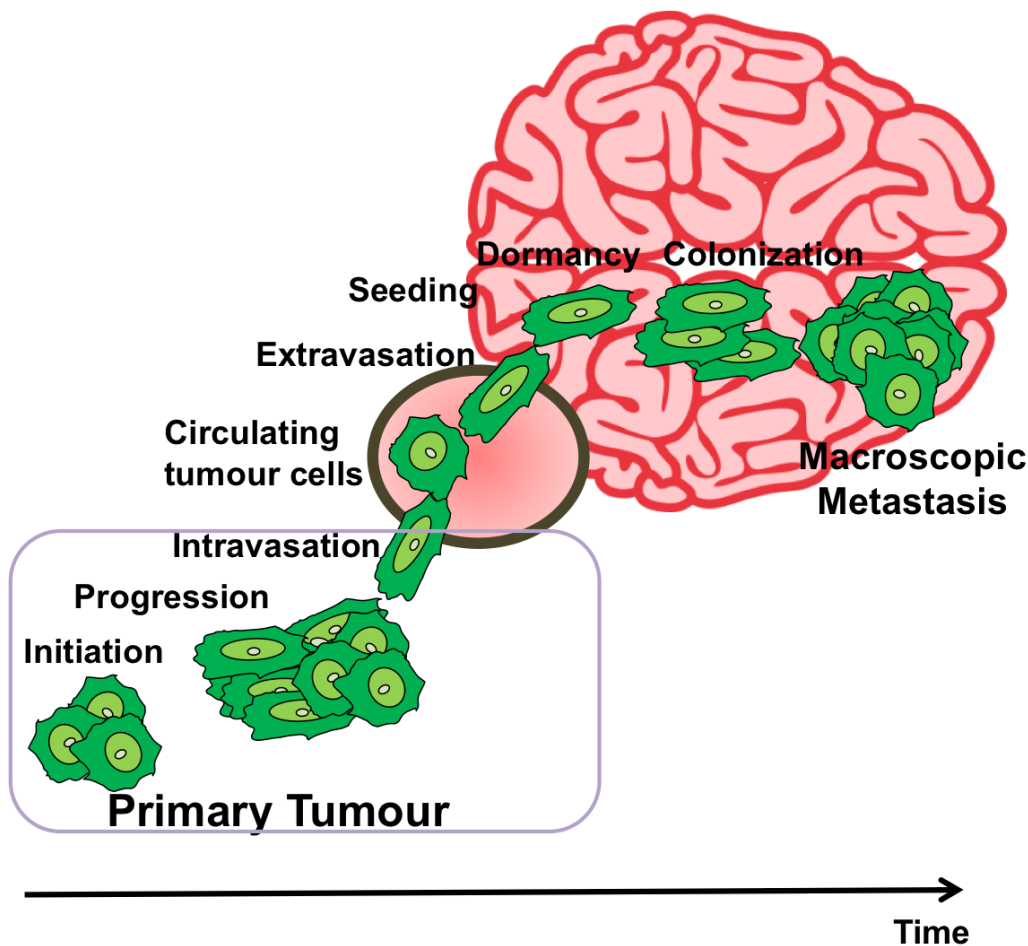
Fig 1: The metastasis cascade (linear model).
Formation of the primary tumour, next tumour cells leaving the primary tumour (initiation and progression), and attack surrounding vessels (intravasation).Surviving cancer cells circulate and arrest in distant organ site before they exit the vessel (extravasation). Followed by seeding and dormancy in the brain. Afterwards metastatic cell colonize in the brain and perform micrometastasis. Micrometastasis grows to macroscopic metastases in the brain.

Importantly, Chambers et al. described in her study that only 0,02% of injected cancer cells were able to colonize in the brain and leading in metastasis (Chambers et al., 2002). This was observed when they injected cancer cells in the vene of mice. Moreover, they investigate the most critical step for the metastatic cells were the colonization of the distant

organ, because the majority of the seeded cells undergo apoptosis, a programmed cell death. This findings have a clinically importance.

Moreover, by the time a primary tumour is detected, it might be already have seeded metastatic cells to the to the secondary side. Therefore treatment of the primary tumour or the early steps of the metastatic cascade can be successful, however, metastasis might be already performed (Fig 2). This knowledge is very important to investigate treatment strategies for metastasis.
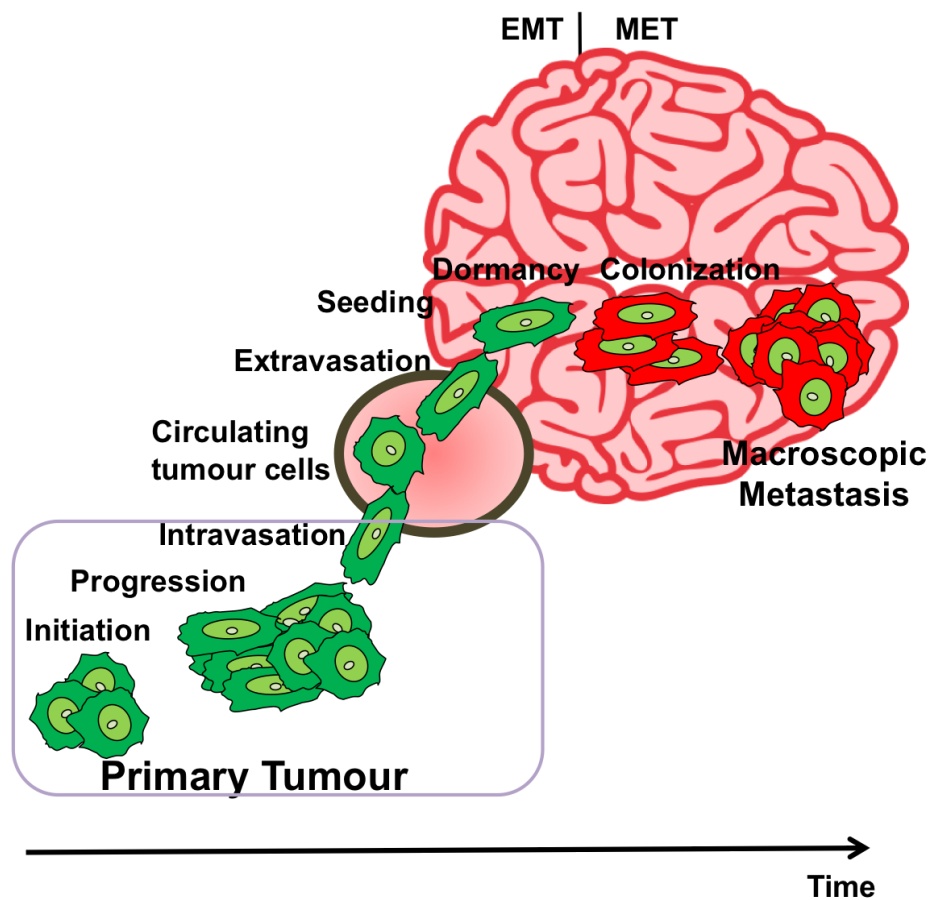
Fig 2: EMT and MET in metastasis formation in the linear model. EMT induces the dissemination of cancer cells.
Cancer cells intravasate into blood vessels, followed by a transport to distant organs. Cancer cells extravasate at secondary sites and can form metastasis through a mesenchymal-epithelial transition (MET).

Moreover, it was demonstrated that cancer cells which survived in this foreign microenvironment were re-initiate efficient proliferative programs at the metastatic sites which leads to metastatic colonization (Valastyan and Weinberg, 2011). For cancer cells to adapt to the new environment they need to have the ability for transformation. Several

genes, which allow this transformation, were identified as so called metastasis initiation genes. These genes can promote epithelial-mesenchymal transition (EMT). EMT is a fundamental process that is essential for morphogenesis. Abnormal expression of developmental transcription factors such as Twist1, Twist2 and Snail might be able to trigger EMT (Nguyen et al., 2009) resulting in increased cancer cell dissemination from the primary tumour (Thiery, 2002).

EMT may mediate the extravasation of cancer cells, which can then disseminate in the secondary environment. EMT is critical in the first steps of metastatic formation, however, MET is required for colonization of cancer cells revert at some point to their epithelial phenotype (Fig 2) (Ramakrishna and Rostomily, 2013).

The transmembrane protein E-cadherin (Ecad) was identified as a marker of an epithelial phenotype. A lack of Ecad decreases cell adhesions and therefore promotes a switch to a mesenchymal phenotype, which is considered as a canonical indicator of metastatic EMT (Ramakrishna and Rostomily, 2013). The loss of Ecad in cancer cells is associated with upregulation of N-cadherin, which is known as the "cadherin switch". Moreover, Ecad is highly expressed in various cancers including breast cancer (Thiery, 2002). Several transcription factors are known to regulate the expression of Ecad, e.g. Snail, Snail2 and Twist. Twist was found to be overexpressed in breast cancer tissue compared to normal breast tissue (Watanabe et al., 2004). A cross talk between cancer cells and the surrounding stroma indicates the importance of various genes in EMT (Mani et al., 2008). Summarised, EMT might be important in generating the initial metastatic phenotype.

Many genes or pathways are necessary for the activation of cancer cells from the step of dormancy to the formation of brain metastases (Eichler et al., 2011a). It is important to understand the process in detail to identify new therapeutic strategies for brain metastasis. Thus, the canonical Wnt/ß-catenin pathway was recently identified to play an important role in EMT.

1.6 The Wnt signalling pathway and its role in tumour progression

The Wnt pathway is not only important for cell-cell communication during embryonic development and for normal tissue homeostasis. It is also involved in tumorigenesis. 19 genes of the Wnt family were identified (Nusse, 2005). The canonical Wnt pathway is per

definition ß-catenin dependent. Here, Wnt binds to Frizzled (Fz) receptor a seven-transmembrane molecule with a long amino-terminal extension containing a cystein-rich domain. Moreover, Wnt signalling requires also the low-density lipoprotein receptor-related protein (LRP) family as co-receptor.

The complex of Wnt, Fz and LRP5/6 recruits dishevelled and axin through the intracellular domains of Fz and LRP5/6. Thus, intracellular Fz interacts directly with dishevelled, which leads to the stabilisation β-catenin by inhibition of ß-catenin phosphorylation. ß-catenin translocates into the nucleus and subsequently binds to transcription factors of the T-cell factor/lymphocyte enhancer factor (TCF/LEF) family thereby activating target gene expression (Clevers and van de Wetering, 1997). Wnt inhibitory factor-1 and secreted Frizzled-Related Proteins can block Wnt signalling by direct binding to Wnt ligands. However, other inhibitors of Wnt, e.g. the Dickkopf family are blocking Wnt signalling by binding to the co-receptor LRP6 (Semënov et al., 2008). Two other Wnt signalling pathways were described within the ß-catenin depended pathway, the planar cell polarity (PCP) pathway and the Wnt/Ca^{2+} pathway. Both non-canonical pathways, Wnt/Ca^{2+} and PCP, can be activated by the Wnt ligand Wnt5a (Yamanaka et al., 2002). Furthermore, the Wnt/Ca^{2+} pathway can also be activated via Wnt4 and Wnt11, both of which induce an intracellular Ca^{2+} release (Kühl et al., 2001).

In the canonical pathway ß-catenin is involved in the regulation of transcription and also in cell adhesion. When Wnt3a or Wnt7a act on their cell-surface receptor, the cytoplasmatic ß-catenin translocates into the nucleus after release from the destruction complex. In the nucleus ß-catenin binds to TCF/LEF and drives the expression of different genes involved in EMT (Clevers and Nusse, 2012). Another important study shows that translocation of β-catenin in the nucleus leads to break the cell-to-cell adhesion formed by β-catenin and E-cadherin, as β-catenin was identified as a cadherin-binding protein (Schäfer et al., 2014a).

1.7 Wnt and EMT

Wnt was recently shown to be involved in EMT. EMT is accompanied with the down regulation of Ecad. The transcription factor Snail functions as a potent receptor of Ecad expression, which can induce EMT. Snail can act alone or with the Wnt/ß-catenin/ LEF. It was demonstrated that Wnt signalling could inhibit Snail phosphorylation and therefore

increase Snail protein levels, which is then driving EMT. Therefore, the Wnt signalling cascade was identified to activate Snail-driven transcriptional programs and Snail activates EMT regulated processes (Yook et al., 2005). In particular, Wnt was demonstrated to activate the Wnt/ß-catenin signalling and promote EMT-like phenotypes in breast cancer cells (Wu et al., 2012). These studies focused on ß-catenin. However, not many studies investigated the role of Wnt ligands on EMT so far. Nonetheless, EMT has been shown to be induced by Wnt in colon cancer cells. This was investigated in human colon cancer tissue, with focus on a specific member, Wnt3a. Low levels of Ecad and higher levels of Vimentin and ß-catenin were found in the Wnt3a expression group compared to the control group with no expression of Wnt. Additionally, Wnt3a is able to promote the expression of the EMT inducing transcription factors, e.g. Snail (Qi et al., 2014). These findings also confirm the importance of Wnt signalling and EMT for the microenvironment.

Wnt genes are expressed in healthy tissues, including the breast. However, diseased breasts showed dysregulated expression of Wnt genes (Huguet et al., 1994a). Moreover, Wnt5a was shown to be overexpressed in many human cancers (Pukrop and Binder, 2008) and Wnt7a was also found to be overexpressed in breast cancers (Kirikoshi and Katoh, 2002). Wnt5a was not only expressed in cancer cells, but also in macrophages at the invasive front of the tumour. Therefore, Wnt genes might be involved in regulating tumour cell invasion induced by macrophages, especially Wnt5a (Pukrop et al., 2006).

1.8 Wnt signalling during cerebral metastasis

The Wnt pathway was identified in breast cancer patients as a contributing factor to facilitate breast cancer metastize into the brain (Smid et al., 2008). The importance of WNT signalling for breast cancer metastasis, especially into the brain was demonstrated in our group (Klemm et al., 2011). Importantly, not only the classical WNT/β-catenin pathway was shown to be involved, also the β-catenin-independent pathway was demonstrated to be relevant in breast cancer progression (Klemm et al., 2011). Furthermore it we showed that the Wnt pathway needs to be activated during microglia-induced invasion (Pukrop et al., 2010a). On the other hand, Wnt genes are act on microglia and are involved in tissue protection in the central nervous system (CNS) (Halleskog and Schulte, 2013). Thus, Wnts are regulated by pro- and anti-inflammatory mechanisms, which also indicate the dual role of microglia in health and disease (Hanisch and

Kettenmann, 2007). Epithelial cells are capable of inducing a damage response following lesions to the brain and that microglia can have a protecting effect on this response inducing apoptosis (Chuang et al., 2013).

In case of infiltration of the malignant cells into the adjacent brain parenchyma, the induction of apoptosis as a damage response is not efficient. Therefore, cancer cells can use the glial interaction to succeed in infiltrating the adjacent brain parenchyma. The exact mechanism how tumour cells can avoid this apoptotic step is not fully understood. However, Wnt signalling is involved in tumour progression rather than in tumour apoptosis and this is process is mediated by glia cells (Chuang et al., 2013). Further studies are required to identify the role of Wnts in the regulation of microglia and the CNS immune response and the role of Wnt in colonization of the distant organs, especially the brain.

1.9 Wnt secretion and inhibition of Wnt secretion

If the Wnt pathway is important in cancer proliferation and spread, the inhibition/the modulation of Wnts may be a good target for therapeutic strategies. However, manipulation at the receptor-level is not trivial because the receptor complexes are very heterogenous and therefore Wnts are not a clear target. The same is true for inhibiting the activating kinase activity. Since, the canonical Wnt pathway is based on the inhibition of a central kinase (GSK3ß), this simple strategy is also not constructive. Modification of the Wnt secretion seems a very rational treatment concept though. However, the mechanisms of Wnt secretion are not fully understood. A crucial step for Wnt secretions is the palmitoylation of Wnt protein, which is mediated by the enzyme Porcupine. This key enzyme belongs to the family of membrane-bound O-acetyltransferase (MBOAT) and is located in the membrane of the endoplasmic reticulum (Siegfried et al., 1994). Inhibition of Porcupine leads to the prevention of Wnt palmitoylation and thereby Wnt secretion (Kurayoshi et al., 2007). These findings and the knowledge of the influence on Wnt in tumour initiation and metastasis formation leads to the idea that inhibition of Porcupine in order to block Wnt secretion might have a beneficial effect on cancer treatment.
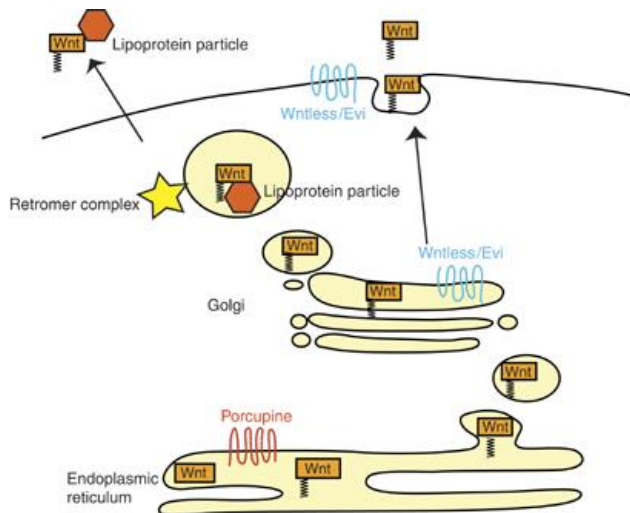
Fig 3: Porcupine is essential for Wnt secretion.
The acyltransferase Porcupine in the endoplasmic reticulum is required for palmitoylation of Wnt proteins and therefore necessary for Wnt secretion (Mikels and Nusse, 2006).

The idea of a promising inhibitory effect of Porcupine to block Wnt secretion was followed up over the last years.

The important role of Porcupine for cell proliferation and activation of the Wnt pathway was shown in gastric cancer exhibiting high expression levels of Porcupine. By using a palmitoyltransferase inhibitor specific for Porcupine (inhibitors of Wnt production (IWP-2)), the cell proliferation, migration and invasion was inhibited in gastric cancer cells. Furthermore, the Wnt/β-catenin signalling pathway activity was downregulated by IWP-2 (MO et al., 2013). Chen and colleagues showed the ability of IWP compounds to selectively target a member of the MBOAT family of acetyltransferases (Chen et al., 2009).

Another Porcupine inhibitor Wnt-C57 (patented by Novartis), a small-molecule inhibitor, was shown to block Wnt palmitoylation, Wnt interaction with the carrier protein Wingless and the Wnt secretion. Wnt driven tumours growth was decreased by using Wnt-C57 in mice (Proffitt et al., 2013). The inhibitory effect of Wnt-C57 was evaluated for all ß-catenin activating Wnts and in all noncanonical Wnts. Summarising, the Porcupine inhibitor, IWP-2, is highly potent and specific in inhibiting Wnt signalling *in vitro* (Chen et al., 2009) (Dodge et al., 2012). WNT-C59 was found to be effective in a Wnt-dependent mouse tumour model (Proffitt et al., 2013). However, pharmacological Wnt inhibitors result in high toxicity and thus have adverse effects at high doses (Chen et al., 2009).

A new and more specific Porcupine inhibitor LGK974 is believed to block tumour progression through inhibition of the Wnt signalling pathway. LGK974 was shown to be well tolerated at the effective doses (Liu et al., 2013a). Therefore, Porcupine inhibition seems a *bona fide* target for cancer treatment. Importantly, in a human based study tumour growth was decreased at well-tolerated doses of LGK974. These results supported the use of LGK974 for clinical use for the treatment of Wnt driven tumours, and Novartis began to use LGK974 in early-phase clinical trials. The study included patients with malignancies dependent on Wnt ligands, (https://clinicaltrials.gov/show/NCT01351103), however, the results from this study have not been published yet.
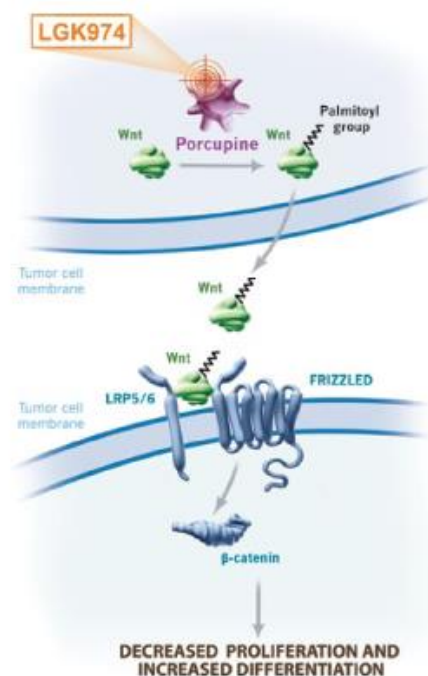
Fig 4: Inhibition of Porcupine.
LGK974 inhibit Porcupine and therefore palmitoylation of Wnt proteins and Wnt secretion

(http://www.novartisoncology.com/ct/pipelineDetails?compound=LGK974&diseaseAcr=BC.)

1.10 Immune response on tumour cell invasion

The role of the tumour microenvironment has been frequently shown to be important in cancer. The malignancy can be suppressed by the immune response, however, most tumours are able to overcome this process and the metastatic potential can be increased, which was shown in mouse models (Joyce and Pollard, 2009). Furthermore, peripheral macrophages can promote the invasiveness of cancer cells. Usually, one role of

macrophages is to destroy malignant cells, however, it has been shown that they are able to secrete factors necessary for cancer progression. Activation of tumour-associated macrophages (TAM) could result in a release of a vast diversity of growth factors, proteolytic enzymes, cytokines, and inflammatory mediators that may facilitate cancer metastasis (Chen et al., 2005). Additionally, tumour cells are able to attract and manipulate cells of the immune system, e.g. the TAM. Therefore, immune cells assist in tumour progression. This was confirmed when invasion inducing macrophages were blocked by using a Wnt inhibitor leading in a decrease or tumour progression (Pukrop et al., 2006). Infiltrating TAM were detected at the invasive front of mammary tumours in human samples. The environment of the brain reacts differently compared to other organs and the immune response of microglia might be different compared to the response of macrophages. Furthermore, astrocytes and microglia were highly activated after seeding of pre-metastatic tumour cells in the brain parenchyma (Lorger and Felding-Habermann, 2010).

1.11 The role of microglia and astrocytes in malignancies

Microglia cells are resident mononuclear phagocytes that play a fundamental role in the protection of normal tissue homeostasis in the central nervous system. Under normal conditions, the immune response of microglia in the brain is mainly the repair of the CNS and the activation of microglia is normally reversible, hyperactivation of microglia often leads to neurotoxic effects (Nakamura, 2002). Microglia and astrocytes were activated in response to proinflammatory stimuli. Astrocytes are identified by the intracellulary expressed cell type-specific marker glial fibrillary acidic protein (GFAP), microglia by cell surface Fc receptors (CSFR) (Kennedy et al., 1980). Astrocytes play an important role in lending support of the Blood-Brain-Barrier (BBB) (Abbott et al., 2006) and regulating the immune response of the CNS. However, it was shown that astrocytes become activated in response to tumour progression, and the size of the tumour is directly correlated to the number of activated astrocytes (Langley et al., 2009). Additionally, microglia cells are regulated by the macrophage growth factor colony stimulating factor-1 (CSF1) which signals via the transmembrane tyrosine kinase receptor (CSFR1). CSFR1 was shown to be also upregulated in injured neurons. CSF1 upregulation also correlates with neurodegeneration and neuroinflammation (Luo et al., 2013). Furthermore, dysregulation

of microglia cells played a central role in cancer (Saijo and Glass, 2011). As the function of microglia cells can be protective but also cytotoxic (Zhang and Olsson, 1997), microglia might influence tumour cell survival. Moreover, microglia are extremely sensitive to changes in the brain microenvironment, which can be an exciting mechanism (Barron, 1995). For experimental design, LPS can induce activations of microglia.

Micrometastatic breast cancer cells are changing the brain microenvironment, which can lead to metastatic progression. The glia cell reaction induces an altered brain microenvironment by e.g. by the formation of a surrounding wall. This might provide the basis for glia-tumour cell interactions thereby influencing metastatic progression. The metastatic tumours cells might change glia cells by unknown mechanisms (Fitzgerald et al., 2008b). Furthermore, it is possible that microglia cells reduce the production of cytotoxic factors after contact with tumour cells allowing tumour cells to colonize. At the onset of brain metastases there is a balance between the protective and cytotoxic effect of microglia cells. This effect is likely to be influenced by signals of the seeded pre-metastatic tumour cells, including different factors (He et al., 2006a). A better understanding of the interactions between tumour cells, glia cells and epithelial cells could help to develop new therapeutic approaches.

1.12 Therapeutic approaches and animal models of cerebral metastasis

It is obvious that the brain microenvironment plays an important role in the formation of metastases. Furthermore, the role of the brain environment in order of breast cancer metastasis is different in comparison to other organs. The special environment of the brain, which includes the BBB and specific immune responses of the CNS, makes it a unique organ. The BBB is composed of a layer of endothelial cells and astrocytes, making the BBB impermeable for most cells. Moreover, the BBB can prevent the entrance of leukocytes and immunoglobulins from the blood. However, once tumour cells attack the BBB, the endothelial cells of the BBB and tumour cells can form a blood-tumour barrier (Fidler, 2011), which can lead to colonisation of tumour cells and therefore to metastasis formation. The leakage of the most cytotoxic agents through the BBB is usually limited, and treatments e.g. chemotherapy, are therefore complicated (Steeg et al., 2011). On the other hand, when the interaction of astrocytes and endothelial cells was disrupted the impermeability of the BBB seemed to be directly related to the uptake of chemotherapeutic

agents. Furthermore, the unique brain microenvironment impedes anti-tumour therapies, therefore it is challenging to develop efficient strategies to target brain metastasis (Eichler et al., 2011b).

To investigate new therapeutic strategies and to understand all of the steps involved in this process, animal models for brain metastasis that are able to mimic the human disease are necessary. Unfortunately, progress in this field of research is still limited by the few spontaneous models available. The chance for metastatic cells to reach the brain is not 100% given because - unlike epithelial cancers - metastatic cells often die before the brain is colonized. Furthermore, while the ability of tumour growth in immune-deficient mouse models gives extremely valuable results to understand tumour biology, the assistance of the immune cells and the lack of immune-signalling- which play an important role in brain metastases-   cannot   be   analysed   in   these   models (http://www.ncbi.nlm.nih.gov/books/NBK100378/). Therefore, a syngeneic mouse mode is more suitable.

Furthermore, a combined treatment involving the stimulation of the immune system by e.g. LPS can further help to investigate the role of immune response on tumour colonization. It has been shown *in vitro* that LPS-activated microglia cells can destroy some metastatic cancer cells (He et al., 2006a). Interestingly, LPS was also found to be neuroprotective and reduced cell death (Bingham et al., 2011).

In a brain slice model it was shown that microglia interact with tumour cells and thereby enhance the invasiveness of breast cancer cells. Moreover, a dense inflammatory infiltrate consisting of active microglia around the tumour mass was observed. Similar results were shown by He et al. (2006), suggesting that the degeneration of neurons can activate microglia, however, the link between neuronal deaths or degeneration and microglia activation could not be made clearly. Later, our group demonstrated that the Wnt pathway plays an important role in macrophage-induced tumour invasion in primary tumours (Pukrop et al., 2006). This was also confirmed in the distant organ, the brain, where Wnt inhibition leads to reduced tumour invasion in the brain slice model (Pukrop et al., 2006). In order to prove the proinvasive effect of microglia and the important role of Wnt signalling during this event, Han-Ning Chuang triggered a proinflammartory response by using LPS in brain slices after adding single tumour cells. Then she analysed gene expression patterns and found Wnt signalling to be one of the most misregulated pathways.

Furthermore Han-Ning demonstrated that LPS affects several Wnt related genes in microglia. Another regulated pathway was the Toll-Like Receptor (TLR) pathway. Also it was shown that TLR4 activation affected several Wnt related genes in microglia.

In this study we built up on these previous results and we aimed to further define the role of the immune system and also the importance of Wnt signalling on tumour colonization. In order to elaborate this in greater detail the goals of this study were:

1) To establish a syngeneic mouse model to investigate the colonization behaviour, the morphological metastatic patterns and analysed Wnt signalling and EMT-markers. EMT marker expression might be critical for tumour invasion. Therefore, we characterized suitable cancer cell lines and focused on epithelial and mesenchymal markers of all analysed cancer cell lines and investigated their colonization behaviour.

2) To investigate whether Wnt secretion is important for colonization of the CNS and therefore might be a good therapeutic target. For this proposes, we tested the Porcupine inhibitor LGK974, which was suggested to block Wnt secretion and therefore tumour invasion.

3) To further elaborate on several exciting findings that we had made in our group by *in vitro* studies on the role of microglia on tumour colonization. We wanted to transfer these *in vitro* findings to the established syngeneic cerebral metastasis mouse model, as this model is physiologically more similar to the human situation.

2 Materials und Methods

2.1 Materials

2.1.1 Biological material

2.1.1.1 Cell Lines

All cell lines used in this study are listed in Tab 1.

Tab 1: Cancer Cell lines

Cell line	Cell type	Characteristics	Obtained from	Culture Medium	References
410.4	murine Mamma-adenokarzinom-cell line	BalbC	Prof. F. Balkwill, London, UK	DMEM medium (Biochrim, Berlin)+10% Fetal calf serum	(Miller, 1983)
4T1	murine Mamma-adenokarzinom-cell line	BalbC	Prof. F. Balkwill, London, UK	RPMI-1640 medium (PAA, Cölbe, Germany) +10% Fetal calf serum (Sigma)	(Aslakson and Miller, 1992b)
E0771	murine medullary breast adenocarcinoma cell line	C57BL/6	Jeffrey Pollard, University of Edinburgh	RPMI-1640 medium (PAA, Cölbe, Germany) +10% Fetal calf serum (Sigma)	(Ewens et al., 2005)
E0771LG	murine medullary breast adenocarcinoma cell line, isolated from experimental lung metastasis foci	C57BL/6	Jeffrey Pollard, University of Edinburgh	RPMI-1640 medium (PAA, Cölbe, Germany) +10% Fetal calf serum (Sigma)	Not published

2.1.2 Cell culture media and additives

All media and additives used are listed in Tab 2.

Tab 2: Cell culture media and additives

Product	Company
DMEM medium	Biochrim (Berlin)
Fetal calf serum (FCS)	Sigma (Munich)
Penicillin/streptomycin (P/S)	Biochrom (Berlin)
RPMI-1640 medium	PAA (Cölbe)
Trysin	Biochrome (Berlin)

2.1.3 Chemicals, Commercial kits and standards

All chemicals, commercial kits and standards used are listed in Tab 3.

Tab 3: Chemicals, Commercial kits and standards

Product	Company
„Cell Proliferation Reagent" WST-1	Roche Applied Science, (Mannheim)
DNA ladder 100kb	Fermentas (St. Leon-Rot)
Extracellular matrix gel (ECM)	Trevigen, R&D, (Wiesbaden-Nordenstadt)
High Pure RNA Isolation kit	Roche (Grenzach-Wyhlen)
iScript cDNA synthesis kit	Bio-Rad (München)
Laemmli loading buffer, non-reducing, 4x	bioPLUS (Mol, Belgium)
Laemmli loading buffer Roti®-Load 1, reducing, 4x	Roth (Karlsruhe)
LGK974 powder	Active Biochemicals (Hong Kong)
LPS from Escherichia coli	Enzo Life Sciences (Lörrach)
Phenol/chloroform/isoamyl alcohol	Roth (Karlsruhe)
Phosphatase inhibitor PhosSTOP, 10x	Roche (Grenzach-Wyhlen)
Ponceau S	Merck (Darmstadt)
SYBR green	Roche (Mannheim)
MTT for MTT assay	Sigma (München)
100xProteaseinhibitor Cocktail	Sigma (München)
Phosphatase inhibitor "PhosStop"	Roche (Mannheim)
4x loading buffer "Roti-Load 1"	Roth (Karlsruhe)
Precision Dual Color Protein Standard	Biorad (München)
Protein loading buffer bioPLUS	Bio-world (USA)
Hybond-C Extra membrane	Amersham Biosciences (Freiburg)
Ponceau S solution	Omnilab Krannich (Göttingen)
Dnase I	Roche (Mannheim)
"ECL Plus"	GE Healthcare (Freiburg)

2.1.4 Antibodies

The antibodies used for Western Blot analyses are listed in Tab 4.

Tab 4: Antibodies

Product	Host species	Application	Company
Wnt5a	rat	1:2000	R&D (MAB645)
Wnt7a/b	mouse	1:250	SantaCruz (sc-365459)

2.1.5 Oligonucleotides

All used Oligonucleotides directed against mouse cDNA are listed in Tab 5.

Tab 5: Oligonucleotides

Name	Sequence (5´-3´)
mm-GAPDH fw	CATCTTGGGCTACACTGAG
mm-GAPDH rv	CTGTAGCCGTATTCATTGTC)
mm-RNA 18s fw	GTAACCCGTTGAACC CCATT
mm-RNA 18s rv	CCAT CCAATCGGTAG TAGCG
mm-CSF1 fw	GCGCTTTAAAGACAACACCC
mm-CSF1 rv	ATGGAAAGTTCGGACACAGG
mm-Vimentin fw	CGGCTGCGAGAGAAATTGC
mm-Vimentin rv	CCACTTTCCGTTCAAGGTCAAG
mm-CSF1R fw	CACCATCCACTTGTATGTC
mm-CSF1R rv	CTCAACCACTGTCACCTC
mm-Ecad fw	GGATATTAATGACAACGCTCC
mm-Ecad rv	GCATTGACCTCATTCTCAG
mm-CK8 fw	ATGAACAAGGTGGAACTAGAG
mm-CK8 rv	ATCTCCTCTTCATGGATCTG
mm-CK19 fw	CCTACAGATTGACAATGCTC
mm-CK19 rv	GTGTTCTGTCTCAAACTTGG
mm-GFAP fw	AACCTGGCTGCGTATAGAC
mm-GFAP rv	CCAGCGATTCAACCTTTCTC
h/mmTwist2 fw	TACATAGACTTCCTCTACCAGG
h/mmTwist2 rv	GGTCATCTTATTGTCCATCTCG
mm Zeb2 fw	CCACGATCCAGACCACAATTA
mm Zeb2 rv	TACTCTTCGATGCTCACTGC
mm Snail1 fw	TGAAGATGCACATCCGAAGC

Name	Sequence (5´-3´)
mm Snail1 rv	CAGTGGGAGCAGGAGAATG
mm-Wnt5a fw	TTACACAACAATGAAGCAGG
mm-Wnt5a rv	ACACTCCATGACACTTACAG
mm-LEF1 fw	TCATCCAGCTATTGTAACACCT
mm-LEF1 rv	TGCTCCTTTCTCTGTTCGT
mm-Zeb1 fw	CAGTATTACCAGGAGGCA
mm-Zeb1 rv	CACACTCGTTGTCTTTCAC
mm-ßcat fw	TACGAGCACATCAGGACAC
mm-ßcat rv	CCAGTACACCCTTCTACTATCTC
mm-Wnt6 fw	GGTTCGAGAATGTCAGTTCC
mm-Wnt6 rv	ATTGCAAACACGAAAGCTG
mm-Wnt5b fw	GAGAAGAACTTTGCCAAGG
mm-Wnt5b rv	GACATCAGCCATCTTATACAC
mm-Porc fw	CTTGTCAAAGCGTTGTCTG
mm-Porc rv	CAAGTTTAAGGCTCGTACC
mm-Wnt3a fw	ATCTTTGGCCCTGTTCTG
mm-Wnt3a rv	TCACTGCGAAAGCTACTC
mm-Twist1 fw	GTACATCGACTTCCTGTACCA
mm-Twist1 rv	TTGCCATCTTGGAGTCCAG
mm-Wnt7a fw	CAGTTTCAGTTCCGAAATGG
mm-Wnt7a rv	GATAATCGCATAGGTGAAGG
mm-Wnt10a fw	AGATCTGATTGACATTCCTCC
mm-Wnt10a rv	TGAGCTAGGAACAGAAAGAG

2.1.6 Equipment

All lab equipment used is listed in Tab 6.

Tab 6: Equipment

Product	Company
Analytical balance, Sartorius excellence	Sartorius (GöttingenFC)
Anatomical tweezers	Carl Teufel GmbH & Co (Liptingen)
Autoclave Varioklav	Thermo Scientific (Bonn)
Axiovert 200M fluorescence microscope	Zeiss (Jena)
Bioanalyzer 2100	Agilent (Santa Clara, USA)
Biolumineszenz Imager (VisiLuxx)	Visitron Systems (Puchheim)
Camera EOS 600D	Canon
CO2 incubator CB150	Binder (Tuttlingen)
Embedding Center EG1160	Leica Microsystems (Wetzlar)
Foreign Body tweezers	Carl Teufel GmbH & Co (Liptingen)
Gavage 0,8Ø	
Hamilton Microliter Syringes, 10µl (26s/51/2)	Hamilton (Bonaduz, Schweiz)
Iridectomy scissors	Carl Teufel GmbH & Co (Liptingen)
Microsurgery tweezers	Carl Teufel GmbH & Co (Liptingen)
Microtome Leica RM 2165	Leica (Wetzlar)
Microwave	Powerwave; Braun
MilliQ water purification system	Millipore (Schwalbach)
NanoDrop ND-1000 spectrophotometer	Peqlab (Erlangen)
Neubauer Improved cell counting chamber	LO Laboroptik (Friedrichsdorf)
PH meter 761 Calimatic	Knick Elektronische Messgeräte (Berlin)
Pipetboy	Integra biosciences (Femwald)
Refrigerated microfuge SIGMA 1-15K	Sigma Laborzentrifugen (Osterode am Harz)

Product	Company
ScanScopeXT	Aperio/Leica (Wetzlar)
Semi-enclosed Benchtop Tissue Processor TP1020	Leica Microsystems (Wetzlar)
Steamer	Braun
Stereotactic apparatus model 900	Kopf Instruments (Tujunga, California)
Surgical lighting Hanaulux 2208	Medap, (Feldkirch)
Sutures Seralon 7/0	DCV- INstrumente (Seitingen- Oberflacht)
Thermal cycler T3000	Biometra (Göttingen)
Vascular clamp	Fine Science Tools (Heidelberg)
Vortex shaker Genius 3	IKA Lab equipment (Staufen)
Water bath	Köttermann (Uetze, Hänigsen)
Mini-gel electrophoresis system	Biometra (Göttingen)
Blotting system	Biometra (Göttingen)
LAS 4000 Imager	Fuji Film / GE Healthcare, (Freiburg)
HT 7900 Real-Time PCR system	Applied Biosystems, (Darmstadt)
"Hybond-C Extra"	Amersham Biosciences, (Freiburg)
"GB33Whatman paper B003"	Heinemann laboratory technology (Duderstadt)
Mikropistill	Faust (Schaffhausen, Scheiz)
Motor for Mikro-Pistill	Faust (Schaffhausen, Scheiz)
Inverted microscope Axiovert 200M	Zeiss (Göttingen)
Microscope Leica DMLB Colorview	Leica (Wetzlar)

2.1.7 Anaesthetics agent and antalgesic

All anaesthetics agents an antalgesic used are listed in Tab 7.

Tab 7: Anaesthetics agent and antalgesic

Medication	Company	Dose
Antisedan® (Atipamezolhydrochlorid)	Pfizer	0,2 mg kg-1 Bodyweight
Hostaket® (Ketaminhydrochlorid)	Intervent	85 mg kg-1 Bodyweight
Rimadyl®	Pfizer	5 mg kg-1 Bodyweight
Domitor® (Xylazinhydrochlorid)	Bayer	7,5 mg kg-1 Bodyweight

2.2 Methods

2.2.1 Cell culture methods

2.2.1.1 Maintenance of cells

Cells were grown at 37°C and 5% CO_2 in a humidified incubator. Cells were first washed with 5ml PBS, separated by incubation in 1ml Trypsin for up to 15 min and splitted in a ratio of 1:10 for passage. In case of BAL17, the cells were centrifuged, washed and then splitted 1:10 daily. Contamination with Mycoplasma was tested frequently for all cell lines. To store cells over a longer period, they were frozen in DMSO +90% FCS and stored at -150°C.

2.2.1.2 LGK974 preparation

2-[5-Methyl-6-(2-methyl-4-pyridyl)-3-pyridyl]-N-(5-pyrazin-2-yl-2-pyridyl)acetamide (LGK974) was delivered as a powder with a molecular weight of 396.44g/mol. Stock solution of 10mM were prepared (3,96mg LGK974/mlDMSO) and frozen. For each experiment performed with LGK974, stock solution were used and diluted.

2.2.1.3 MTT assay

Cell viability was measured by MTT assay (Mosmann, 1983). Treatment with or without inhibitor was tested to compare the viability of the cells. The assay is based on the conversion of the water-soluble, yellow tetrazolium salt 3-(4,5-Dimethylthiazol-2-yl)-2,5-diphenyltetrazoliumbromid (MTT) to an insoluble, purple formazan. This reduction is mediated by NAD(P)H-dependent enzymes in the endoplasmic reticulum (Berridge and Tan, 1992) and therefore highlights apoptotic or necrotic cells which have an altered cell metabolism.

For the MTT assay, $2x10^4$ cells of E0771LG, $4x10^4$ cells of 4T1, $4x10^4$ cells of 410.4, $1x10^5$ human Mφ per well were seeded in triplicate in a 24-well-plate and incubated with the LGK974 inhibitor at the indicated concentrations and time periods. Afterwards, the cells were incubated with 500µl equivalent culture medium +10% MTT (stock solution: 5mg/ml) for 4h at 37°C and 5% CO_2. The medium was aspired and cells lysed in 500µl 5% formic acid containing 63% isopropanol and 32% DMSO. The extinction at 540nm was measured in triplicate using a photometer and was normalized to the extinction of the untreated control.

2.2.1.4 WST-1 test

The WST-1-test measured the viability of cells. The principle of the reaction is the conversion of the tetrazolium salt WST-1 by succinate-tetrazolium reductase to formazan. The measured change in colour of the sample from light red to dark red is proportional to the amount of enzyme in the culture that will be used. For the WST-test $2,5x10^4$ microglia cells per well were seeded in triplicate in a 24-well-plate and incubated with the LGK974 inhibitors at the indicated concentrations and time periods. Subsequently, the cells were incubated with 500µl culture medium for 24 hours before incubation in 500µl and 50µl WST 1 substrate for 2h at 37°C and 5% CO_2. The extinction at 540nm was measured in triplicate using a photometer and compared to the extinction of the untreated control.

2.2.1.5 xCelligence

As an additional method for real-time monitoring of cell viability and proliferation measurements the xCelligence system (RTCA DP Analyzer, Roche), an electronic impedance-based cell sensing measurement system, was used. Here, $5x10^3$ cells of 410.4, $2,5x10^3$ cells of 4T1 and $2x10^3$ cells of E0771LG, respectively, were seeded per well in E16 plates (Roche) and stimulated with concentration of 2.5µM and 5µM of LGK974 for 48h. The bottom of these wells is covered with a gold microelectrode, therefore, changes in electrical impedance can be measured when the cells attach and spread on the electrode surface. Consequently, cell growth and spreading result in increased impedance while detachment or rounding up of cells lead to a reduction. With this method, which is comparable to the MTT-assay and as well to the WST-test, the cell index is determined.

2.2.1.6 Cell invasion assay (modified Boyden chamber)

The microinvasion assay was performed with a modified Boyden chamber system, which has been described previously (Hagemann et al., 2004). The membrane consists of polycarbonate (pore diameter: 10µm, Pieper Filter) and was coated with 1:4 dilution extracellular matrigel (ECM) in serum-free RPMI-1640 medium. Cancer cell invasion was determined by counting the cancer cells in the lower chamber that invaded through the artificial basement membrane. In case of 410.4 cells, cells were cocultured with microglia. Cells were performed with cell culture inserts (BD, Heidelberg, Germany) in the upper chamber, without cell-to-cell contact to the cancer cells. The experiments were performed twice, once with pre-stimulation once without 24h pre-stimulation with LGK974. For all experiments $1x10^5$ cells were used.
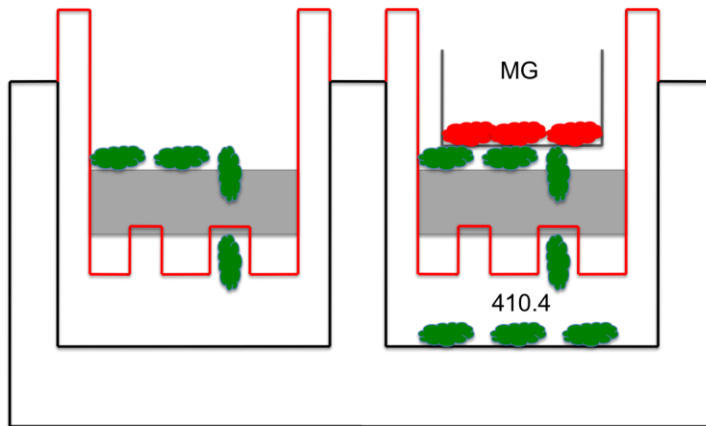
Fig 5: Schema of Microinvasion assay.
The invasive cancer cells were seeded in the upper well of the chamber. In case of 410.4, microglia cells were added. After 96h the numbers of invasive cells, which had degraded the ECM gel to the lower wells, were counted und compared with unstimulated cancer cells.

2.2.2 Protein biochemistry

2.2.2.1 Protein Isolation from cells

For the isolation of total protein the generation of lysates, all used cell lines were seeded in 6-well plates in a concentration of 1x 10^6 cells per well. The possibility to adhere was given for at least for 4hours and then incubated with or without stimulation. After the indicated time points cells were washed once with cold PBS. Afterwards 100µl RIPA lysis buffer was added before cells were detached from the well with a cell scraper on ice, and transferred into 1,5ml tubes. After an incubation of 10-20min, lysates were centrifuged for 5min at 20.000xg and 4°C to pellet cell debris and DNA. Supernatants were collected in 1,5ml tubes and stored at -20°C.

RIPA lysis buffer:	Tris, pH 7,2	50 mM
	NaCl	150 mM
	SDS	0,1%
	Na-deoxycholat	0,55 %
	Triton X-100	1%

For protein lysates from cells, protease inhibitors ("100xProteaseinhibitor Cocktail") as well as phosphatase inhibitors ("PhosStop") were added to the lysis buffer according to the manufacturer's instructions.

2.2.2.2 Protein quantification by Lowry assay

Protein concentrations were determined by Lowry assay (DC protein assay, Bio-Rad) using a BSA standard curve. According to the manufacturer's instructions all samples were diluted 1:10 in 10µl ddH$_2$O. The Lowry assay is based on the colorimetric detection of copper (I) ions, which bind to Bicinchoninsäure (BCA). In the presence of proteins copper (II) ions are reduced to copper (I) in a concentration-dependent manner. The violet product was measured in a photometer at 750nm (Lowry et al., 1951).

2.2.2.3 SDS Polyacrylamidgelelectrophoresis (SDS-PAGE)

For detecting proteins in cell lysates by Western blot, SDS-PAGE (Laemmli, 1970) was used for size fractionation. Therefore, proteins pass through a polyacrylamide gel with two layers within an electric field. First the stacking gel (neutral pH) collects the proteins in one band before the resolving gel (basic pH) separates them. In order to allow their separation in an electric field, the protein lysate were mixed with the anionic surfactant SDS. This surfactant binds proteins proportional to their size based on their negative charges. Prior to electrophoresis, protein lysates were incubated with 4x loading buffer "Roti-Load 1" and boiled for 5min at 95°C to denature the proteins. The loading buffer contains ß-mercaptoethanol, which reduces the protein disulfide bonds. Also, the SDS binds to proteins and applying negative charge in proportion to their mass. The electrophoresis was performed in a vertical mini-gel electrophoresis system (Biometra) using Tris-Glycine running buffer. The focusing of proteins in the stacking gel was carried out for 30min at 90V, the subsequent separation in the resolving gel for approximately 90min at 130V. For the determination of the protein sizes a standard was applied ("Precision Dual Colour Protein Standard").

In the case of Wnt5a protein PAGE was performed under non-denaturing conditions with β-mercaptoethanol-free loading buffer (bioPLUS).

5% Stacking gel:	Tris + 2% SDS (1,5 M; pH 6,8)	630µl
	Acrylamid/Bisacrylamid 30%	830µl
	APS (10%)	50µl
	TEMED	5µl
	H_2O (bidest.)	3,45ml

10% Separating gel:	Tris + 2% SDS (1,5 M; pH 8,8)	5ml
	Acrylamid/Bisacrylamid 30%	6,7ml
	APS (10%)	200µl
	TEMED	20µl
	H_2O (bidest.)	7,9ml

1× Electrophoresis buffer:	Tris	3g
	Glycin	14,4g
	SDS	1g
	H_2O (bidest.)	ad 1l

2.2.2.4 Western Blot

Western blot analyses were used to transfer proteins from a gel onto a nitrocellulose membrane. Subsequently proteins were detected with antibodies (Towbin et al., 1979). A semi-dry blotting system was used for all proteins.

The nitrocellulose membrane "Hybond-C Extra" (Amersham Biosciences) and "GB33Whatman paper B003" (Heinemann laboratory technology), were equilibrated for 5min in transfer buffer before the membrane was put on three "Whatman paper".

Afterwards, the polyacrylamide gel was washed with transfer buffer and placed on the nitrocellulose membrane, and topped by three layers of "Whatman paper" soaked with transfer buffer "GB33 Whatman FilterB003". Then, the blot chamber was closed and the protein transfer was carried out at 10V for 75min. To verify a successful transfer, the nitrocellulose membrane was stained with Ponceau S solution, which stains all proteins. To

detect specific proteins, the nitrocellulose membrane was incubated with antibodies specific for the respective proteins. Therefore, the membrane was incubated for 1h in blocking solution at room temperature to prevent non-specific binding. Afterwards, the primary antibody was diluted according to the manufacturer's instructions in block solution and incubated with the membrane overnight at 4°C., followed by three washing steps for 5min with TBS + 0.1% Tween. Next, the membrane was incubated with the secondary antibody for one hour at room temperature. The secondary antibody was conjugated to horseradish peroxidase (HRP), to visualize the proteins. After incubation with the secondary antibody, the membrane was washed again three times for 5min with TBS + 0.1% Tween. The membrane was incubated for 5min with the detection reagent "ECL Plus" (GE Healthcare) according to the manufacturer's instructions. The substrate of the working solution and HRP are generating a light emitting precipitate, which binds to the antigen-antibody complex. This precipitate was visualized using the "LAS 4000 Imager".

Blockingsolution:	Tris	2,4g	
	NaCl	8g	TBS
	H_2O (bidest.)	ad 1l	
	Tween	0,1%	
	BSA	5%	

2.2.3 Gene expression analysis

2.2.3.1 RNA isolation from cells

The isolation of mRNA from cultured cells was carried out with the spin column- based High Pure RNA isolation kit (Roche**) according to the manufacturer's instructions. Briefly, the cells were seeded at a concentration of $1x10^6$ cells per well in 6-well plates and stimulated as indicated. Subsequently, cells were washed once with PBS and lysed in 400μl of the lysis- /binding buffer supplemented with 200μl PBS. While RNases are inactivated, the buffer also contains Triton X-100, which mediates the permeabilization of the cell membrane as well as guanidine hydrochloride, which induces protein denaturation. The samples were vortexed for 15sec to boost cell lysis and subsequently applied onto a

spin column that consists of glass fiber fleece. Columns were centrifuged at 8000xg for 15sec, which leads to the binding of the nucleic acids to the column, while proteins, salts and cellular debris are eluted. Contaminating DNA was digested directly on the column by incubation with DNase I for 15min. The remaining RNA was washed three times, before 50µl nuclease-free water was added to the column to elute the RNA. Concentration and purity were measured with the NanoDrop ND-1000.

2.2.3.2 RNA isolation from tissue

RNA from tissue was isolated with a modified TRIzol method incorporating a Dnase I digestion step.

For the isolation of total RNA from mice brain, tissue samples were treated with the TRIzol (Invitrogen) reagent. First, samples were homogenized, by a motor driven micropistille, in 1ml TRIzol in a 1,5ml eppendorf tube, before 200µl chloroform was added. This was followed by hand-shaking for 15seconds and incubation at room temperature for 5min. Tubes were then centrifuged at 20.000xg for 15min at 4°C which results in the formation of three phases with the RNA being present in the colourless upper aqueous phase. The upper phase was transferred to a new tube and 500µl isopropanol were added. For the precipitation of the RNA, the samples were incubated for 10min at room temperature followed by centrifugation at 13.000xg and 4°C for 30min. The pellets were washed in 1ml 70% ethanol and centrifuged at 20.000xg and 4°C for 10min. To remove DNA, the pellets were resuspended in 50µl DNA digestion mix and incubated for 20min at 37°C. To purify the RNA, 150µl nuclease-free water and 200µl phenol/chloroform/isoamyl alcohol were added. The samples were vortexed for 30sec and subsequently centrifuged for 2min at 20.000xg and 4°C. The upper aqueous phase, which contains the RNA, was transferred to a new tube. 20µl sodium acetate (3M, pH 4,8) and 200µl isopropanol were added and samples were incubated for 30min at 4°C to precipitate the RNA before centrifugation for 30min at 20.000xg and 4°C. The pellet was washed twice once with 1ml 70% ethanol and once with 900µl 70% ethanol for 5min each followed by centrifugations at 20.000 g and 4°C. Finally pellets were air dried at 37°C for 15min and the RNA was resuspended in 20µl to 50µl (depending on the size of the pellet) nuclease-free water. The concentration and purity was determined using a NanoDrop ND-1000 spectrophotometer (Peqlab).

DNA digestion mix:

5µl DNase I incubation buffer (10x, Roche)

1µl DNase I (10U/µl, Roche)

0,5µl RNase OUT (40U/µl, Invitrogen)

Ad 50µl nuclease-free water

2.2.3.3 Reverse transcription

In the first step to analyse changes in gene expression by qRT-PCR, the isolated RNA was transcribed into complementary DNA (cDNA) by using reagents from the iScript cDNA synthesis kit, which includes reverse transcriptase, an RNA-dependent DNA polymerase. All mRNA´s were reverse transcribed using random hexamer oligonucleotides or oligo(dT) primers, the latter being complementary to the poly-A tail of eukaryotic mRNAs.

Reaction mix:

5x iScript reaction mix	4µl
iScript reverse transcriptase	1µl
RNA template (1µg)	xµl
Nuclease-free water	xµl
Total volume	20µl

Standard program:	25°C	5min
	42°C	30min
	85°C	5min

Each sample was diluted in a ratio of 1:5 with nuclease-free water and stored at -20°C.

2.2.3.4 Quantitative real-time (qRT-PCR)

For quantification of gene expression levels and changes in gene expression in tissue or

cell lysates qRT-PCR was used. This commonly used method for single gene expression consists of two reaction steps. In the first step the RNA is transcribed into cDNA in the second step this cDNA is used for amplification by PCR. For detection SYPR- Green was used. This fluorescence marker intercalates into dsDNA and therefore, the reaction product can be detected as the reaction progresses in real time For the qRT-PCR a thermo cycler was used with the capacity to illuminate samples with a beam of light of a specified wavelength and to detect such fluorescence. The method follows the general principles of the polymerase chain reaction: After activation of a hot-start polymerase, the protocol consists of 40 cycles each including three steps: Denaturation of nucleic acids double strand, annealing of the primers and DNA polymerization.

10× PCR-Puffer:	Tris-HCl pH 8,8	0,75M
	Ammoniumsulfat	0,2M
	Tween-20	0,1% (v/v)
SYBR-Green Master Mix:	10x PCR-Puffer	2,5ml
	25 mM MgCl2	3ml
	1:100 SYBR-Green	31,3µl
	20mM dNTP-Mix	250µl
	5 U/µl Taq-Polymerase	100µl
	10% Triton X-100	652µl
	1M Trehalose	7,5ml

All dilutions were performed with DEPC-H_2O and the Trehalose was diluted with Tris-HCl (pH 8,0).

PCR-Reactionmix:	SYPR-Green Master Mix	5,6 µl
	fw-Primer (10µM)	0,3µl
	rv-Primer (10µM)	0,3µl
	cDNA 5ng/µl	2µl
	H_2O	1,8µl

Standard qRT-PCR program:

95°C	12min	Activation Taq-Polymerase
95°C	15sec	Denaturation
60°C	1min	Annealing/Elongation
95°C	15sec	
60-95°C	2°C/min	

(40x applies to Denaturation and Annealing/Elongation steps)

The reaction mix was placed in a 384-well plate. All qRT-PCRs were performed using the HT 7900 Real-Time PCR system. Gene expression was analysed by using the SDS software version 2.4 (Applied Biosystems) normalizing the expression to two reliable housekeeping genes, murine 18S ribosomal RNA and murine GAPDH. Fold changes or ΔCt values were plotted with GraphPad Prism for Windows or Mac (version 6.0e). For analysis the comparative cycle threshold (Ct) method was applied as described by Livak and Schmittgen, 2001 (Livak and Schmittgen, 2001):

ΔCt = Ct of gene of interest − Ct of housekeeping gene

$\Delta\Delta$Ct = ΔCt of sample - ΔCt of reference

Fold change = $2^{-\Delta\Delta Ct}$

2.2.3.5 Establishing primers for qRT-PCR reaction

All used primer pairs were designed with the software PerlPrimer version 1.1.21 (Marshall, 2004) before they were tested for their efficiencies. The primer pairs were chosen from the database BioGPS (Wu et al., 2009). For primer testing, cDNA with a known concentration was used. Under optimal conditions each PCR cycle should results in a doubling rate of the die, which corresponds to an efficiency of 100% of the respective primer. Only primers within a range of 90%-110% efficiency were chosen for experiments. As described before, the Ct- values were measured and plotted against the amount of input cDNA. The slope of the resulting graph was calculated with SDS software version 2.4; a slope result of -3,33

equals a primer efficiency of 100%. The efficiency can be calculated using the following formula:

$$10^{-1/\text{slope of the line}}$$

Furthermore, to verify that a single gene product with the correct size was generated, the PCR-products of all used primer pairs were visualized on a 2% agarose gel.

Primer sequences are listed in the supplementary Table 7.

2.2.4 Histology

2.2.4.1 Perfusion, Fixation and Tissue Processing

Mice were anesthetized with ether before perfusion. Therefore, the skin of the abdomen was cut open quickly as well as the pericardium using scissors. A small hole was then cut into the right cardiac atrium through which the blood could leave the animal's body. Then 10ml phosphate buffered saline (PBS) was thoroughly injected into the left main heart chamber thereby pumping the blood out of the circulation system. Total brains were dissected out. The anterior part (Fig 6) of the brain (bulbus not included) was snap frozen in liquid nitrogen and stored at −80°C until homogenized for gene expression analysis. Furthermore, for fixation all tissues were stored for 48hours in 4% Paraformaldehyde (PFA at room temperature) at a ratio of fixative to tissue of 10:1. Tissues were stored in PBS before further processing. All fixed tissue were processed into a cassette, dehydrated and cleared automatically.
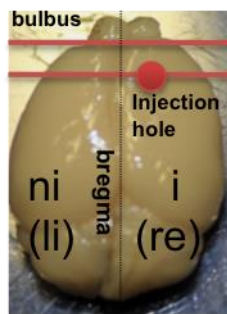
Fig 6: Schema of a mouse brain and tissue processing.
The tissue between the red lines was snap frozen, right side (i) as the injected side with the injection hole and left side non- injected side (ni) as the control.

Tab 8: Dehydration Protocol

Time	Substance
3x60min	75% Ethanol
2x90min	96% Ethanol
3x75min	100% Ethanol
2x120min	Xylol

Tissue were picked out of the cassette and embedded with pure molten paraffin. For microscopic analysis sections of 3µm thickness were cut with a microtome, floated on a warm water bath to help remove wrinkles before they were picked up with a glass microscopic slide.

Tab 9: Deparaffinization Protocol

Time	Substance
3x5min	Xylol
2x5min	100% Ethanol
3min	96% Ethanol
3min	80% Ethanol
3min	70% Ethanol
3min	H_2O

2.2.4.2 Histology staining

To visualize the morphology haematoxylin and eosin staining, the gold standard was used for all samples.

Tab 10: Hematoxylin - Eosin (HE) Protocol

Time	Substance
3min	Roti-Histol
3min	Roti-Histol
3min	Roti-Histol
2min	100% Ethanol
2min	100% Ethanol
2min	96% Ethanol
2min	70% Ethanol
2min	50% Ethanol
2min	30% Ethanol
3min	Aqua dest.
5min	Haematoxylin
10min	Tap water
2min	Aqua dest.
3min	1% Eosin
1sec	Aqua dest.
1min	70% Ethanol
1min	80% Ethanol
1min	90% Ethanol
1min	96% Ethanol
2min	100% Ethanol
2min	100% Ethanol
2min	Roti-Histol
2min	Roti-Histol
2min	Roti-Histol

2.2.4.3 Immunostaining

Immunohistochemistry (IHC) was performed on all sections of 3μm thickness from 4% formalin-fixed, paraffin-embedded tissues.

2.2.4.3.1 Cytokeratin 8 (CK8)

Sections were deparaffinised, unmasked in a steamer for 40min with Citrate buffer (Dako Real Target Retrieval Solution 1:10 dilution), washed, and then rinsed with PBS+H_2O_2 for 20min before incubation overnight at room temperature with anti- Cytokeratin 8 (dilution 1:100 Abcam ab 59434). Sections were washed with Tris Buffer and then incubated for 1h at room temperature with goat anti rabbit biotinylated antibody (dilution 1:250 Dianova 111-065-144), washed in Tris buffer, incubated for 1h with Peroxidase (dilution 1:1000, Sigma ExtrAvidin – Peroxidase E-2886) and visualized with DAB substrate (DAB 500plus Zytomed).

2.2.4.3.2 Ionized calcium binding adaptor molecule (IBA)

Sections were deparaffinised, unmasked in a steamer for 40min with Citratbuffer (Dako Real Target Retrieval Solution 1:10 dilution), washed, and then incubated in PBS+H_2O_2 for 20min before incubation overnight at room temperature with Rb Anti Iba-1 (dilution 1:1000 Wako 019-19741). Sections were washed with Tris Buffer and then incubated at room temperature with goat anti rabbit antibodies (dilution 1:250 Biotinylated Dianova 111-065-144), washed in Tris buffer, incubated for 1h with Peroxidase (dilution 1:1000 Sigma ExtrAvidin – Peroxidase E-2886) and visualized with DAB substrate (DAB 500plus Zytomed).

2.2.4.3.3 Ki67

Sections were deparaffinised, unmasked in a steamer for 40min with Citrate buffer (Dako Real Target Retrieval Solution 1:10 dilution), washed, and then incubated in PBS+H_2O_2 for 20min before incubation overnight at room temperature with Anti- Ki-67 antibody (dilution 1:200 Abcam ab15580). Sections were washed with Tris Buffer and then incubated for 1h at room temperature with goat anti rabbit antibodies (dilution 1:250 Biotinylated Dianova 111-065-144), washed in Tris buffer, incubated for 1h with Peroxidase (dilution 1:1000 Sigma ExtrAvidin – Peroxidase E-2886) and visualized with DAB substrate (DAB 500plus Zytomed).

2.2.4.3.4 CD34

Sections were deparaffinised, unmasked in a steamer for 40min with Citratbuffer (Dako Real Target Retrieval Solution 1:10 dilution), washing, and the incubated in PBS+H_2O_2 for 20min before incubated overnight at room temperature with CD34 rat anti mouse (dilution 1:500, Klon MEC14.7, Serotec MCA1825GA). Sections were washed with Tris Buffer and then incubated at room temperature for 1h with Rabbit Anti-Rat (dilution 1:500 Biotinylated Dako E0468) washed in Tris buffer, visualized with 3,3'-diaminobenzidine (DAB) or either with DAB substrate (DAB 500plus Zytomed).

2.2.4.3.5 Glial fibrillary acidic protein (GFAP)

Sections were deparaffinised, unmasked in a steamer for 40min with Citratbuffer (Dako Real Target Retrieval Solution 1:10 dilution), washing, and the incubated in PBS+H_2O_2 for 20min before incubated overnight at room temperature with anti-GFAP antibody (dilution 1:200, Dako Z0334). Sections were washed with Tris Buffer. Afterwards they were incubated at room temperature with Alkaline Phoshatase/red/rabbit/mouse system for 10min to 15min (Dako Real Detection System K5005).

2.2.4.3.6 Myeloperoxidase (MPO)

Sections were deparaffinised, unmasked in the microwave for 30min with Tris/EDTA (10x Dako S2367 Target Retrieval Solution pH 9), washing, and the incubated in PBS+H_2O_2 for 20min before incubated overnight at room temperature with Anti-Myeloperoxidase (MPO) antibody (dilution 1:200, Abcam 9535). Sections were washed with Tris Buffer and then incubated at room temperature for 1h with goat anti rabbit biotinylated (dilution 1:250 Dianova 111-065-144), washed in Tris buffer, incubated for 1h with Peroxidase (dilution 1:1000 Sigma ExtrAvidin – Peroxidase E-2886) and visualized with DAB substrate (DAB 500plus Zytomed).

2.2.4.3.7 CD3

Sections were deparaffinised, unmasked in the microwave for 30min with Citratbuffer (Dako Real Target Retrieval Solution 1:10 dilution), washing, and the incubated in PBS+H_2O_2 for 20min before incubated overnight at room temperature with Anti-CD3

antibody (dilution 1:150, DCS C1597C01). Sections were washed with Tris Buffer and then incubated at room temperature for 1h with goat anti rabbit biotinylated (dilution 1:250 Dianova 111-065-144), washed in Tris buffer, incubated for 1h with Peroxidase (dilution 1:1000 Sigma ExtrAvidin – Peroxidase E-2886) and visualized with DAB substrate (DAB 500plus Zytomed).

2.2.4.3.8 B220

Sections were deparaffinised, unmasked in the microwave for 30min with Citratbuffer (Dako Real Target Retrieval Solution 1:10 dilution), washing, and the incubated in PBS+H_2O_2 for 20min before incubated overnight at room temperature with rat Anti-mouse CD45R antibody (dilution 1:200, BD Pharmingen 557390). Sections were washed with Tris Buffer and then incubated for 1h at room temperature with goat anti rat biotinylated (dilution 1:200 Sigma B7139), washed in Tris buffer, visualized with 3,3'-diaminobenzidine (DAB) and nuclei counterstained with haematoxylin.

Nuclei were counterstained with haematoxylin for all staining.

2.2.5. Light microscopy

For the documentation of all preparations the stereomicroscope (Leica Microsystems) was used to examined and photographed.

2.2.6 Animal monitoring

Before injection mice were monitored for their physical fitness. Sensory, or motor deficits in the animals that might interfere with their normal behaviour were checked before and after surgery. Therefore, all mice were tested for several parameters, including poor grooming, changes of the fur, bald patches in the coat, absence of whiskers, laboured breathing and body weight loss and abnormalities were recorded. The following tests were used to reveal neurological dysfunctions.

2.2.6.1 Wire Hang Test

This test is used to evaluate motor function: It investigates neuromuscular strength of animals. The mouse is placed on the wire cage lid and the lid is gently waved so that the

mouse grips the wire (Fig 7A). The lid is then turned upside down approximately 50cm above the surface of the bedding material.

The latency to fall onto the bedding was recorded. This task was used as a measure of grasping ability and an indication for motor function deficiency.

2.2.6.2 Rotarod Test

This test is widely used to measure motor coordination and balance and can reveal ataxic behaviour. The rotarod measures the ability of the mouse to maintain balance on a rotating rod (Fig 7B). Performance is measured as "latency until drop-off". There are two methods:

Rotarod: Each mouse is placed on the rotating rod and the time until fall off is measured (cut-off time: 60sec). Different constant rotation speeds are used in this paradigm.

Accelerod: An accelerating rotarod allows the rotation speed to be constantly increased from 4 to 40 revolutions per minute (rpm), over a five-minute period.

Each mouse is placed on the rotarod at a constant speed (12rpm) for a maximum of 120sec and the latency and frequency to fall off the rotarod within this time period is recorded.
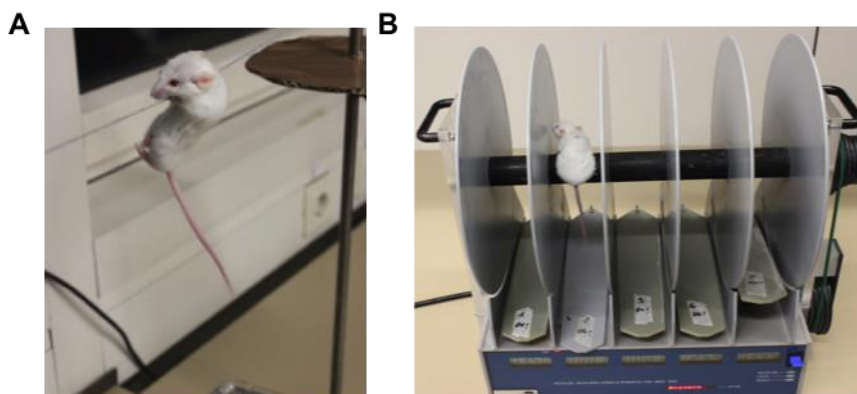
Fig 7: Behaviour testing systems.
(A) Wire Hang system and **(B)** Rotarod system for behaviour testing.

2.2.7 Stereotaxis

2.2.7.1. Animal use and intracranial cancer cell injection

Mice, of approximately 20g body weight and eight weeks of age were bred in-house from animals purchased from JANVIER SAS and were used for all studies. Female mice were

group-housed in Macrolon cages, provided with nesting material without environmental enrichment. Mice were provided with water and phytoestrogen-free and soy-free food (ssniff Spezialdiäten GmbH), available ad libidum. Cages were held under standard conditions within a temperature- and humidity-controlled holding room (22°C; 55-60% relative humidity on a 12:12 hour light:dark schedule (lights phase: white light; illumination: ~80lx; dark phase: no light)) and housed for four weeks to acclimatise before they were used for experiments. Physical examinations were performed before and after surgery in an experimental room. Testing was commenced at least one hour after onset of the light phase. Thus, potential abnormalities, sensory, or motor deficits, which might interfere with data interpretation, would have been detected before the procedure. Mice with abnormalities were not used for further studies.

At an age of 12 weeks, mice were anesthetized with ketamine 100mg/kg intraperitoneal (IP) ×1 and Domitor® 0,25mg/kg IP ×1 before injection. Mice were placed into a stereotactic frame (Fig 8). This frame employs two devices: a head holder and a thumbscrew driven ear-bar advance.
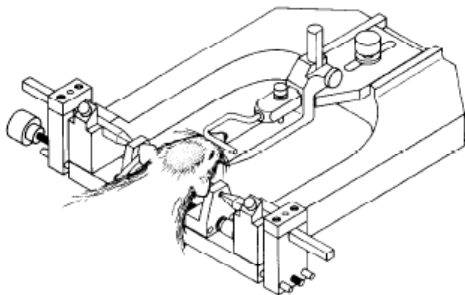
Fig 8: Stereotaxis frame.
Mouse was fixed in the front and also from the left and right side with ear-bar advance (Marchand and Riley, 1979).

Different amounts of cells were tested and injected. 3µl (mixture 1:3 cells and extracellular matrix (ECM)) were stereotactically injected through a 0.5- 1mm burr hole by using a Hamilton 10µl syringe. Brain coordinates relative to bregma (Franklin KBJ, Paxinos G.; The Mouse Brain in Stereotaxic Coordinates. San Diego: Academic Press; 1997. 10.1111/j.1469-7580.2004.00264.x.), were posterior -2.0, lateral 1.0, ventral -3.5 and

dorsal +0.5 to the right hemisphere. The opening of the needle pointed to the left. The syringes remained in place for a period of 3min to minimize reflux through the needle track. Afterwards, the needle was removed under simultaneous rinsing with physiological saline solution from the brain. The burr hole was then closed with bone wax and the scalp stitched.

Mice were weighed and checked on biweekly basis at minimum to monitor metastasis development.

2.2.7.2 Cancer cell preparation for injection

In case of adherent cells, cells were observed before for they had reached 70-80% confluency. Cells were washed with PBS and detached by incubation with 1ml Trypsin (1:5) for up to 15min. Cells were calculated in Neubauerzählkammer.

2.2.7.3 Application of LGK974

For application of LGK974 gavage (stomach tube) was used. LGK974 was diluted in sterile H_2O 50µl to 60µl depending on the body weight were applied with a concentration of 3mg/kg body weight.

2.2.8 Chorioallantoic Membrane (CAM) Assay

This method is widely used as a method to study angiogenesis, cancer cell invasion and metastasis. Murphy (1912) used the fertilized chicken egg membrane as a respiratory organ and studied tumour invasion using this method. The advantage of this model are a highly nature vascularisation which can promote tumour cell growth, it is very reproducible and comparable to animal models with less but at lower costs. Furthermore, the CAM itself contains ECM and therefore mimics the physiological cancer cell environment.

Here, cancer cells are placed on the developing embryo of a chicken egg at the tenth day after fertilisation. Alternatively cancer cells that have been treated with the substance to be tested can be used. The embryos are incubated for a desired time before the effects of the substance or tumour growth can be analysed. Specific pathogen free eggs were used, which

were purchased from Charles River (Sulzfeld). Eggs were incubated at 37°C and at a relative air humidity of 80%. To amenable access of the tumour cells to the CAM, eggs were windowed on the third day of incubation. Therefore eggs were sawed in the bubble, so that the air can escape from the egg and the embryo can descend and separate from the shell. Furthermore, a small opening was sawed into the shell above the embryo. Before the eggshell was lifted, a Locke's solution was used to separate the shell from the membrane. Next, the opening was covered with Leukosilk S (BSNmedicalGMBH, Hamburg) and eggs were incubated for another seven days. In the next step, different cancer cells or cancer cells plus inhibitor were placed on the CAM. In case of 410.4, 3×10^6 cells in 40µl ECM (R & D Systems, Wiesbaden-north city) were resuspended and then placed directly on the CAM. Additional 1×10^5 of 4T1 cell and 1×10^5 E0771LG cell were resuspended in 40µl ECM and placed on the CAM. After covering with Leukosilk S, eggs were incubated for another seven days. For fixation CAM and tumour tissue was removed from the eggs and incubated overnight in 4%PFA. Afterwards the tissue was washed in stored in PBS before tissue Processing as described.

Locke's solution:	NaCl (1,61M)	100ml
	KCl (0,16M)	37ml
	CaCl$_2$ (0,14M)	21ml
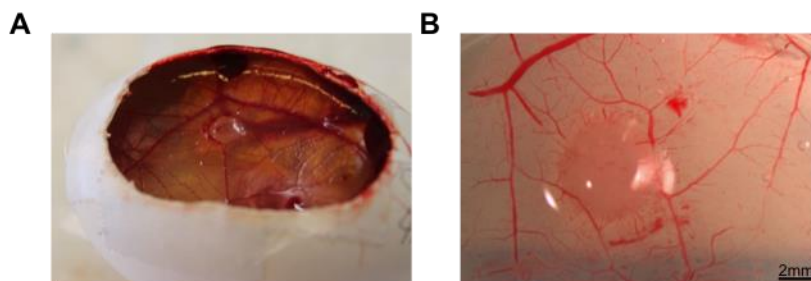
Fig 9: Preparation of CAM.
(A) Opened Egg with tumour. **(B)** Membrane with tumour

2.2.9 Software analyses

Aperio ImageScope viewing software from Leica practical on digital slide images, which can adjust enlargement and can compare different stains, interpret areas of interest, and perform image analysis. Analysis provides automated quantification for the exact evaluation of staining patterns. Therefore, slides were digitised on a scanner and volume of the tumours were measured and evaluated.

2.2.10 Statistics

GraphPad PRISMA® Version 6.0e software was used for the calculation of significance with the two-sided unpaired t-test. Results with a p-value <0.05 were considered significant. GraphPad PRISMA® Version 6.0e software was also used for the Kaplan Meier survival curves. All experiments were performed at least in biological triplicates. All data are displayed as means±SD (standard deviation).

3 Results

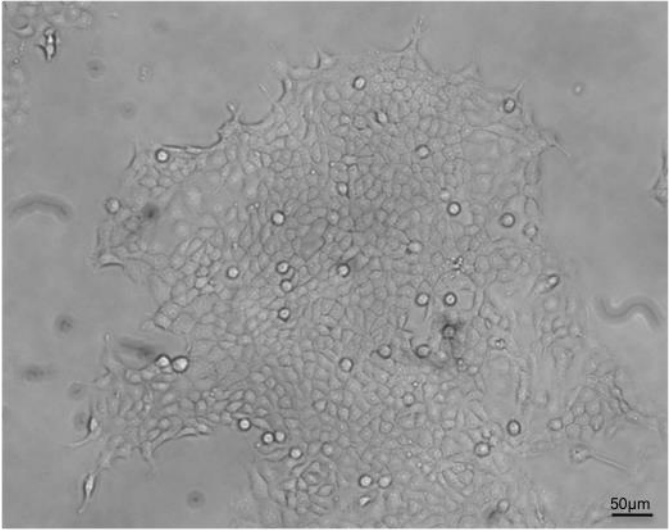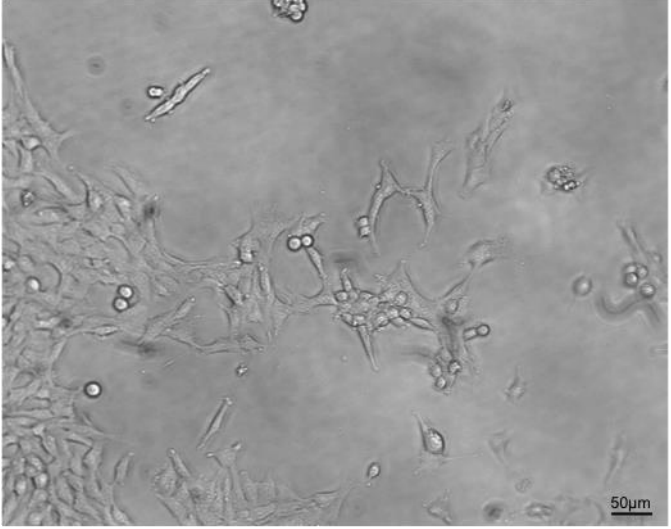## 3.1. Characterisation of cancer cell lines

One of the major aims of this thesis was to establish a syngeneic mouse model to investigate the colonization of cancer cells in the central nervous system. Therefore, we first had to identify suitable breast cancer cell lines from mice, test their biological features and characterize their gene expression profile.
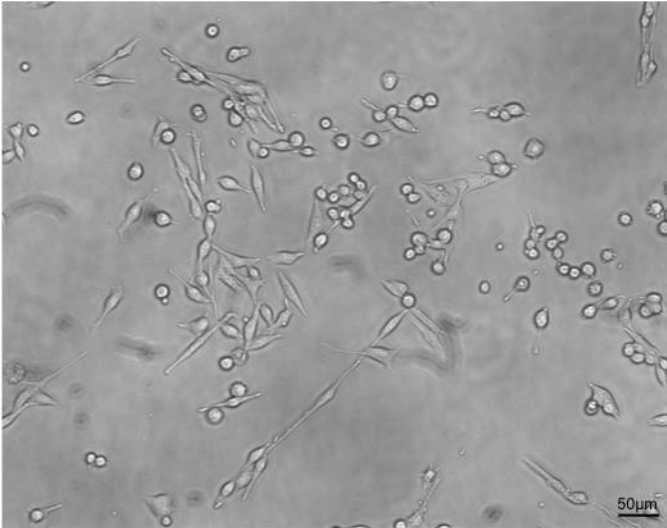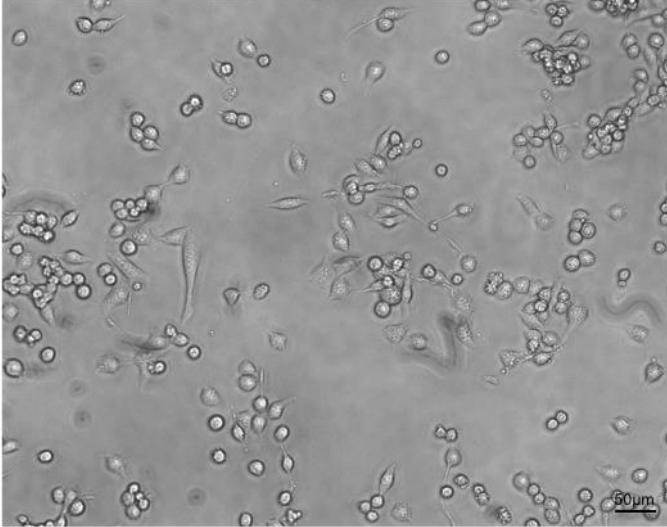
One of the potential cell lines we came up with is the breast cancer cell line 410.4. This mamma- adenocarcinoma cell line was originally isolated from a single spontaneously arising mammary tumour from a BalbC mouse (Miller, 1983). The subclone 4T1 was derived from 410.4 after treatment with thioguanine, which resulted in a thioguanine-resistent 4T1 cell line (Aslakson and Miller, 1992b). The 4T1 cancer cell line is able to metastasise spontaneously in the lungs and liver and appears to enter the blood stream without involvement of the lymph nodes while the metastatic potential of 410.4 has not been investigated yet. The third breast cancer cell line used in this study is the adenocarcinoma cell line E0771. EO771 was originally isolated from a spontaneous cancer of a C57BL/6 mouse. The E0771LG we used was provided by Jeffrey Pollard. This is a more aggressive subclone of the EO771. In the laboratory of Jeffrey Pollard, E0771 cells were injected intravenously into C57BL/6 mice, and the cells isolated from lung metastatic foci were cultured to obtain the highly metastatic subclone EO771LG (Ewens et al., 2005).

3.1.1 Cell lines morphology

First, to identify differences in cancer cell morphology, cancer cell lines 410.4, 4T1, E0771, and E0771LG were cultivated for 48hours until they had reached a confluency of 70%. For documentation, pictures were taken with an inverted microscope. The cancer cell lines 410.4 and 4T1 grew with a comparable morphology and typical epithelial characteristics (Fig 10). The E0771 and E0771LG showed no differences, however, in contrast to 410.4 and 4T1, they revealed obvious mesenchymal morphology (Fig 10).

Cell line	Morphology
410.4 The cells grow as a monolayer with epithelial morphology. Cells are polygonal in shape with more regular dimensions, and grow in patches/groups.	
4T1 Cells grow similar to 410.4. 4T1 cells grow as single cells before they grow in patches.	

Cell line	Morphology
E0771 The cells grow as a monolayer. Fibroblast-like cells are bipolar or multipolar and have elongated shapes.	
E0771LG Cells grow similar to E0771	

Fig 10: The morphology of the four breast cancer cell lines used in this study.
The morphologies of the cancer cell lines 410.4, 4T1, E0771 and E0771LG are shown.

3.1.2 Gene expression for the characterisation of cancer cell lines

The morphology of the E0771 and E0771LG cell lines indicates a more mesenchymal phenotype as compared to the other lines implicating differences in the epithelial and mesenchymal characters of these cell lines (3.1.1). In order to examine this implication, further and to prove the impact of EMT and MET in metastasis, cancer cell lines were characterised for their gene expression patterns using Real-Time-quantitative-PCR. Typical markers were used for epithelial (Ecad) (Fig 11A) and for mesenchymal characterisation (Vimentin) (Fig 11B).
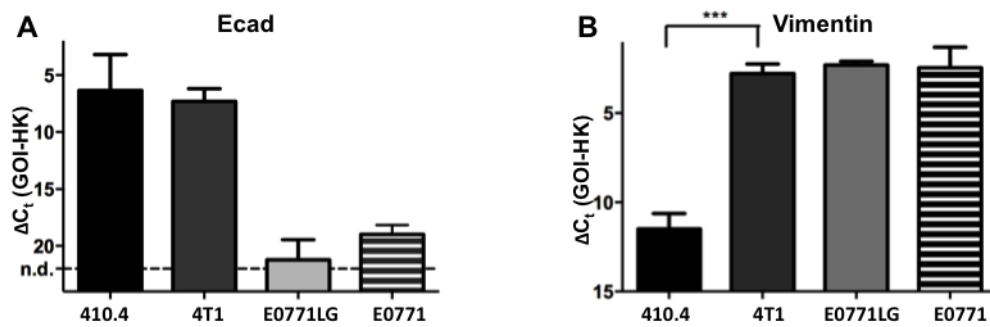
Fig 11: The expression level of E-cadherin (A) and Vimentin (B) revealed differences in the epithelial or mesenchymal character of the different breast cancer cell lines.
The expression of E-cadherin (Ecad) and Vimentin was assessed by qRT-PCR from total RNA samples of the cancer cell lines 410.4, 4T1, E0771LG and E0771 (GOI = gene of interest, HK = housekeeper). Error bars show SD, values, statistics sign was tested using unpaired, two tailed students t-test. **(A)** Both, the 410.4 and the 4T1 showed high expression levels of Ecad compare to the both EO771 cell lines. **(B)** The 410.4 showed low expressions levels of Vimentin compare to all other cell lines. Interestingly, the 4T1 demonstrated significantly higher expression of Vimentin compared to 410.4 (p= <0.0001).

Ecad as a marker for epithelial cells was highly expressed in the cancer cell lines 410.4 and 4T1, which underlined the epithelial character of these cell lines. The expression level in all other cell lines was lower compared to 410.4 and 4T1 and therefore an indicator for a mesenchymal character. Vimentin, an intermediate filament protein, which is expressed in mesenchymal cells, is often used as a marker for cells undergoing EMT during normal development as well as during metastatic progression (Thiery, 2002). In our tests lowest significant expression of Vimentin was measured in the 410.4 cell line, and high expression was detected in 4T1, E0771LG and E0771. With respect to 410.4 it would be of interest, if these cell types differ in their colonization capacity in the planned *in vivo* experiments.

To be able to demonstrate the presence of cancer cells in tissue samples obtained from mice later, after the injection of these carcinoma cells into the brain, we screened them for typical markers. Breast cancer cells often express increased levels of Cytokeratin 8 (CK8). Indeed, CK8 was highly expressed in all four cell lines and could therefore be used as a potent marker to measure the content of breast cancer cells in the brain tissue, which normally expresses low amounts of CK8 (Fig.12).
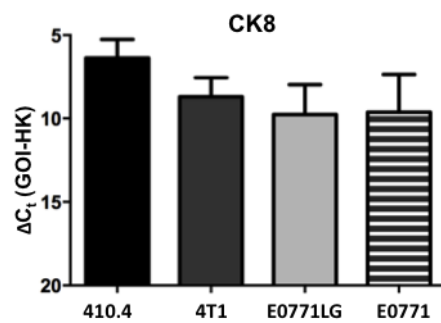
Fig 12: Gene expression of CK 8 in different cancer cell lines.
The expression of CK8 was assessed by qRT-PCR from total RNA samples of the cancer cell lines 410.4, 4T1, E0771LG and E0771 (GOI = gene of interest, HK = housekeeper), qRT-PCR for Cytokeratin 8 in murine mamma carcinoma cell line 410.4, 4T1, E0771LG and E0771. Statistics sign was tested using unpaired, two tailed students t-test Interestingly, there were no significant differences between the four breast cancer cells.

After establishing CK8 as a suitable marker to identify tumour masses that may develop from the injection of breast cancer cell lines we plan to use in this study, we can now focus on the next step: establishing syngeneic *in vivo* models, which I will describe in the next section.

3.2. Establishing of a syngeneic mouse model

3.2.1 Investigation of cerebral metastasis development

Cerebral metastasis is a severe clinical implication with mostly fatal outcomes for the patients. Almost 30% of metastasized breast cancer patients suffer from brain metastases and this incidence is increasing. However, animal models for brain metastases are limited. Furthermore, the immune cells and immune signalling play an important role during the colonization of the brain (Lorger and Felding-Habermann, 2010). In order to investigate the role of the resident innate immune cells, the microglia, during cerebral metastasis, the establishment of syngeneic mouse models is needed. Also, to test immune based therapeutic strategies *in vivo* as well as for a better understanding of the role of blood-derived immune cells during the colonization of the brain, immune-competent mouse models are required. However, until now the majority of the investigations on metastatic diseases are performed using a Xenograft model, that is in immunocompromised mice (Morton and Houghton, 2007).

In order to establish syngeneic cerebral metastasis mouse models, different amounts of 410.4, 4T1, E0771LG, and E0771 cancer cells were intracranially injected in immune-competent BalbC or C57BL/6 female mice, respectively. After the procedure, all mice were observed carefully and behaviour tests (Hanging wire and Rotarod tests) as well as weight measurements were performed to screen and follow–up the injected mice (data not shown and Fig 7). Mice displaying abnormal neuronal deficiencies as revealed by the inability to successfully complete the Hanging wire or Rotarod tests, or losing weight (>20%), were dissected immediately. The inability to complete these tests was documented through movies and photos. After sacrificing, potential tumour mice, the brain tissues were dissected and macroscopically photographed to document the tumour growth (Fig 13). Furthermore, every mouse was catalogued by age, injection date and dissection date and based on this data survival curves for experimental groups were generated (Fig 14).
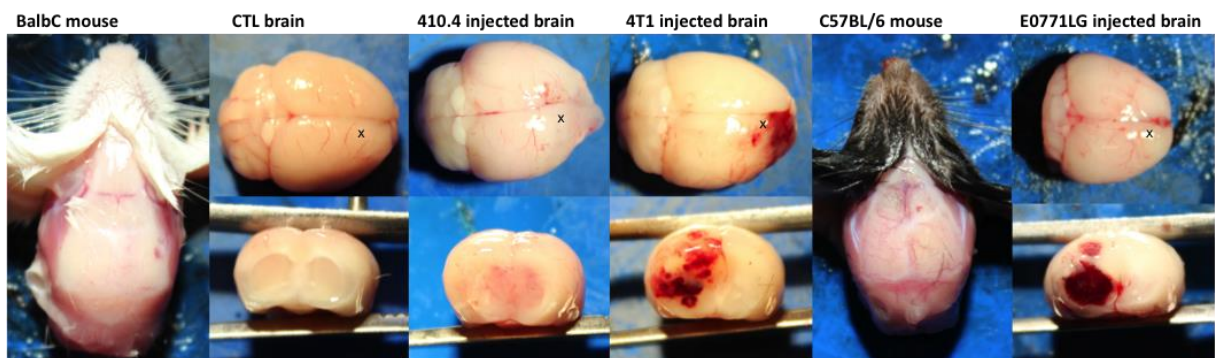
Fig 13: Preparation of mouse brains after the colonization of different cancer cell lines.
BalbC mice were injected with 410.4 and 4T1 cancer cells and compared with the control (CTL =injected only with ECM/medium without breast cancer cells). C57BL/6 mouse were injected with E0771LG. Injection whole was labelled with "x".

BalbC mice were injected with different amounts of 410.4, 4T1 and E0771LG embedded in ECM, and ECM alone as controls (CTL).
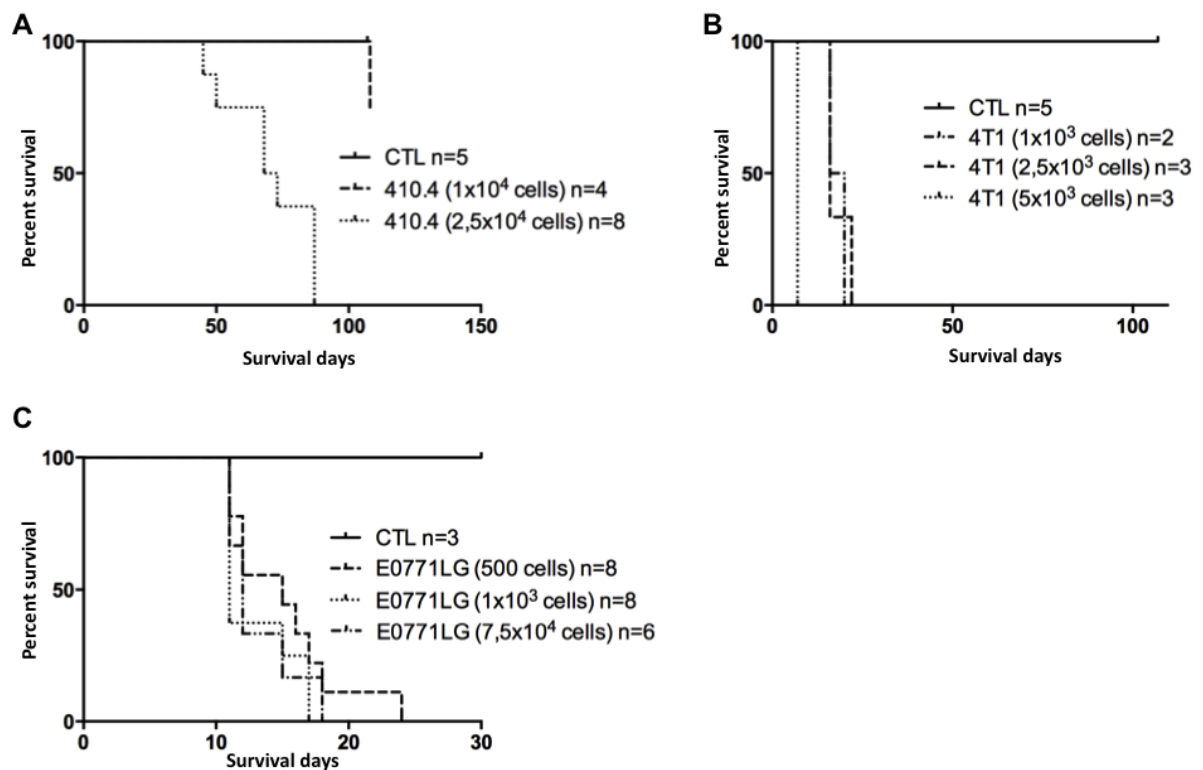
Fig 14: Kaplan Meier survival curves of mice.
(A-C) Survival days of mice after injection of different amounts of cancer cell lines 410.4, 4T1 or E0771LG as well as a control. **(A)** Control (n=5) vs. $1x10^4$(n=4) or $2,5x10^4$(n=8) injected 410.4 cells**. (B)** Control (n=5) vs. $1x10^3$ (n=2) or $2,5x10^3$ (n=3) or $5x10^3$ (n=3) injected 4T1 cells. **(C)** Control (n=3) vs. 500 (n=8) or $1x10^3$ (n=8) or $7,5x10^4$ injected E0771LG cells.

In case of $1x10^4$ injected 410.4 cancer cells, only one out of four mice developed cerebral metastasis (n=4) while all mice developed metastasis after the injection of $2,5x10^4$ 410.4 cancer cells. Interestingly, this finding indicated that there is a threshold regarding the amount of 410.4 cells for successful colonisation of the brain.

In parallel, $1x10^3$ cells, $2,5x10^3$ cells, $5x10^3$ cells and $1x10^4$ cells (data not shown) of cancer cell line 4T1 embedded in ECM were injected in BalbC mice (Fig 14B). All injected mice with the 4T1 cancer cell line developed metastasis independently of the amount of injected cells. Furthermore, the amount of cells seemed also not to influence the overall survival of the mice. All mice died in the same range between day seven and 22. Therefore, we underlined the assumption that the subclone of the 410.4, 4T1 has a significant better ability to colonize the brain tissue. Here, injecting $1x10^3$ 4T1 cancer cells is enough for cerebral metastasis development and can be used for further experiments.

To test the colonisation capacity of the EO771LG breast cancer cell line C57BL/6 mice were injected with 250 cells (data not shown), 500 cells, $1x10^3$ cells, $1x10^4$ cells (data not shown), $2,5x10^4$ cells (data not shown) and $7,5x10^4$ cells embedded in ECM (Fig 14C). Additionally, as a control (CTL), C57BL/6 mice were injected with ECM alone. All mice developed metastasis within 21 days. For this reason we decided to perform further experiments with 500 cells.

Interestingly, the mean overall survival (OS) of mice injected with the cancer cell line 410.4 was 50 days (Fig 14A), in comparison to the mean OS of 21days following injection with cancer cell line 4T1 (Fig 14B). C57BL/6 mice injected with lower amounts of the cancer cell line E0771LG survived 15days (Fig 14C). During and after dissection, brain tissues were macroscopically observed. We observed frequent bleedings in the E0771LG model in contrast to the 410.4 and 4T1 models (Fig 13). Even after the very short OS of the EO771LG injected mice, we could detect massive tumour cell colonization. In contrast to the 410.4 and 4T1, mice injected with the cancer cell line E0771LG died immediately after the first observation of behavioural symptoms. All injected BalbC mice - independent of the cancer cell line - showed first symptoms without the necessity to sacrifice the mice immediately. These first symptoms include motor function abnormalities e.g. hyperactivities or ambulation with at least one full 360° turn. There was a period of up to one week between observation of first symptoms and the failure of the described behaviour.

In summary, four syngeneic cerebral metastasis mouse models were established by stereotactic injection of four different breast cancer cell lines. Additionally, the amount of cancer cells for metastasis development was experimentally determined and was used for the following studies. Significant differences in OS and the amount of cells for successful metastasis were detectable between 410.4 and 4T1. However, there were no differences between the cancer cell lines E0771LG and E0771. Moreover, different colonization patterns of the cancer cell lines were investigated.

3.2.2 Histological investigation of colonized breast cancer cells metastasis

To confirm the macroscopic results and to analyze the induced tumours in greater detail, histology, IHC and qRT-PCR from the brain tissue samples were performed. Therefore,

tissue sections of each mouse were stained using the gold standard HE, to see whether they show the presence of colonized breast cancer cells in the brain.
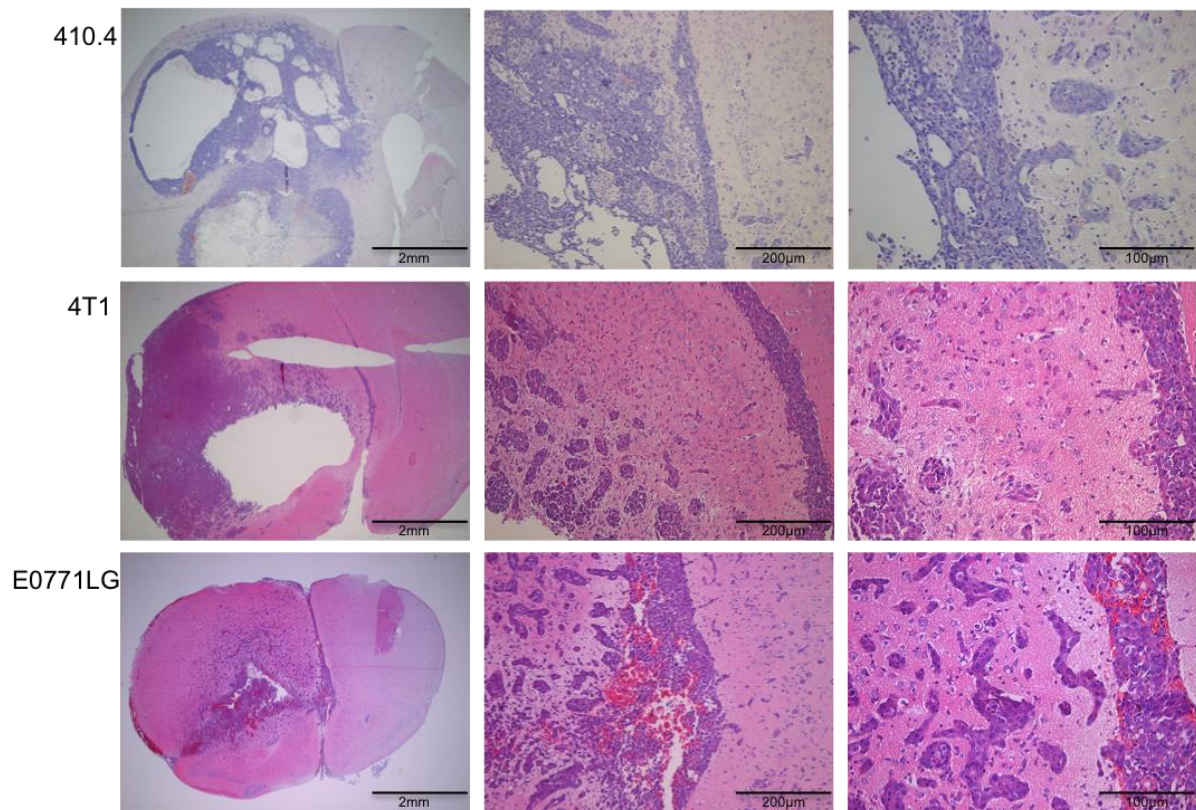
Fig 15: Cell lines derived from BalbC/C57BL/6 mice have metastatic potentials.
Intracranial injection of 410.4 ($2,5 \times 10^4$ cells), 4T1 (1×10^3 cells) and E0771LG (500cells) were tested for metastatic potentials in BalbC or in case of E0771LG in C57BL/6 mice. HE stained sections show the presence of colonized cancer cells in the brain.

All HE stained sections displayed the presence of metastasis in the brain. Here, the differences of cancer cell lines on metastasis development are conspicuous (Fig.15).

Most importantly, in contrast to previous reports we detected that the colonized cells not only form a macroscopic metastasis but also that colonizing cells detach from the metastatic mass and infiltrate into the adjacent brain tissue. This is in contrast to the current view that cerebral metastasis growth only displacing with a glial pseudo-capsule and without infiltration. This unexpected finding raised several questions, in particular, what is the biological consequence of these cells infiltrating brain parenchyma. Additionally, we detected carcinoma cells at the meningeal and in distinct samples also in the ventricles. These findings indicated that the cells are potential sources for further dissemination in the affected brains. In some experiments we detected contralateral to the

injection site also colonized metastatic cells confirming this hypothesis. Thus taken these findings together, it seems that metastasis have the potential to disseminate and metastasize again, at least in the brain.

Moreover, the infiltration pattern into the adjacent brain parenchyma varied between the syngeneic models. While the 410.4 injected cancer cells showed cohort infiltration patterns (Fig 15). 4T1 cancer cells showed the same cohort infiltration pattern, however, with a significantly higher extent. In contrast, the E0771LG cancer cell line demonstrated single cell, diffuse infiltration into the adjacent brain parenchyma. To demonstrate the presence of colonized cancer cells in the brain and confirm previews findings, we used the marker CK8 (Fig 16). Therefore, CK8 staining was performed in one of each sectioned, injected mouse brain with 410.4, 4T1 and E0771LG cancer cells.
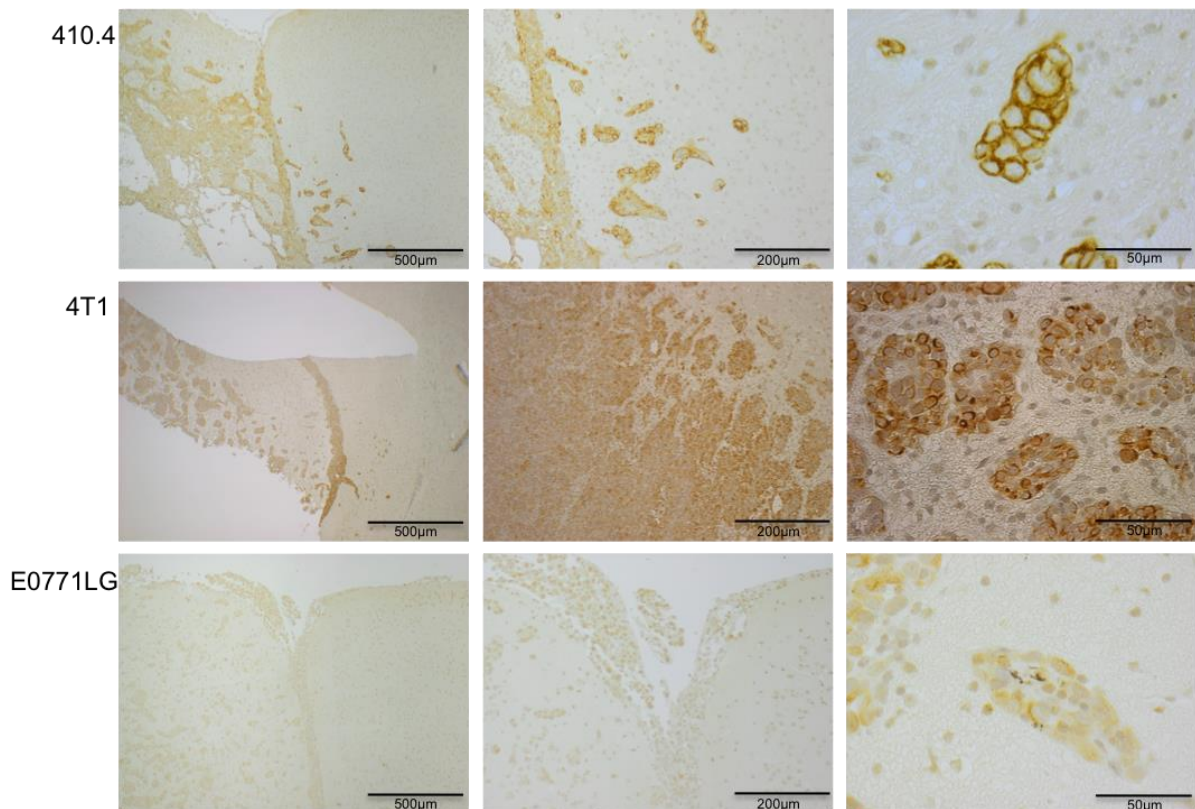
Fig 16: Quantification of cancer cell lines and metastatic potentials.
Intracranially injection of 410.4 ($2,5x10^4$cells), 4T1 ($1x10^3$cells) and E0771LG (500cells) were tested for CK8. CK8 staining was performed for sections with injected cancer cell lines 410.4, 4T1 and E0771LG. CK8 staining show clearly the presence of colonized tumour cells in the brain.

Here, it was possible to verify the gene expression results. These findings correlate well with the results of cancer cell gene expression obtained by qRT-PCR (Fig 12). CK8 was

highly expressed in the metastasis of the cancer cells 410.4 and 4T1. Expression of CK8 in E0771LG could also be detected, however with lower intensity. This important observation might be useful for the quantification of metastasis development in the brain. The slightly lower expression of CK8 in E0771LG could be explained by the fact that Cytokeratin expression in primary human mammary carcinomas correlates with clinicopathologic variables (Willipinski-Stapelfeldt et al., 2005). CK19 was highly expressed in E0771LG, however, CK19 showed low expression in the other cancer cell lines (data not shown). Therefore, CK8 was routinely used as a standard in further experiments.
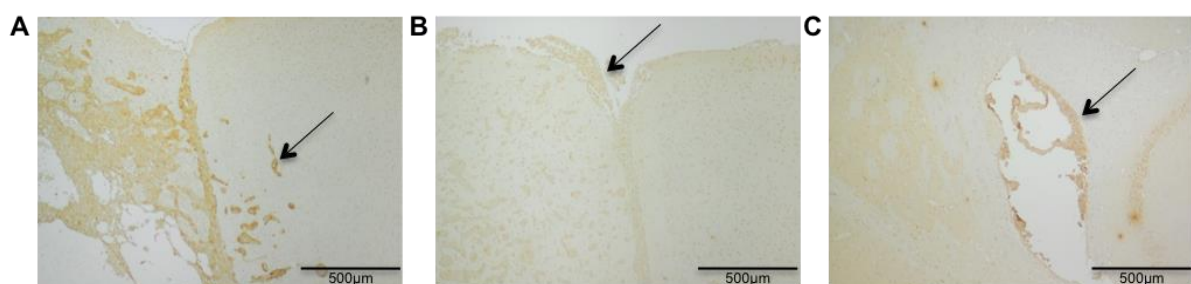
Fig 17: Representative examples for different infiltration patterns of cancer cell lines.
CK8 stained sections reveal different infiltration patterns. **(A)** Infiltration of cancer cells over the hemisphere gab in the brain, **(B)** colonization decay of meningeal and **(C)** colonization decay of ventricle.

After staining, the metastatic potential was investigated and histological sections were compared with the corresponding cell lines. In case of 410.4 injected cancer cells, metastasis were growing particularly over the gap to the other hemisphere (Fig 17A). Vascularisation of the metastasis was detectable. Metastasis enlarge as a cohort and therefore similar to the cell line-growth pattern. Also, lots of necrosis leads to lesions in the tissue. A metastasis growth pattern similar to that of 410.4 was observed after injecting of 4T1 cancer cells (Fig 15). These metastases enlarge as cohort, with a more aggressive behaviour. They perform more vascularisations and grow rapidly through the brain over the hemisphere gap. A representative example was shown in Figure 17A. Metastasis resulting from the injection of E0771LG cells grows differently: Single colonized tumour cells or small groups of colonized tumour cells were detectable and vascularisation was performed. Colonized tumour cells attacked meningeal. An example for attacked meningeal was shown in Figure 17B. A representative example for attacked vessels and ventricles were shown in Figure 17C and were spread within the brain. Also, here the colonized tumour cells grow similar to the cell line. The differences in infiltration patterns are listed in Tab 11.

Tab 11: Differences in the infiltration behaviour of the syngeneic mouse models

Cell line infiltration patterns	410.4	4T1	E0771LG
Single-cell-infiltration	yes	yes	yes
Cohort colonization	yes	yes	
Colonization decay of Meningeal			yes
Colonization decay of Vessels	yes	yes	yes
Hemisphere gab	yes	yes	yes
Colonization decay of Ventricle			yes

In our group it was recently demonstrated that microglia are critical for the invasion of cancer cells into the brain. Moreover, Giulian already confirmed (1993) this finding and also that the brain responds to brain injuries with a glial reaction. Microglia and astrocytes are found next to the injured site where they build a "glial-wall". To confirm these findings in our syngeneic models one section of each mouse brain was stained with a marker for astrocytes (GFAP), (Fig 18) and macrophages/microglia (IBA), (Fig 19). Additionally, in terms of an immune reaction CD3 and MPO were stained on consecutive brain sections.
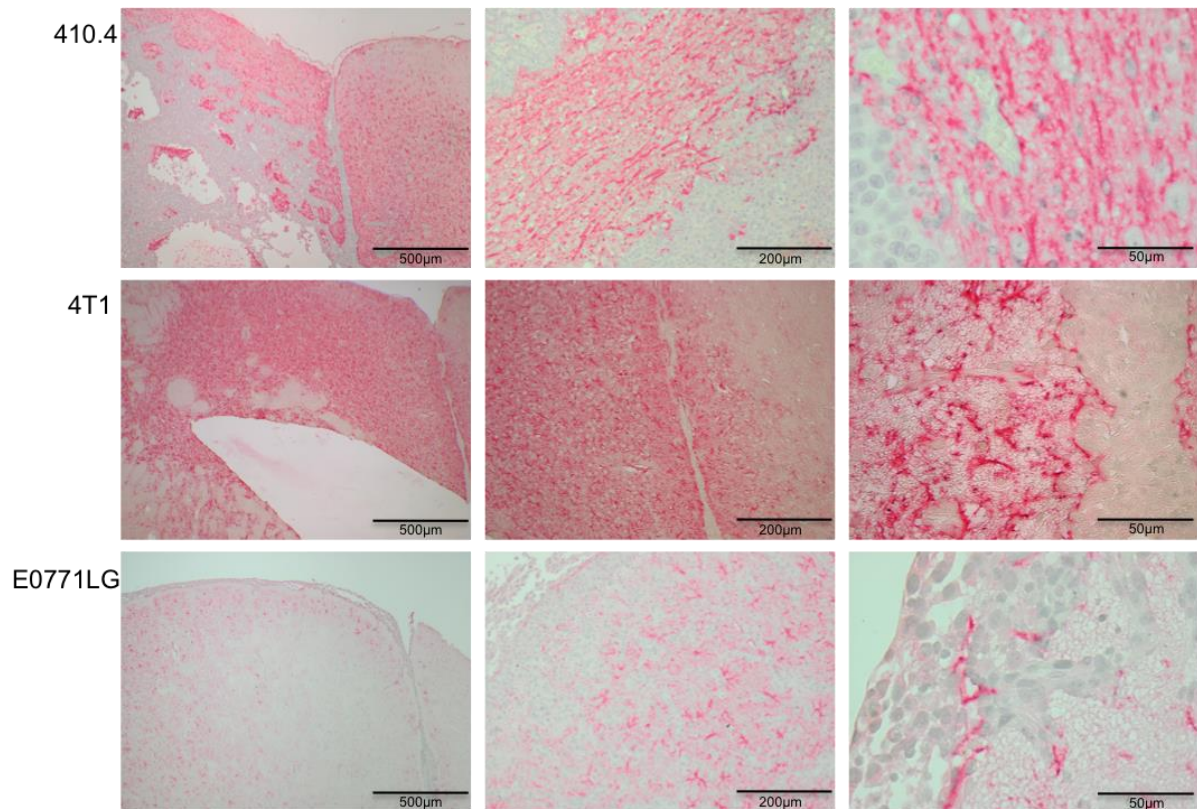
Fig 18: Identification of immune reaction after injection of cancer cell lines (GFAP).
Intracranial injection of 410.4 ($2,5x10^4$cells), 4T1 ($1x10^3$cells) and E0771LG (500cells) were immunologically tested for astrocytes activation with GFAP. GFAP staining was performed for all sections. All staining showed clearly the presence of astrocytes activation in the brain.

GFAP was detected in all slices, which indicates the presence of activated astrocytes. Interestingly, there were differences in the localisation of the astrocytes. In the sections of the injected brain with cancer cell line 410.4, the metastasis was clearly separated from the astrocytes; they were able to build a wall around the metastasis. In case of injected brains with 4T1 cancer cells, astrocytes were also found partly in the metastasis, however astrocytes were able to build a wall around the metastasis and the infiltration was similar to the infiltration of 410.4 cancer cells. Indeed, in cancer cell lines E0771LG, astrocytes were found in the metastasis and around. No wall was built by the astrocytes here. Nevertheless, in all cases activation of astrocytes was found around the metastasis but much less in the non-injected healthy side. In a next step, the microglia activation was investigated on sections stained with the macrophages/microglia marker IBA.
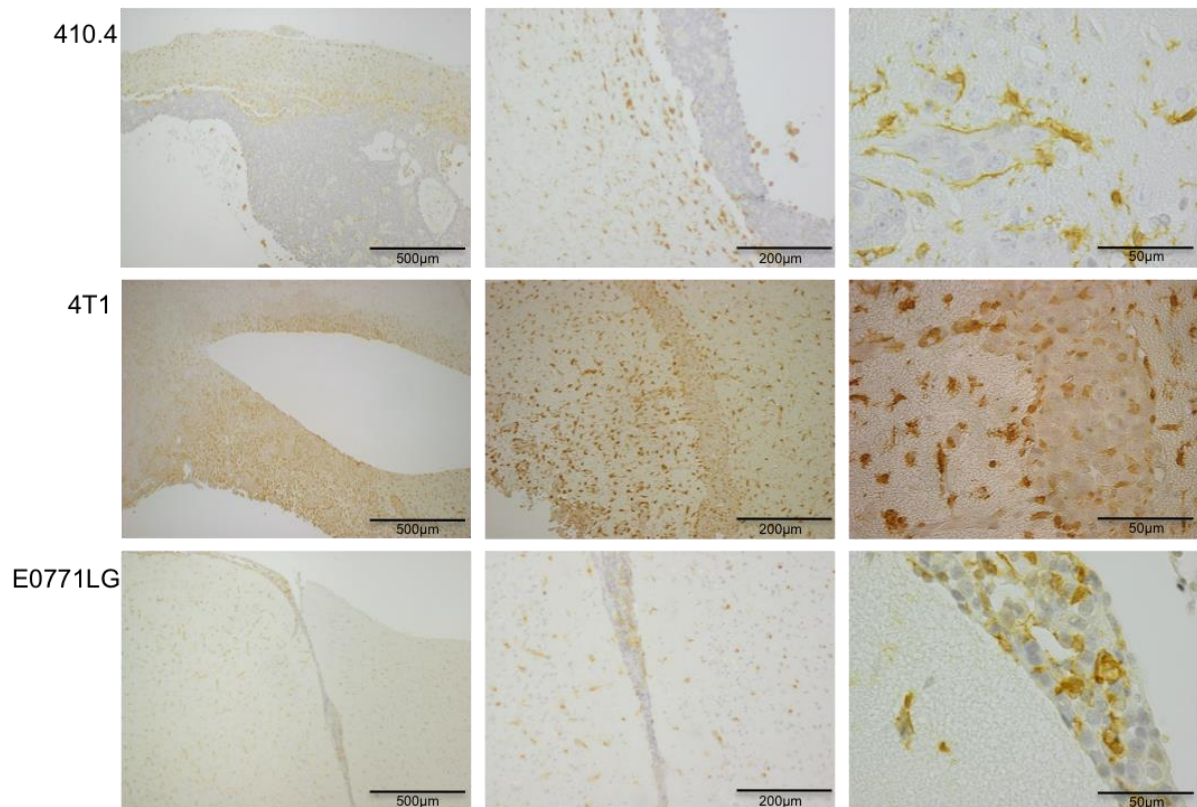
Fig 19: Identification of immune reaction after injection of cancer cell lines (IBA).
Intracranial Injection of 410.4 (2.5×10^4 cells), 4T1 (1×10^3 cells) and E0771LG (500 cells) were immunologigally tested with the macrophages/microglia marker IBA. Staining was performed for all sections. All staining showed clearly the presence of microglia activation in the brain.

All sections showed the presence of activated microglia cells/ macrophages (Fig 19). In contrast to the activation patterns of astrocytes, microglia cells were present around and between the colonized tumour cells. Furthermore, activated microglia were present in the brain, also in the healthy non-injected side. Microglia cells were found mostly close to vessels or colonized breast cancer cells.

This leads us to suggest, that the immune response to colonized cancer cells is very diverse. First, injection of different cancer cells showed different localisation patterns of activated astrocytes and microglia. In particular, the localisation of astrocytes was different. Astrocytes were able to build a wall in case of metastasis developed from 410.4 and 4T1 but not in metastasis developed from E0771LG. Second, microglia cells are located differentially: No wall was built by microglia comparable to that of astrocytes. This interesting finding will give the possibility to investigate the role of the glial response in different metastasis in more detail.

Furthermore, immunostaining with other markers such as Ki67 was performed (data not shown). Ki67 is a common marker for proliferation and is often correlated with clinical courses of cancer. Here, in all sections Ki67 was expressed (data not shown). In order to investigate differences in the proliferation of metastatic cells, Ki67 needs to be further quantified in the near future. Next, staining with CD34 (data not shown), which is established as a marker of microvascular structures in breast cancer (da Silva et al., 2009), was performed to investigate differences between metastasis. Further analyses need to be done to detect differences in the vascularisation induced by various cancer cells. In the near future, we plan to analyse these histological sections with the software "Definiens Tissue Studio", which allows us to quantify the expression levels in great detail and to reveal potential variance.

These results present previously unknown differences in colonization capacity, infiltration pattern into the adjacent brain parenchyma as well as in the glial reaction against breast cancer cells of various origins.

3.2.3 Gene expression in the metastasis and corresponding cancer cell lines

In the first part of this thesis, various gene expression markers were established and investigated in the cancer cell lines by qRT-PCR. The first two markers, Ecad and Vimentin were used to investigate the epithelial and mesenchymal character. In order to investigate these characteristics after injection of the cancer cell lines into the brain, these genes were analysed in the parts of the brain tissues containing metastases (Fig 20).
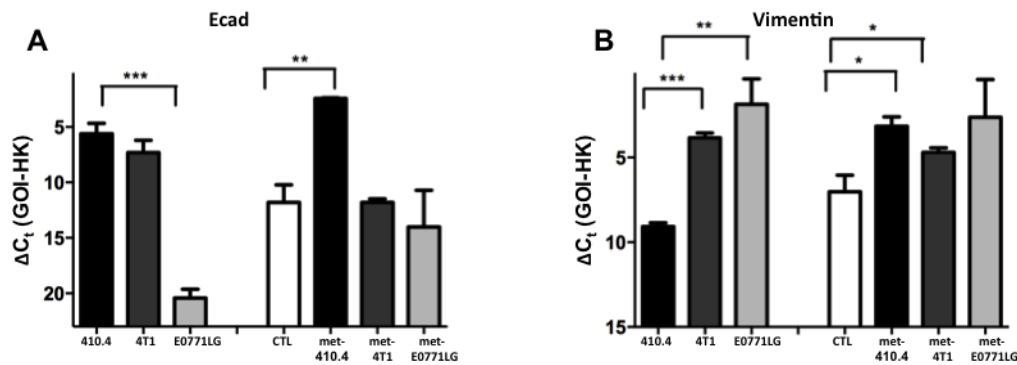
Fig 20: Gene expression of E-cadherin and Vimentin in cancer cells and metastasis.
The expression of Ecad and Vimentin was assessed by qRT-PCR from total RNA samples of the cancer cell lines 410.4, 4T1 and E0771LG, also RNA samples from control brain and developed metastases of the cell lines (GOI = gene of interest, HK = housekeeper). Error bars show SD, values, statistics sign was tested using unpaired, two tailed students t-test. **(A)** Ecad is highly expressed in the cancer cell line 410.4 and 4T1. E0771LG show lower expression of Ecad. Injected brains with ECM were used for control (CTL), metastases (=met) developed from 410.4, 4T1 and E0771LG show high level on Ecad expression, the highest significant expression was demonstrated in metastasis developed from 410.4 compare to the control **(B)** Vimentin was highly expressed in cancer cell lines 4T1 and E0771LG and lower expression level in cancer cell line 410.4. Vimentin was expressed in the control, significantly higher expression in metastases developed from 410.4 and 4T1. Vimentin was expressed in metastasis developed from E0771LG.

When comparing the cell lines by using 410.4 as a reference, Ecad was significantly decreased in the cancer cell line E0771LG ($p=<0.0001$) (Fig 20A). Metastatic samples of 410.4 expressed significantly more Ecad compare to the control tissue ($p=0.0041$) (Fig 20A). Metastasis and corresponding cancer cell line 410.4 demonstrated significant higher expression levels of Ecad. However, there are no significant changes between metastatic tissue and the cell line. Interestingly, the cancer cell line E0771LG showed low expression levels of Ecad, while the metastasis expressed higher levels of Ecad. In a next step gene expression-studies of Vimentin were performed (Fig 20B). Metastatic samples of 410.4 expressed significantly higher expression of Vimentin compared to the control tissue ($p=0.0264$) (Fig 20). When comparing the cell lines by using 410.4 as a reference, Vimentin was significantly increased in cell lines 4T1 ($p=0.0009$) and E0771LG ($p=0.01$)

(Fig 20B), and the corresponding metastasis also showed high expression levels of Vimentin, which were clearly higher than the control in all syngeneic models. Vimentin expression in metastatic samples of 4T1 was significantly higher (p=0.0246) (Fig 20B) as in control samples.

The next gene expression analysis was to confirm Cytokeratin 8 as a quantification marker for tumours developed from the injection of cancer cell lines.
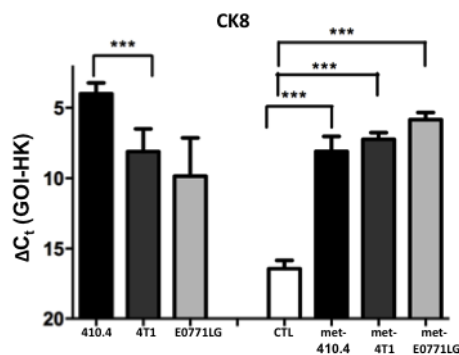
Fig 21: Gene expression of Cytokeratin 8 for quantification in cancer cells and corresponding cerebral metastatic tissue.
The expression of CK8 was assessed by qRT-PCR from total RNA samples of the cancer cell lines 410.4, 4T1 and E0771LG, also RNA samples from control brain and developed metastases of the cell lines (GOI = gene of interest, HK = housekeeper). Error bars show SD, values, statistics sign was tested using unpaired, two tailed students t-test. CK8 is expressed in all cancer cell lines. Injected brains with ECM were used for control (CTL) shown low expression on CK8. Metastases (=met) of 410.4, met of 4T1 and met of E0771LG show high levels CK8 expression.

Here, CK8 expression in the cancer cell lines was confirmed (Fig 21A) and metastasis of the cell lines 410.4, 4T1 and E0771LG show significant higher expression levels of CK8 compared to the control. When comparing the cell lines by using 410.4 as a reference, CK8 was significantly decreased in the cancer cell line 4T1 (p=0.0395) (Fig 21). In all metastatic samples, CK8 expression was significantly higher in comparison to the control sample (p=<0.0001) (Fig 21). Thus, expression of CK8 detected by qRT-PCR confirmed the findings of metastatic cells in the brain tissue and can be used for quantification. The results clearly showed that after injection of cancer cell lines, the corresponding developing metastasis can express characteristic genes – such as CK8- which can be used for quantification and are reproducible in subsequent experiments.

All these results underline that a syngeneic cerebral metastasis mouse model for the study of cancer metastasis has been established here. This model is applicable for different cancer cell lines displaying different characteristics with respect to their epithelial and

mesenchymal character and therefore metastatic potential. All cell lines were able to colonize the brain and to develop cerebral metastasis. Colonized cancer cells can be quantified with CK8. Importantly, all developed metastasis present different colonization patterns, which might be related to differences in their phenotype as well as differences in their gene expression, we investigate the epithelial and mesenchymal character of colonized cancer cell.

3.3. Application of a syngeneic cerebral metastasis mouse model

In the next part of the thesis we aimed to use the new established syngeneic cerebral colonization models of breast cancer to study the impacts on innovative therapeutics. Current treatments are of limited efficiency in the treatment of CNS metastasis because of several reasons. One is that so far very little is known about how breast cancer cells and others colonize this well protected organ and which signalling cascades orchestrate this process. Previously, others and we have demonstrated that the dysregulation of Wnt signalling is associated with cerebral metastasis in breast cancer (Chuang et al., 2013) (Klemm et al., 2011) (Smid et al., 2008) (Pukrop et al., 2010b). In general, the Wnt pathway is known to play a role in various processes in cancer initiation, proliferation and the first steps of metastasis, thus inhibitors of the Wnt pathway may be valuable for a therapeutic strategy also during colonization of the CNS. Therefore we studied a Wnt inhibitor in our established syngeneic cerebral metastasis mouse models (4T1 and EO771LG) that has already entered clinical trials.

3.3.1 Wnt expression levels of cancer cells

In order to confirm that the Wnt inhibitor LGK974 has an impact on Porcupine and therefore on Wnt secretion, cancer cell lines 410.4, 4T1 and E0771LG were tested for gene expression levels of Wnt molecules. Additionally, Porcupine expression levels were analysed in these cancer cell lines. Identification of markers, which are specifically expressed in cancer cells, could prove the inhibitory effect of LGK974 on Porcupine in later experiments.
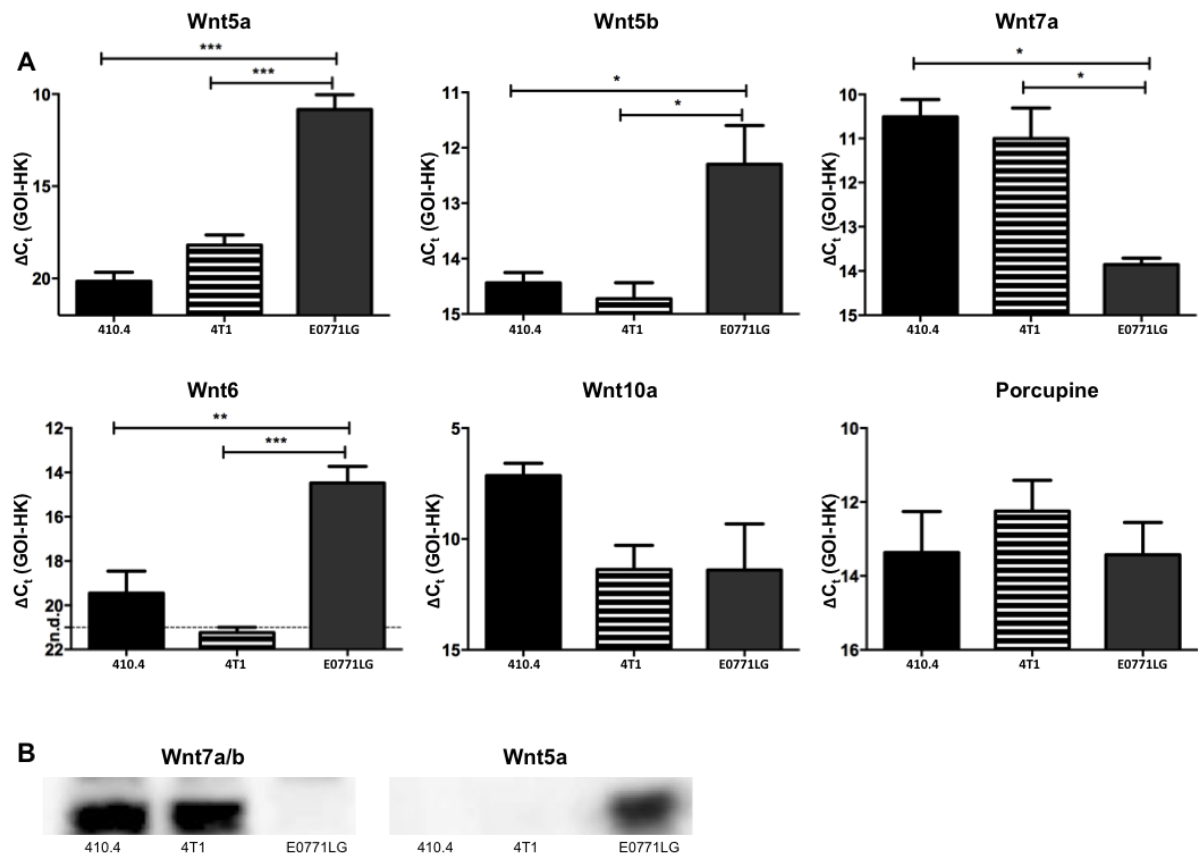
Fig 22: Gene and Protein expression level of cancer cells.
(**A**) Gene expression level of Wnt5a, Wnt5b, Wnt7a, Wnt6, Wnt10a and Porcupine in cancer cell lines 410.4 (n=3), 4T1 (n=3) and E0771LG (n=3) (GOI = gene of interest, HK = housekeeper). Error bars show SD, values, statistics sign was tested using unpaired, two tailed students t-test. Wnt5a, Wnt5b, Wnt6 was highly expressed in cancer cell line E0771LG. Wnt7a was highly expressed in cancer cell lines 410.4 and 4T1. Wnt10 was expressed in cancer cell line 410.4. Porcupine was expressed in all tested cancer cell lines. (**B**) Protein expression levels of Wnt7a/b and Wnt5a in cancer cell lines 410.4, 4T1 and E0771LG. 410.4 and 4T1 show high expression of Wnt7a/b, Wnt5a was expressed in E0771LG.

Wnt genes and Wnt pathway components were screened, by using the NanoString technology (http://www.nanostring.com) (data not shown). Out of the 105 tested genes in the cancer cell line E0771LG Wnt5a, Wnt5b and were highly expressed and therefore selected for further investigations. In order to investigate expression levels of Wnt5a, Wnt5b, Wnt7a, Wnt6, Wnt10a and Porcupine qRT-PCR were performed (Fig 22A). Wnt5a was significantly higher expressed in the cancer cell line E0771LG compared to the cancer cell lines 410.4 (p=0.0003) and 4T1 (p=0.0009) (Fig 22A). In contrast, Wnt7a was highly expressed in both 410.4 (p=0.0024) and 4T1 (p=0.0139) cancer cell lines (Fig 22A) compared to the cancer cell line E0771LG. This significant difference was confirmed on the protein level (Fig 22B). Furthermore, the potential therapeutic target Porcupine was

expressed in all tested cancer cell lines. These results provide the basis for targeting Wnt signalling in the above described established syngeneic cerebral metastasis models of these cell lines by inhibition of Porcupine.

3.3.2 Investigation of treatment application

In order to investigate the effect of the Porcupine inhibitor LGK974 on cellular viability, MTT measurements were performed with various cancer cells and different LGK974 concentrations (Fig 23A): Additionally, some concentrations of LGK974 were tested in xCelligence measurements (Fig 23B). Here, cells were stimulated for 24hours before the xCelligence measurements (pre-treatment). Based on these testing's we used 2,5µM and 5µM LGK974 in further functional tests.
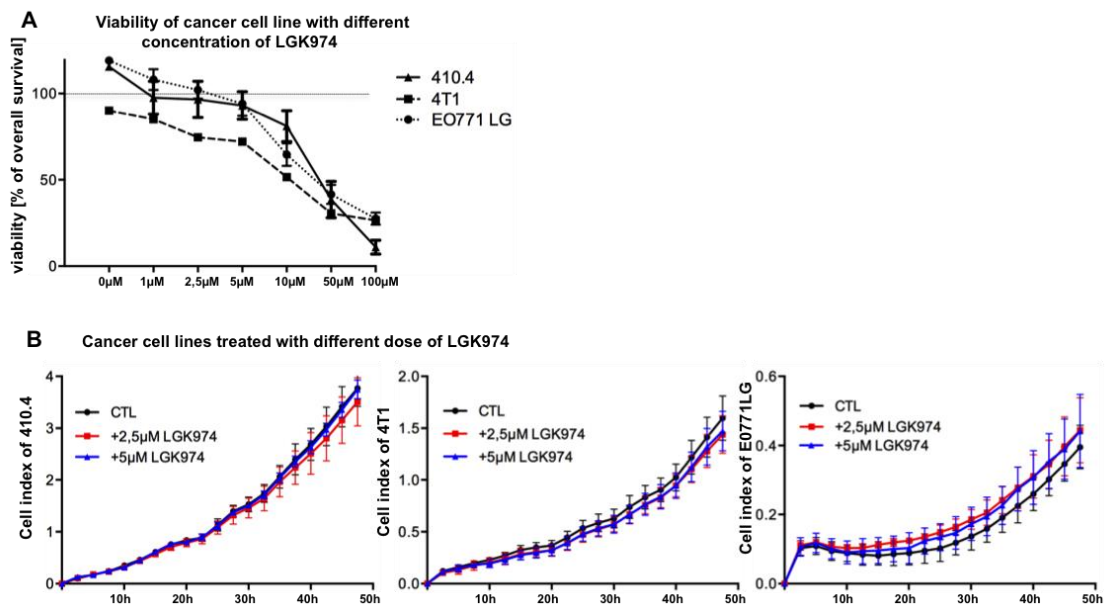
Fig 23: Viability of cancer cells after treatment with different doses of LGK974.
(A) MTT assay LGK974 treated for 96h of 410.4 (n=3), 4T1 (n=3) and E0771LG (n=3). Tested dose of LGK974 between 1µM and 100µM (0µM for control) and **(B)** 2,5µM and 5µM for all cell lines, xCelligence measurements of 410.4 (n=3), 4T1 (n=3) and E0771LG (n=3) pre-treated for 24h and treated for 48h with LGK974.

The MTT results of the proliferation assay (data not shown) demonstrated, that an inhibitory effect of LGK974 was increased, when cancer cells were pre-stimulated with LGK974, without a toxic effect on these cells. Based on viability (Fig 23A) and proliferation tests (Fig 23B), an effective dose of 5µM of LGK974 for further experiments

was investigated. Moreover, a pre-treatment for 24hours with an LGK974 dose of 5μM was determined to be optimal.

Next, to confirm the effects of Porcupine inhibition on the Wnt-release of the LGK974 treated cells, cancer cells were treated with 2,5μM, 5μM and 10μM of the Porcupine inhibitor for 24h. Untreated cancer cell lines served as controls. A concentration of 5μM was used to test the time dependent effect of the Porcupine inhibitor LGK974 and cancer cells were stimulated for 0, 4, 12, 24 and 48hours. The control was the untreated cancer cell line at the corresponding time. To investigate the inhibitory effect of LGK974 on Wnt secretion, expression levels of Wnt7a/b and Wnt5a were analysed in the whole cell lysates of the treated cells.
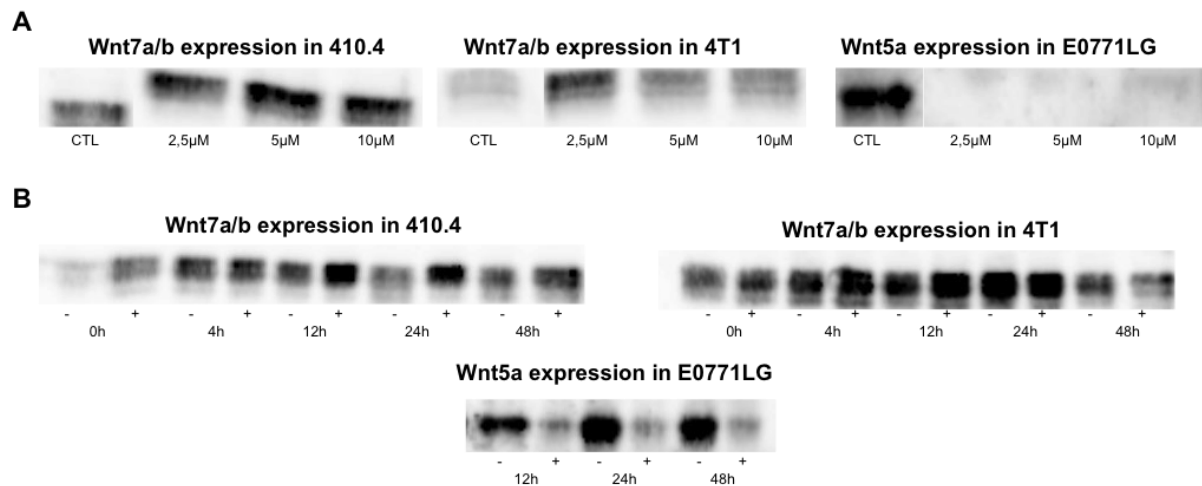
Fig 24: Effect of LGK974 on protein expression of Wnt7a/b and Wnt5a in cancer cells.
(A) Westernblot: Comparison Wnt7a/b or Wnt5a expression with different concentration of LGK974 on cancer cells lines to the additional untreated control cell line (CTL). **(B)** Comparison of Wnt7a/b or Wnt5a expression with a concentration of 5μM LGK974 of different time points on cancer cell lines.

Wnt5a expression was clearly decreased in E0771LG after LGK974 treatment; however, interestingly, the inhibitory effect of LGK974 on protein level seemed to cause an enrichment of the protein in 410.4 and 4T1 cancer cell (Fig 24A). These results were confirmed with the time dependent treatment strategy, when cancer cells were pre-stimulated 24hours with 5μM LGK974 and afterwards also stimulated with the same concentration of LGK974. After 24hours and 48hours we detected the strongest effect of LGK974. Wnt7a/b was enriched in the cancer cells 410.4 and 4T1 treated with LGK974.

Thus, the effect of LGK974 was clearly shown, and the Porcupine inhibitor influenced Wnt secretion as expected.

Afterwards, we investigated the invasion capacity of various breast cancer cells after treatment with these two LGK974 concentrations and the stimulation for 24hours before. The results are demonstrated in Figure 25.
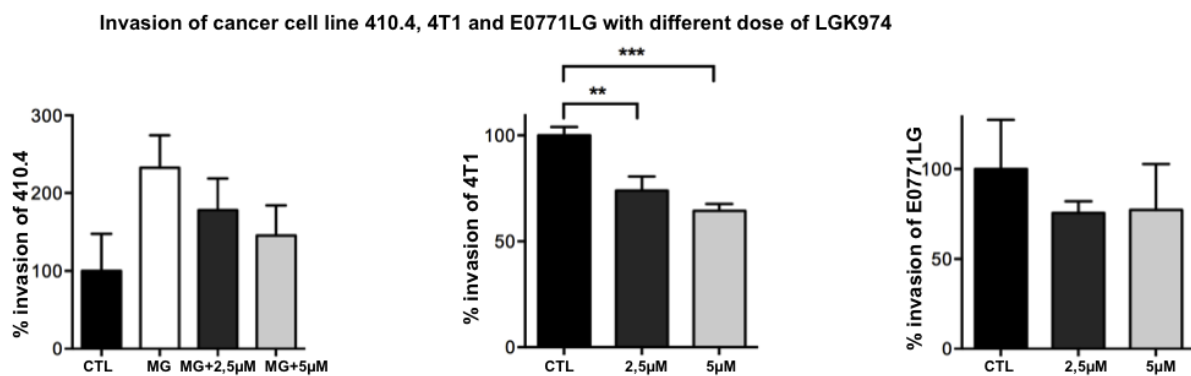
Fig 25: Invasion of cancer cells after treatment with different doses of LGK974.
Invasion assay of 410.4 were performed with microglia (MG) (n=3) to increase invasion of cell line 410.4 and pre-treated 24h and treated 48h with 2,5μM and 5μM LGK974, 4T1 (n=3) and E0771LG (n=3) were pre-treated 24h and treated 48h with 2,5μM and 5μM LGK974.

The expected inhibitory effect was detected in the 4T1 cell line with LGK974 (Fig 25). LGK974 were able to decrease 4T1 invasion in a dose-dependent manner (**$p<0,01$, ***$p< 0,001$). Surprisingly, LGK974 did not significantly inhibit invasion of the cell lines 410.4 or E0771LG. These results indicate that additional activities of the inhibitor beyond the Wnt pathway are possible. Therefore, further experiments were performed to prove this indication and to increase the N numbers. However, LGK974 was effective at a concentration of 5μM. To prove whether this effect is an inhibitory effect of the Wnt pathway needs to be investigated.

3.3.3 CAM assay with LGK974 treatment

In order to confirm the inhibitory effect of LGK974 on Wnt signalling and therefore an effect on colonization of tumour cells independently, Chorioallantoic Membrane Assays (CAM) were performed (Murphy, 1913). Cancer cells or cancer cells pre-treated for 24

hours with LGK974 were placed on the developing embryo of a chicken egg, on a special membrane. In case of 410.4, 3×10^6 cells were re-suspended in 40µl ECM and then placed directly on the membrane. Additionally $1x10^5$ of 4T1 cells and $1x10^4$ E0771LG cells respectively were re-suspended in 40µl ECM and placed on the membrane. In this step, the different cancer cells or cancer cells pre-treated with LGK974 were placed on the membrane. Afterwards, eggs were covered with Leukosilk S and incubated for another seven days. Then, Leukosilk was removed and the membranes with the tumours were prepared and analysed. Tissues were fixed in PFA and sectioned. HE staining was performed in order to locate the tumour on the membrane.
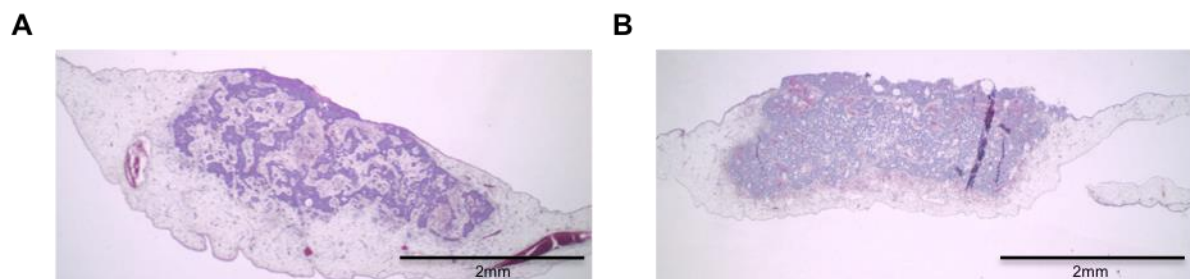
Fig 26: Effect of LGK974 by CAM assay.
(A) Example for CAM assays, tumours of 410.4 cancer cells are shown (control) and (B) tumours of LGK974 treated 410.4 cancer cells.

The histological sections of the CAM assays indicate differences between the tumours of the control group compared to the treatment group. A typical example is shown in Figure 26. The amount of the tumour cells in the control group compared to the tumour of the treatment group was decreased. Also, in most cases tumours of the treatment group seemed significantly enlarged. It can be speculated, that in cancer cells stimulated with LGK974 tumour cell colonization might be increased. In order to prove this finding, all sections were scanned by Image Scan and analysed with the basic software Image Scope. The tumour sizes of each scanned section were measured and tumours of the control group were compared with tumours of the treatment group.
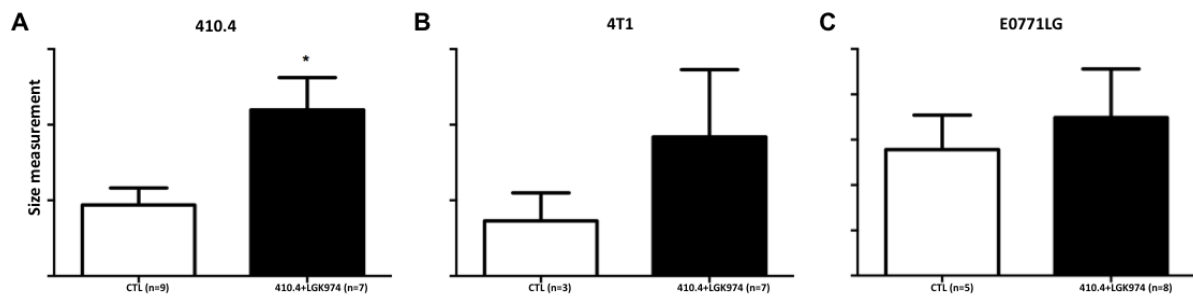
Fig 27: Tumour enlargement by CAM assay.
(A) CAM assays of cancer cell lines 410.4, **(B)** 4T1 and **(C)** E0771LG were shown. All tumour sizes of the control group were compared to tumour sizes of the treatment group. Error bars show SD, values, statistics sign was tested using unpaired, two tailed students t-test.

Quantitative analysis of the HE stained sections revealed that tumours derived from the cancer cell line 410.4 treated with LGK974 (n=7) were significantly increased compare to the control group (n=9) (p=0.0149) (Fig 27A). This result verified the suggestion that the Porcupine inhibitor LGK974 support tumour cell colonization. However, tumours derived from cancer cell line 4T1 treated with LGK974 (n=7) were not significantly different in comparison to the control group (n=3) (p=0.4297). Also, the tumours derived from E0771LG (n=8) were not significant different to the control group (n=5) (p=0.5019).

The effect of LGK974 needs to be clarified for a better understanding of this process. However, tumours developed from cancer cell line 4T1 or E0771LG treated with LGK974 show no significant differences compared to the control group (Fig 27B and C). In case of 4T1, the control group contained only a low number of samples (n=3) (Fig 27B). In order to investigate and prove the results, the number of CAM assays need to be increased and quantitative analyses of the tumour size need to be further improved to measure the exact sizes of the whole tumours. Furthermore, proliferation and angiogenesis need to be investigated; other histological staining for such markers will properly reveal further differences between these tumours in future studies.

3.3.4 *In vivo* model with LGK974 treatment

The established syngeneic mouse models for cerebral colonization of 4T1 and EO771LG were used to transfer the *in vitro* findings to an *in vivo* model.

First, in order to use a non-toxic effective dose of LGK974, based on the study of Liu et al., we used a dose of 3mg/kg body weight (Liu et al., 2013b). Next, the application

method of LGK974 was tested in a pre-study as part of this work. These results were used to design a schedule (Fig 28). In order to do so, behaviour test were performed and mice were pre-treated with 3mg/kg body weight for five days with LGK974 (treatment group) or H_2O (control group). For the application of LGK974, or H_2O, gavages were used. Afterwards, mice were injected intracranially with the respective cancer cell lines. Mice were not treated on the day of surgery, or the day following surgery. Mice were weighed on the day of surgery and on recovery days, the day following surgery was the recovery day. Then, H_2O or LGK974 was applied for another 35 days or until neurological symptoms became apparent. The weight of each mouse was measured daily. For a control, mice were pre-treated and treated with the same volume of H_2O compared to LGK974, which was 50-60µl depending on the weight of the mouse.
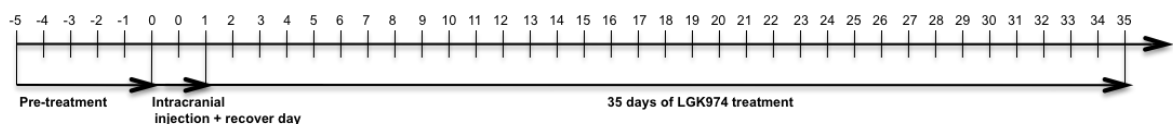
Fig 28: Schedule of experiment performance.
Day -5 to -1 (five days) pre-treatment with LGK974 or H_2O was performed. Cancer cells were intracranially injected on day 0. The day after surgery was the recovery day. Day 1 to day 35 (35days) mice were treated with H_2O (control group) or LGK974 (treatment group), followed by the observation of survived mice.

First BalbC mice were pre-treated with 3mg/kg body weight LGK974 in the treatment group and with H_2O additional for the control group over XY days (d-5 to d-1 before stereotactical injection d0). At day 0, mice were injected intracranially with $1x10^3$ cancer cells of 4T1. In a second experiment, mice were injected with a lower number of the cancer cell line 4T1 ($1x10^2$). The survival of these mice is shown in Figure 28A-C as a Kaplan Meier diagram. In the following experiments (Fig 29 and Fig 30), H_2O and LGK974 were applied daily for 35days accompanied with daily observation and weight measurements. Hanging wire and Rotarod test were performed as an additional indicator for developing cerebral metastasis. Mice with abnormalities in motor function or neuronal deficiencies as well as a weight loss of >20% were dissected immediately. Furthermore, every mouse was listed by age, injection date and dissection date and survival curves were calculated.
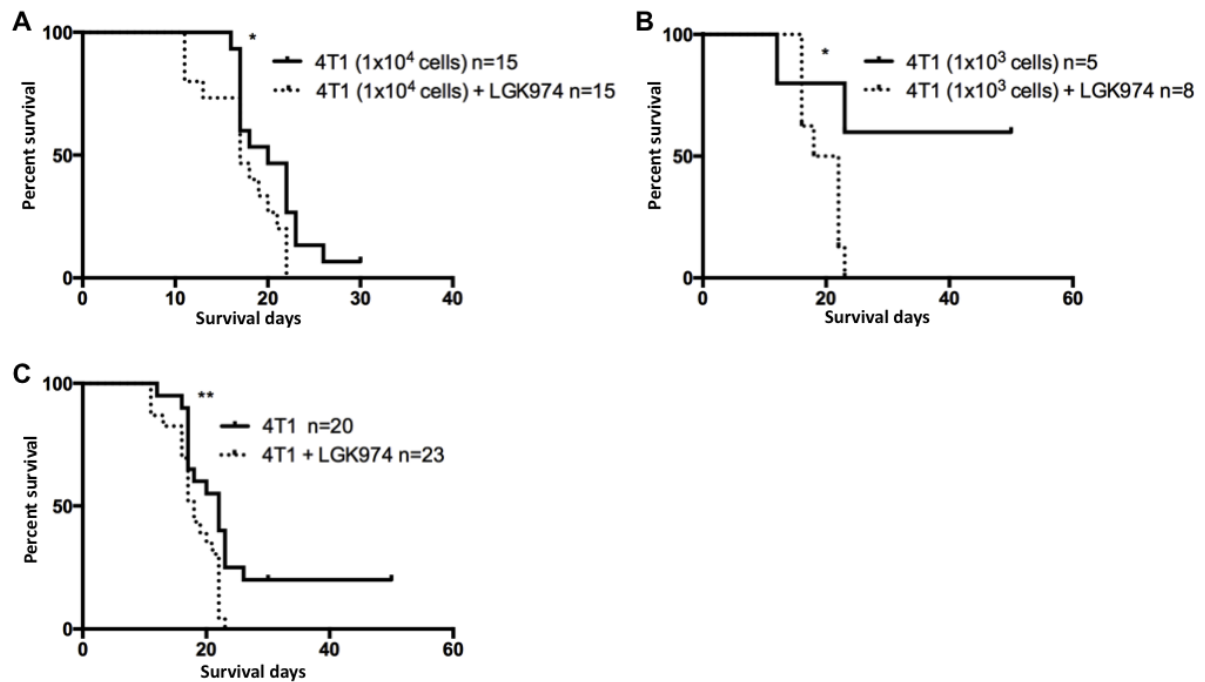
Fig 29: Kaplan Meier surviving curves after cancer cell line 4T1 injection and LGK974 treatment.
(**A**) Survival curves of $1x10^4$ or (**B**) $1x10^3$ injected 4T1 cancer cells with LGK974 treatment or additional in controls. (**C**) Survival curve of both experiments together ((**A**)+(**B**)) to increase the numbers of animals.

After the injection of $1x10^4$ cancer cells of 4T1, all mice in the LGK974 treatment group (n=15) developed metastasis that were significantly more aggressive than in the control group (n=15) based on both size of the metastasis and survival of the mice (p=0.0334) (Fig 29A). Even after the injection of $1x10^3$ cancer cells of 4T1, all mice treated with LGK974 (n=8) developed metastasis within 21days (Fig 29B). In the control group (n=5) mice developed metastasis on average later and one mouse even survived until the end of the experiment. Differences between the treatment group and the untreated control group were significant (p=0.0292). The OS of mice injected with cancer cell line 4T1 and treated with LGK974 of both experiments together (Fig 29A and 29B) was significantly decreased compare to the control groups (p=0.0072) (Fig 29C).

The next experiment was performed with the cancer cell line E0771LG. Here, C57BL/6 mice were pre-treated for five days with H_2O or 3mg/kg body weight LGK974 were injected intracranially with 250 cancer cells of E0771LG (Fig 30).
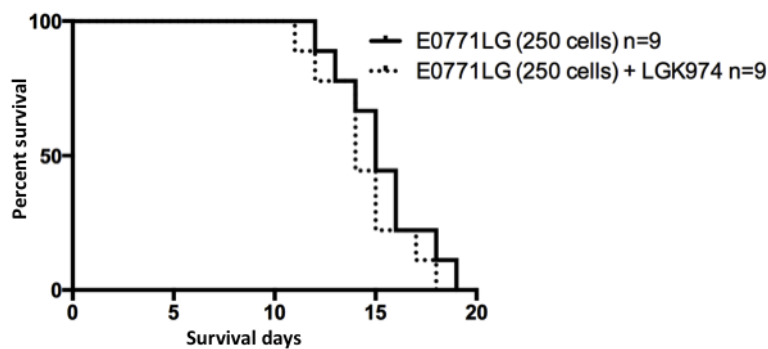
Fig 30: Kaplan Meier surviving curves after E0771LG cancer cell injection and LGK974 treatment.
Survival curve of 250 injected E0771LG cancer cells with LGK974 treated or additional control (n=9 in control and treatment group).

After the injection of 250 cancer cells of E0771LG, all mice in the LGK974 treatment group (n=9) developed metastasis. Also, all mice in the control group (n=9) development metastasis. Unfortunately, there was no significant difference on survival between the treatment and control group (p=0.2425) (Fig 30). These results did not confirm the idea, that LGK974 underlines the results of the CAM assays and do not prevent tumour cell colonization, despite, *in vitro* studies showed an inhibitory effect of LGK974 on Wnt signalling.

To test if colonization of the tumour cell resulting in metastasis were different, tissue sectioning and HE staining were performed next.
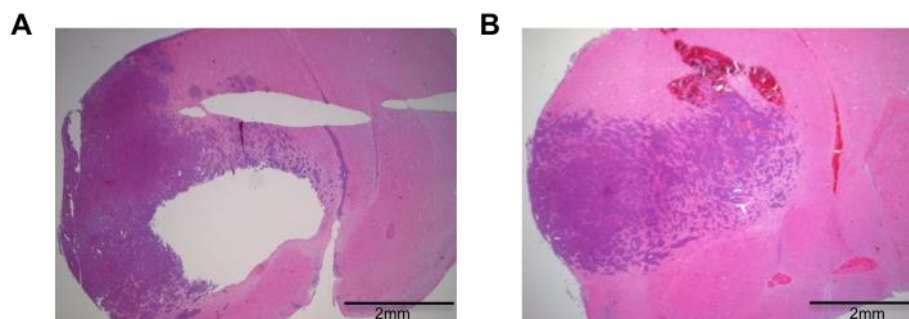
Fig 31: HE staining on control vs. LGK974 treatment sections.
Representative examples of developed **(A)** metastases after injection of cancer cell line 4T1 vs **(B)** 4T1 with LGK974 treatment.

HE staining was performed on sections, however, no obvious differences in the metastasis could be detected microscopically at first glance. Therefore the effect of the Porcupine inhibitor in terms of limitation of survival *in vivo* could not be investigated with HE staining.

Remarkably, the injection of the cancer cell line E0771LG and treatment of LGK974 had no effect on the survival (Fig 30). After HE staining of sections derived from respective metastasis also no obvious differences were detectable. The reason for this might be a different growth rate and colonization behaviour of tumour cells resulting in metastasis developed from E0771LG cell line compared to metastasis developed from 4T1 cell line and suggests that LKG974 has no effect on fast colonizing tumour cells.

To gain more information about the role of LGK974 on Wnt signalling and colonization of tumour cells, we analysed selected brain tissue from mice injected with 4T1 cancer cells for their gene expression levels of EMT markers and their Wnt profile. First, to characterise the epithial charcater of metastasis, Ecad and Vimentin were analysed by qRT-PCR. Brains were separated into two halves, the injected side of the brain (i.) and the non- injected side (n.i.). Both sides were compared to each other and the control group was compared to the treatment group (Fig 32).

In this study it was shown that indeed LGK974 inhibits Porcupine, which leads to changes in Wnt secretion (Fig 24). Consequently, gene analyses on the Wnt pathway were also performed. The injected (n=12) and the non- injected sides (n=12) of the control group were compared and the injected (n=12) and the non- injected (n=12) sides of the LGK974 treatment group were compared (Fig 32). Both, the injected and the non- injected hemispheres of each group were then compared to the respective other group, either LGK974 treatment group or non-treatment control group. Based on previous analyses (3.3.1), we measured the Wnt family members, which were expressed in the breast cancer cell lines, Wnt5a, Wnt5b, Wnt7a, Wnt6 and Wnt10a as well as the target of the LGK inhibitor, Porcupine.
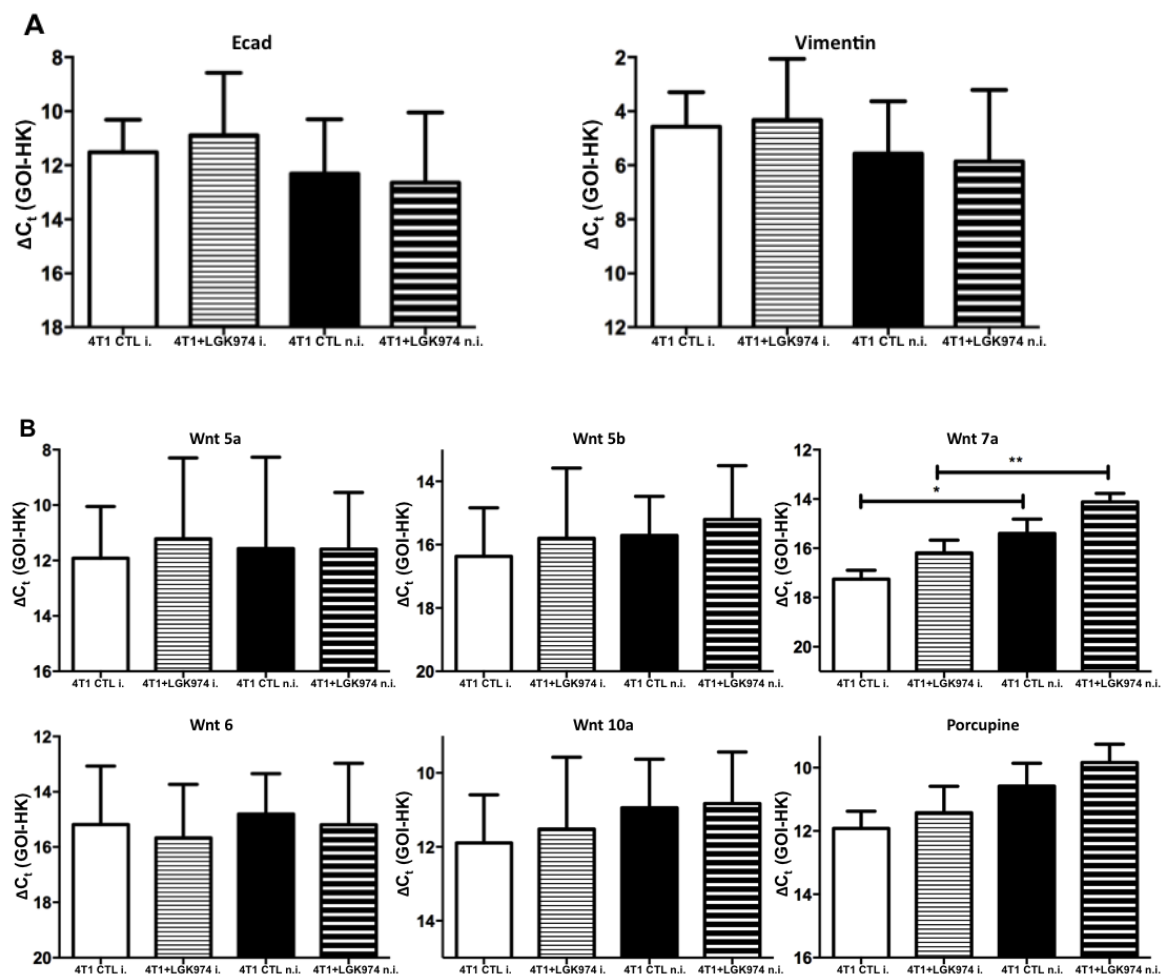
Fig 32: Analyses of developed metastasis from cancer cell line 4T1.
(A) Ecad and Vimentin were evaluated to prove changes in epithelial or mesenchymal character of the cell line in metastasis (GOI = gene of interest, HK = housekeeper). **(B)** Wnt profile was used to detect eventual changes in the Wnt profile after LGK974 treatment (GOI = gene of interest, HK = housekeeper). Error bars show SD, values, statistics sign was tested using unpaired, two tailed students t-test. In all, expression of Ecad or Vimentin and Wnt analyses, 4T1 injected brains (4T1 CTL i.) were compared to 4T1 injected brains with LGK974 (4T1+LGK974 i.) treatment. Additionally, 4T1 brain tissues of the non- injected side (4T1 CTL n.i.) were compared to 4T1 brain tissues with LGK974 treatment of the non- injected side (4T1+LGK974 n.i.). The LGK974 treatment group (4T1+LGK974 i/ni) were compared with the control group (CTL i/ni).

These experiments did not support the notion that metastasis derived from the cancer cell line 4T1 - that had been treated with LGK974 - underwent EMT and MET. No differences in the epithelial (Ecad) or mesenchymal (Vimentin) character of the metastasis developed from 4T1 cell line were detectable when the treatment and the control groups were compared (Fig 32A). Furthermore, the inhibition of LKG974 on Porcupine and Wnt secretion could not be confirmed in the metastasis.

In the next step we investigated various Wnt ligands to test if they showed changes in the Wnt profil after the treatment with LGK974. We were not able to detect any significant differences in expression levels of Wnt5a, Wnt5b, Wnt6 or Wnt10a in the issue samples (Fig 32B). However, Wnt7a was significantly increased in the non- injected side after LGK974 treatment in comparison to the injected side (p=0.0021) (Fig 32B). Also, Wnt7a was increased in the non- injected side of the control group compare to the injected side of this group (p=0.0108) (Fig 32B). The expression of Wnt7a was increased in the injected side of the treatment group compared to the injected side of the control group, however the difference was not statistically significant (p=0.1087), (Fig 32B). Also, the expression of Wnt7a was not significantly increased in the non- injected side of the treatment group compared to the non- injected side of the control group (p=0.0050) (Fig 32B). Interestingly, the cancer cell line 4T1 expresses high levels of Wnt7a. However, metastases developed from 4T1 showed reduced expression levels of Wnt7a. Nevertheless, metastasis developed within 4T1 treatment group showed significant differences in their Wnt7a expression levels between the non- injected and the injected sides. The Wnt7a expression was significantly reduced in the injected side compared to the non- injected side, in both, treatment group and control group. We demonstrate that LGK974 might have an effect on Wnt7a expression by inhibiting Porcupine in metastasis derived from the 4T1 cell line or changing the composition of the metastatic cells and their microenvironment. To further elaborate on this interesting hypothesis and also to investigate EMT and MET on tumour cell colonization in greater detail, other markers for EMT and MET, e.g. those for specific transcriptions factors need to be established.

Unexpectedly, the survival of the LGK974-treatment group was significantly decreased compared to the control group in the 4T1 trials. Therefore, it was suggested, that LGK974 might induce EMT and MET thereby triggering tumour cell colonization and boosting the metastatic potential of these cells. However, Ecad and Vimentin were not regulated as indicators for EMT or MET. Therefore, we could not demonstrate that LGK974 induced EMT and MET yet.

Suggestions that LGK974 impacts on Wnt signalling and that Wnt signalling could induce transcriptional changes, thereby driving EMT and MET need to be followed up. Consequently, additional EMT and MET markers need to be investigated. Therefore, we stimulated the cancer cell line 4T1 for 24hour and 48hours with LGK974. The unstimulated cancer cell line 4T1 was used as a control (Fig 33).
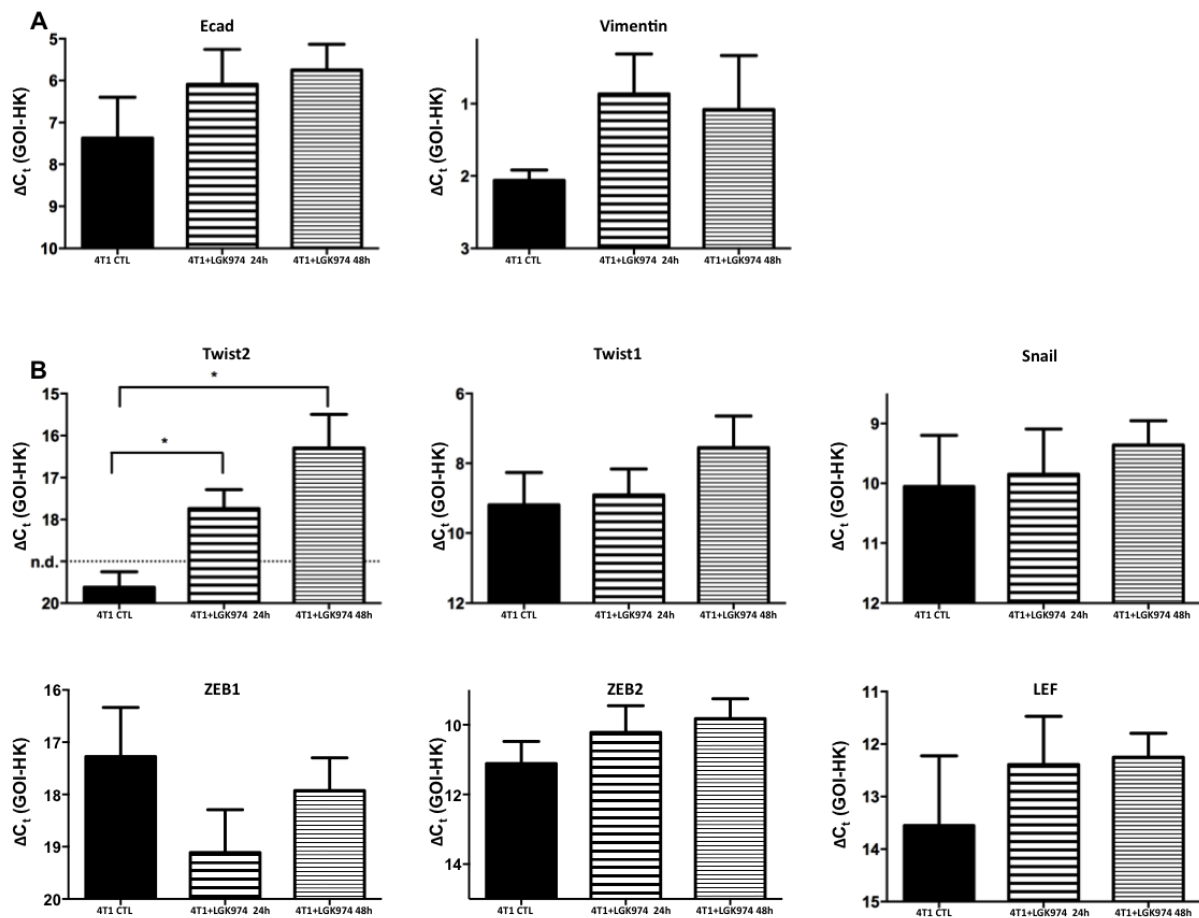
Fig 33: Expression level of EMT and MET markers of cancer cells +/- LGK974.
(**A**) Ecad and Vimentin and (**B**) Twist2, Twist1, Snail, ZEB1, ZEB2 and expression of cancer cell line 4T1, 4T1 treated for 24hours with LGK974 and 4T1 treated for 48hours with LGK974 (GOI = gene of interest, HK = housekeeper). Error bars show SD, values, statistics sign was tested using unpaired, two tailed students t-test.

After stimulating the cancer cell line 4T1 with LGK974, there were no significant differences in the epithelial (Ecad) or mesenchymal (Vimentin) characters of the 4T1 cell line treated with LGK974 compared to the control (Fig 33A). However, the expression of Twist2 was significantly increased, compared to the untreated control (Fig 33B). Furthermore, the stimulation with LGK974 for 48hours (p=0.0196) was more effective compared to that for 24hours (p=0.0329) revealing a time dependent effect of the treatment. However, for all other tested transcription factors relevant for EMT and MET, no significant differences are shown when 4T1 was stimulated with LGK974. This experiment needs to be repeated using higher N number and more time point's stimulation. However, the preliminary data show significant differences in the expression of the transcription factor Twist2 after stimulation with LGK974 and the other data indicate the

possibility that the cancer cell line 4T1 underwent EMT and MET after treatment with LGK974. In the future gene expression analyses of the brain tissues from LGK974-treated mice might confirm this suggestion.

In a brief summary, we found that the brain microenvironment reacts against the colonization of secondary malignancies, which has consequences on therapeutic strategies such as the application of drugs and the precise manipulation of important cancer pathways.

3.3.5 *In vivo* model with LPS

When we realized that interfering with the Wnt signalling by inhibiting Porcupine had unexpected treatment effects we searched for alternative treatment strategies. In our previous *in vitro* coculture-experiments we found that switching microglia into an acute inflammatory phenotype lead to improved treatment results. In brief, microglia-induced invasion was significantly reduced by treatment with Lipopolysaccharide (LPS) in modified Boyden chamber experiments (Pukrop et al., 2010b). To further elaborate on these *in vitro* findings the established syngeneic cerebral metastasis mouse model is ideal. First steps into this direction have already been performed as part of this study. Brain tissue from previous experiments - were we tested the right amount of cells for the metastatic potential (3.2.1) - was used for the gene analysis of immune-related markers. To investigate the impact of the immune response on tumour cell colonization, GFAP, CSF1 and CSFR1 were used as markers for inflammation (Fig 34B-D). Additionally, CK8 was used as a marker for colonized tumour cells (Fig 34A). In case of the control group, ECM and medium were injected, and animals were sacrificed at the same time the last mouse of the group with injected cancer cells was sacrificed. Injected and non- injected side of the control or injected cancer cell group were compared. Additionally, the injected side of the control was compared to the injected side of the cancer cell group. Also, the non- injected side of the control group was compared to the non- injected side of the cancer cell group.
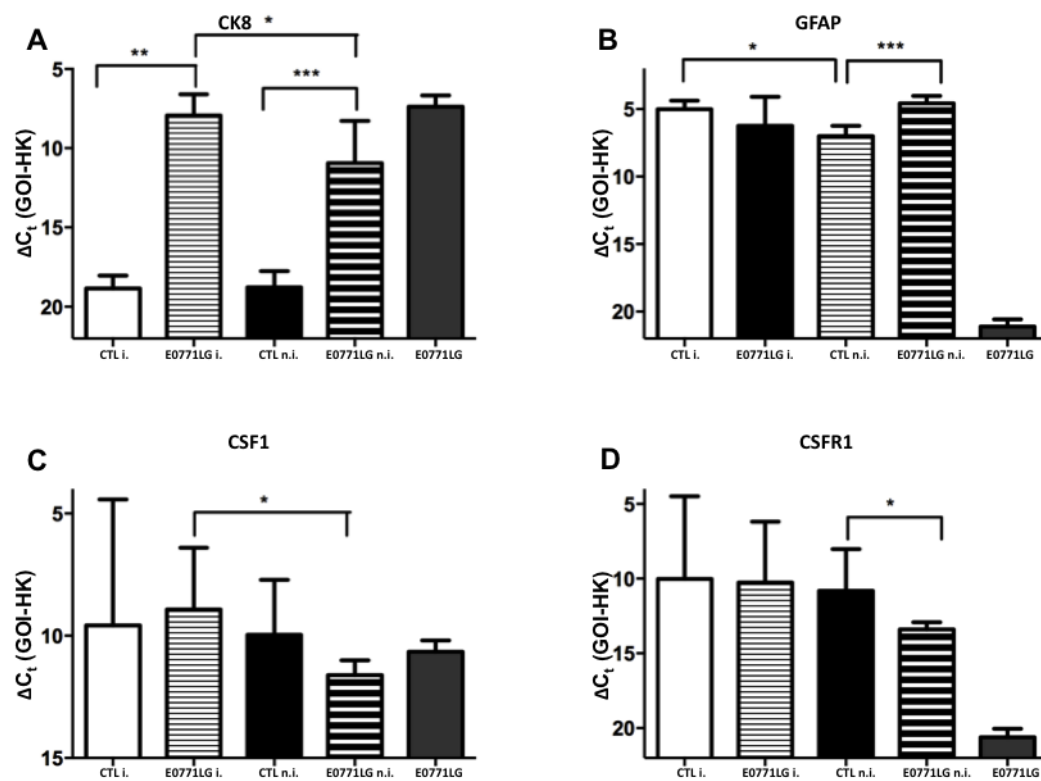
Fig 34: Analyses of developed metastasis from cancer cell line E0771LG.
(A-D) The gene analysis was performed with three control samples and seven samples of the injected cancer cell line. Injected side of control (CTL i.) was compared to the control non- injected side (CTL n.i.). Injected side with E0771LG (E0771LG i.) was compared to the non- injected side of E0771LG (E0771LG n.i.). Control group was compared E0771LG group. Cancer cell line E0771LG was used and compared with the tissue (GOI = gene of interest, HK = housekeeper). Error bars show SD, values, statistics sign was tested using unpaired, two tailed students t-test. **(A)** CK8 was evaluated to prove the presence of colonized tumour cells. **(B)** GFAP as a marker for astrocytes was used and CSF1 **(C)** and CSFR1 **(D)** were used as marker for microglia cells.

Consistent with the notion that colonized tumour cells express CK8 compared to the normal brain tissue, CK8 was significantly increased after cancer cell injection compared to controls (p=0.0014), (Fig 34A). The control, which was injected with ECM/medium showed significantly lower amounts of CK8. Interestingly, also the non- injected side of the cancer cell injected group, showed high levels of CK8, which was significantly increased compare to the non- injected side of the control group (p=<0.0001), (Fig 34A). However, the injected side showed significantly more CK8 expression as compared to the non- injected side (p=0.0206), (Fig 34A). The latter finding further underlined the previous finding that cells can disseminate also to the other, non-injected hemisphere

Moreover, there was a significant increase of GFAP after the injection of E0771LG on the non-injected side in comparison to the non- injected side of the control (p=<0.0001), (Fig

34B). GFAP was significantly increased in the injected side of the control compared to the non- injected side (p=0.0258). GFAP was also highly expressed also in control brain tissue. Possibly, because of the high expression levels of GFAP in these samples, small differences in gene expression could not be discerned. However when we looked at the expression levels of CSF1, differences between the cancer cell-injected side and the non-cancer cell-injected side were significant (p=0.0178), (Fig 34C). These results suggest that the injection of cancer cells activates microglia. However, analyses of CSFR1 could not confirm this conclusion (Fig 34D). Here, significant differences were only shown between the non- injected side of the control group and the non- injected side of the cancer-cell injected group, but not between the injected sides of both groups. These results could not demonstrate significant differences on the presence of microglia or astrocytes between control group and the cancer cell-injected group and further experiments are necessary including higher N numbers. However, sections stained against markers for microglia and astrocytes clearly show the presence and localisation of microglia cells (Fig 35A) or astrocytes (Fig 35B). It might be interesting to monitor the activation state of microglia, perhaps by having a closer look at their morphological appearance.
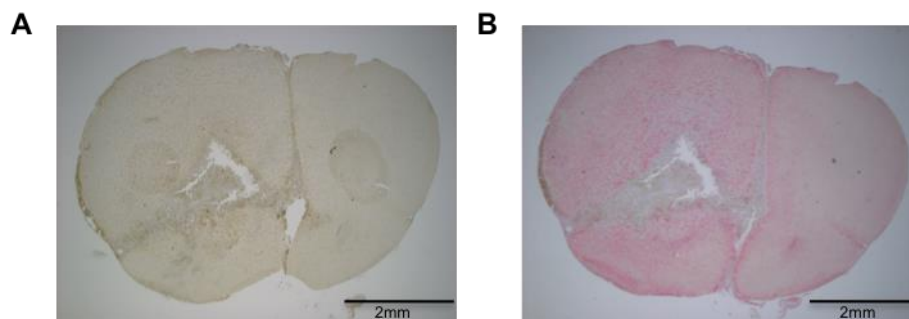
Fig 35: Identification of immune reaction after injection of cancer cell line E0771LG.
500 cells of cancer cell line E0771LG injected in the brain were immunologigally labelled with the macrophages/microglia marker IBA **(A)** and **(B)** with the astrocytes marker GFAP. The staining clearly showed the presence of microglia and astrocytes activation in the brain. Left side of the hemisphere=injected side, right side of the hemisphere= non- injected side.

In comparison to the non- injected side, the injected side of these brains show a strong increased of activated microglia cells and astrocytes. Collected control brains, which were injected with ECM and medium alone, showed no expression of the immuno-markers (data not shown). It might be possible to use the stained sections in Fig 35 at higher magnification to analyse a possible morphologically detectable interaction between colonized tumour cells and immune cells in the future.

The effect of LPS had been tested in our group before and a dose of 1μg/μl was determined to be non-toxic for the E0771LG cancer cell line. These results can now be confirmed in the background of this syngeneic mouse model, using - in a first step - the E0771LG cancer cell line.

Mice were injected intracranially with an amount of 500 E0771LG cancer cells as described before. For the treatment group 1μl of LPS was added to the mix of cells/medium/ECM. The control group was injected with cells/medium+1μl/ECM. Behaviour tests were performed before and after surgery and used as an indicator for the developments of metastases (Fig 36).
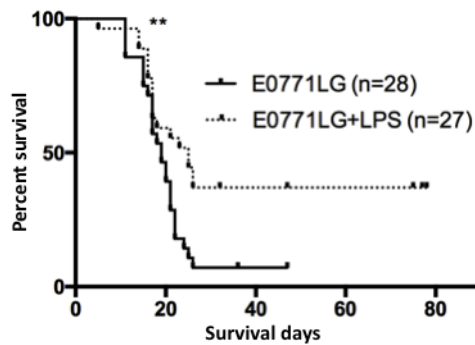
Fig 36: Kaplan Meier surviving curve after E0771LG cancer cell injection +/- LPS.
C57BL/6 mice were injected with cancer cell line E0771LG and treated (n=27) or not treated (n=28) with LPS. The survival of mice injected with E0771LG was significantly decreased compare to the survival of treatment group.

All mice of the control group died within 50days. Surprisingly, mice treated with LPS were identified as long-term survivors. The surviving prognosis for the treatment group was significantly (p=0.0090) increased with 40% survival and no more mice from this group died within the next month when the experiment was stopped. These first results gained with this model indicate that LPS has a positive treatment effect (Fig 36).

Specifically, LPS was shown to activate the immune response by activating the Toll-like receptor pathway. Especially, TLR4 is responding to LPS (Regen et al., 2011). Moreover, TLR4 signals in a MyD88- and TRIF-dependent way, adaptor molecules that are specific for the TLR signalling pathway (Hagemann et al., 2008). This indicates that two adaptors in TLR signalling, MyD88 and TRIF, which are responding differently to LPS, may regulate tumour progression via different mechanisms. MyD88 was shown to play a role in promoting metastasis, which was driven by macrophages. In order to investigate the role of

MyD88 and TRIF and the TLR signalling on tumour cell colonization, we designed experiments for an *in vivo* study. Three groups of mice were used to compare the survival prognosis with or without LPS treatment. WT mice, MyD88 knockout mice and TRIF knockout mice were intracraniallay injected as described before, with 500 cancer cells of E0771LG or 500 cancer cells of E0771LG and LPS. 1µl (1µg/µl) of LSP was added to the mixture of cells, medium and ECM. All mice and the respective cancer cell line E0771LG have a C57BL/6 background, which allows us to use them as a syngeneic mouse model for further analyses. Behaviour tests were performed before and after surgery and used as an indicator for metastasis development.

Tab 12: Mean survival of different mice strains and +/- LPS treatment

Mice strain	Mean survival days without LPS treatment	Mean survival days with LPS treatment	Hazard Ratio untreated/treated	P value
WT injected with E0771LG	19	29	2.027 CI 95% [1.129-3.637]	P=0.0179
TRIF knockout injected with E0771LG	18,5	15	0.7372 CI 95% [0.2825-1.578]	P=0.9382
MyD88 knockout injected with E0771LG	16	16	0.8049 CI 95% [0.3335-1.554]	P=0.2200

WT mice injected with the cancer cell line E0771LG and LPS survived much longer than all other tested mice here (Tab 12). In WT mice the protective effect of LPS could thus be confirmed. WT mice injected with the cancer cell line E0771LG and LPS (n=35) survived significantly longer than mice injected with E0771LG alone (n=33) (p=0.0179). MyD88

knockout mice injected with the cancer cell line E0771LG (n=12) or E0771LG and LPS (n=15) showed a slight difference regarding their survival (p=0.2200). However, here LPS showed no protective effect, the effect of LPS seems to have an adverse effect in Myd88 knockout mice. The injection of TRIF knockout mice with the cancer cell lines E0771LG (n=12) or E0771LG and LPS (n=13), revealed no differences on survival (p=0.9382) either. These first preliminary results indicate the importance of Myd88 and TRIF for the protective effect of LPS and showed differences between MyD88 and TRIFF. In order to investigate the protective effect of LPS via TLR signalling in greater detail, available brain tissue from all experiments can be used for further analysed.

4 Discussion

4.1 Characterisation of different cancer cell lines

It is well accepted that not the primary tumour of breast cancer but its metastasis is the main cause of death in these patients. Until now has not been possible to safely predict the risk of metastasis development of the individual patient. Therefore, great efforts have been made the last decades to identify for example by gene-expression signatures of the primary breast cancers (Weigelt et al., 2005) prognostic markers to better predict the individual risk for metastasis. However, this is still not recommend for the daily routine to use this as decision instrument. Moreover, the manifestation of metastasis e.g. in the brain is not predictable. In order to detect metastatic tumour cells seeding specifically the brain, markers on (circulating) tumour cells were analysed *in vivo* experiments (Bos et al., 2009). One method others tried to investigate the CTCs, was the identification by Cytokeratin expression. In breast cancer CK8, CK18, CK5 and CK17 were typically expressed and therefore potential suitable markers to study successful colonization of breast cancer cells in the Cytokeratin negative brain tissue (Perou et al., 2000). In order to transfer these findings of the human studies to an experimental design for mice, first, we characterised available murine breast cancer cells in terms of their relevant gene expression levels. We identified typical characteristic markers of these cell lines and measured significant CK8 expression in all murine breast cancer cell lines. So, CK8 gene expression was an ideal candidate to quantify the breast cancer metastatic load in the negative brain parenchyma.

In the next step, we wanted to better understand biological process. Therefore, we first focused on EMT markers which have been demonstrated that these factors facilitate metastasis development and their expression in the primary tumour are correlated with poor prognosis (Thiery, 2002). Consequently, we analysed EMT markers on available murine breast cancer cell lines, which were differently expressed in the respective breast cancer cells. The hypothesis was now, that these features should influence the cerebral colonization capacity of three murine breast cancer cell lines.

It was shown that activated Wnt signalling promotes EMT-like phenotypes in breast cancer cells (Wu et al., 2012) and Wnt signalling was also shown to play an important role in the cerebral metastatic process (Pukrop et al., 2010b) (Klemm et al., 2011) (Smid et al., 2008).

To confirm the role of Wnt signalling in cerebral metastasis development, we characterised the murine breast cancer cell lines with respect to their Wnt profile. The qRT-PCR and protein measurements revealed high expression levels of Wnt5a in the cancer cell line E0771LG, while high expression of Wnt7a was detected in the cancer cell line 410.4 and 4T1. Our available cancer cells were later used to study the role of glia contact to colonized tumour cells in an *in vivo* model. Taken together, in the first step we characterised the murine breast cancer cells for their epithelial and mesenchymal character and Wnt profile bases for our further investigations in the functional *in vitro* tests and finally *in vivo* experiments. Importantly, the profiles of the murine cells were already detected in human breast cancer samples (Huguet et al., 1994b) (van de Vijver et al., 2002) (Perou et al., 2000).

4.2 Establishing of an *in vivo* syngeneic cerebral metastasis model

The impact of the tumour microenvironment in the primary tumour got more and more impact on outcome of the disease. We and others also described that the metastatic microenvironment has also significant impact on many features of the pre-metastatic cells seeded the distant organ, in particular the brain (Pukrop et al., 2010b) (Chuang et al., 2013). However, the majority of the *in vivo* studies are performed in Xenograft models, which systematically exclude or at least massively influence this very important force during metastasis in comparison to the human situation.

Thus, firstly only an immune-competent model reflects the real impact of the metastatic microenvironment and secondly is applicable for studies of immune-based therapeutic strategies. Moreover, it has been demonstrated, that the genetic background from which cancer arises also has an effect on the capacity of mouse mammary cancer cells to metastasis and support the hypothesis that the genetic make-up of the host and background of the cancer cells need to be similar (Lancaster et al., 2005). With this knowledge our main goal was to establish a syngeneic cerebral metastasis mouse model to investigate colonization and involved interaction of the metastatic microenvironment. This is at least a prerequisite to develop new therapeutic targets in both, "seed and soil", which might lead then to more successful intervention strategies for breast cancer metastasis.

Mammary fatpad of syngeneic mouse models injected with the cancer cell line 4T1, which originally derive from a spontaneous mouse mammary primary tumour of a BALB/C mouse, metastasise to the brain and therefore metastatic outgrowth can be studied (Aslakson and Miller, 1992a). Not all of our cancer cell lines are able to metastasize spontaneously. Therefore, we injected cancer cells intracranially considering the background of these cells and mouse strains. Very importantly, we used cancer cells that were embedded in extracellular matrix (ECM) before applied to the brain.

Different types of cancer cells tested to develop metastasis here were used for further experiments and the establishment of *in vitro* markers. Importantly, all cell lines were able to develop metastasis caused by various amounts of injected cells and their colonization patterns. Interestingly, we found different infiltration patterns of the cancer cell lines. The cancer cell lines 410.4 and 4T1 showed cohort infiltration, whereas the cancer cell line E0771LG showed diffuse infiltration. Based on personal communication with L. Siam (manuscript on preparation), we know that those different infiltration patterns are relevant for the OS in patients with cerebral metastasis. Those patients with no infiltration have a much better prognosis than patients with cohort or diffuse infiltration. With this finding, we are able to investigate the biological consequence of the infiltration of the adjacent brain parenchyma. Until know, these features are not addressed at all.

Quantification of the developed metastasis of cancer cell lines was performed with the marker CK8. Interestingly, an important finding was observed when CK8 was used to detect colonized tumour cells (Fig 30A). Unexpectly, we found colonized tumour cells also in the non- injected side (other hemisphere of the brain) derived from the injected cancer cells. This finding indicates that the into the benign brain parenchyma infiltrating carcinoma cells are not only a surrogate parameter for worse OS but also a potential source for further metastasis in complete other regions of the affected organ. This would mean those established metastases are a potential source for new metastasis, at least in the same organ. Taken together, this is one of the very few *in vivo* results demonstrating that metastases metastasize.
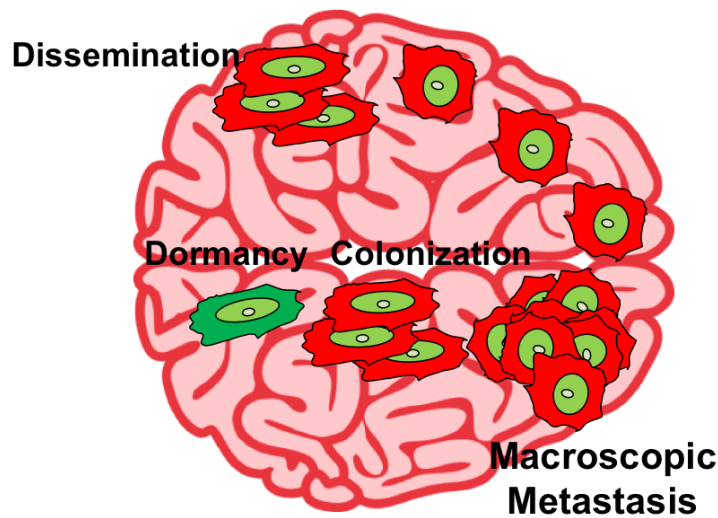
Fig 37: Colonized tumour cells are able to disseminate.
Colonized tumour cells perform metastasis. These cells can disseminate in the brain.

So far we have identified different colonization patterns of metastatic cells. However, systematically analyses should be performed to further quantify the infiltration and new breast cancer colonies of the disseminated cells. Additionally, the amount and patterns of the affected menigeal and ventricles should also be measured. Therefore, we cooperate in future with Trevor Do, a group member of the research group at STTARR in Toronto, who routinely uses an analysing software which could measure these features.

Further, we might be also able to identify the different zones of the metastatic tissue and there cellular composition. We therefore aim to investigate the astrocytes, microglia and immune responses in the core of the metastasis, at the interface to the benign brain parenchyma and infiltration zone. This is of major interest because we already see significant differences of at least the astrocytes and microglia, which accumulate at the interface. However, we detected differences in respect to the syngeneic models. For example, astrocytes and microglia were detectable around the metastasis of all injected cancer cell lines, but in case of cancer cell lines 4T1 and E0771LG also between the metastatic cells. Gene expression analyses also indicate differences in the three models. Further, we were able to quantify colonized tumour cells with CK8. Hence, we conclude that in terms of infiltration patterns of the carcinoma cells and the response of the brain tissue varies in dependency of the features of the carcinoma cells. Some features, in

particular the infiltration patterns of the carcinoma cells, might be related to differences in gene expression based on the role of EMT and MET in tumour cell colonization and metastasis development. Therefore, EMT and MET markers should be further investigated as EMT and MET changes can potentially be used for new therapeutic strategies. In summary, we established four syngeneic cerebral metastasis mouse models to study the colonization of the brain and the resulting response of the brain microenvironment against the metastatic progression, which can now be used for further experiments and intervention studies.

4.2 Clinical applications

Breast cancer metastasis indicate a poor survival prognosis due to limited treatment options and the lack of proven effectively targeted therapies. Recently new therapeutic strategies focused on the inhibition of the Wnt signalling pathway have been developed. One of these novel promising treatment strategies for Wnt manipulation might be the Porcupine inhibitor LGK974 of Novartis.

Currently this inhibitor is in use in clinical Phase 1 trial in advanced cancer patients. The idea was that LGK974 might be a useful novel drug for the treatment of Wnt dependent cancer progression. Therefore, patients with triple-negative breast cancer have been also included in this study. Excluded from this study were patients with brain metastasis that had not been adequately treated. Novartis evaluated in cell-based models that LGK974 inhibits the Wnt pathway by specifically binding Porcupine, a membrane-bound O-acyltransferase that catalysis the palmitoylation of Wnt ligands and functions on Wnt secretion. Furthermore, in preclinical studies they found that inhibition of Porcupine with LGK974 is associated with anti-tumour activity.
(http://www.novartisoncology.com/ct/pipelineDetails?compound=LGK974&diseaseAcr=BC)

This was confirmed by a study by Liu et al. (2013a). They showed the successful use of LGK974 as a potent, selective, and orally bioavailable Porcupine inhibitor on the initiation and development of primary tumours. This *in vivo* study demonstrated on a Wnt dependent murine breast tumour model (mouse mammary tumour virus-driven Wnt1 model), that the inhibition of Wnt signalling at well-tolerated doses is associated with a reduction of

tumour growth. In our study we investigated a tolerable dose of LGK974 *in vitro* and confirmed the effect of LKG974, to cause a reduced invasiveness of cancer cells *in vitro*, however, only for the cancer cell line 4T1 and with a positive trend in 410.4. However, this effect could not be confirmed for EO771LG cell line with the different Wnt profile, which mainly expresses Wnt5a. Therefore, these results indicate that the action of LGK974 might depend not only on Wnt secretion but also on a specific Wnt profile. We additionally detected differences in the inhibitory effect of LGK974 on the protein level using cancer cell lines 410.4, 4T1 and E0771LG. Interestingly, Wnt5a abolished in the cancer cell line E0771LG treated with LGK974. In contrast, Wnt7a/b seemed to accumulate in the cytosol of the cancer cell lines 410.4 and 4T1 as expected by the mechanism of action of the drug. Thus, this indicates that the inhibition of Porcupine can have different effects on Wnt proteins levels that might also depend on the type of the cancer cells. However, it could also be a technical effect when the missing palmitoylation of Wnt5a changes the tertiary form of Wnt5a, which could not be recognized by the antibody anymore. So, further analyses are required to explain why the cancer cell lines tested here react differently to the treatment with LGK974, which has potential therapeutic implications. Notably, Porcupine was investigated to be necessary for all of the Wnt pathways (Dodge et al., 2012) and as we detected an effect of LGK974 on both tested Wnts, we were able to confirm the Wnt inhibitory effect of LGK974.

Next we proved effects of the LGK974 inhibition on Wnt signalling *in vivo*. The physiological conditions can have serious impacts and therefore it is important to address possible therapeutic treatment side effects on *in vivo* experiments. Therefore, we treated mice orally with LGK974 by using the established cerebral metastasis mouse models. Surprisingly, in further experiments on LGK974, we detected another effect of the inhibition of Porcupine with LGK974. In contrast to the *in vitro* experiments, the cancer cell line 4T1 in combination with LGK974 lead to a significant decrease of OS, independent from the amount of cancer cells that were injected *in vivo*. This effect was observed in all the *in vivo* experiments that were performed with the cancer cell line 4T1 *in vivo*. Also, this was confirmed via CAM assay where we found that cancer cells 410.4, with a comparable Wnt profile like 4T1, stimulated with LGK974 increased tumour cell colonization. The 4T1 showed the same trend, and more experiments have to be performed to underline this effect. However, in none of the functional and *in vivo* experiments we saw any treatment effect in the Wnt5a driven by EO771LG. So, our results significantly

underlined that Wnt ligand expression is not sufficient for treatment effects. Most important, here we demonstrate negative treatment effects in the 4T1 model. As described above, Liu et al demonstrated in their study a positive treatment effect of LGK974 in early stages of breast cancer. However, our model represents late stage of cerebral metastasis when the breast cancer cells colonized the brain tissue. Our finding demonstrates that biological treatments, which affect stem cell features or EMT, could lead in early stage *in vivo* models beneficial outcome but with an opposite effect on late stage tumour models (Fig 35). The conclusion of this study is that biological inhibitors seem to be not only dependent on the profile of the cancer cells but also stage dependent.
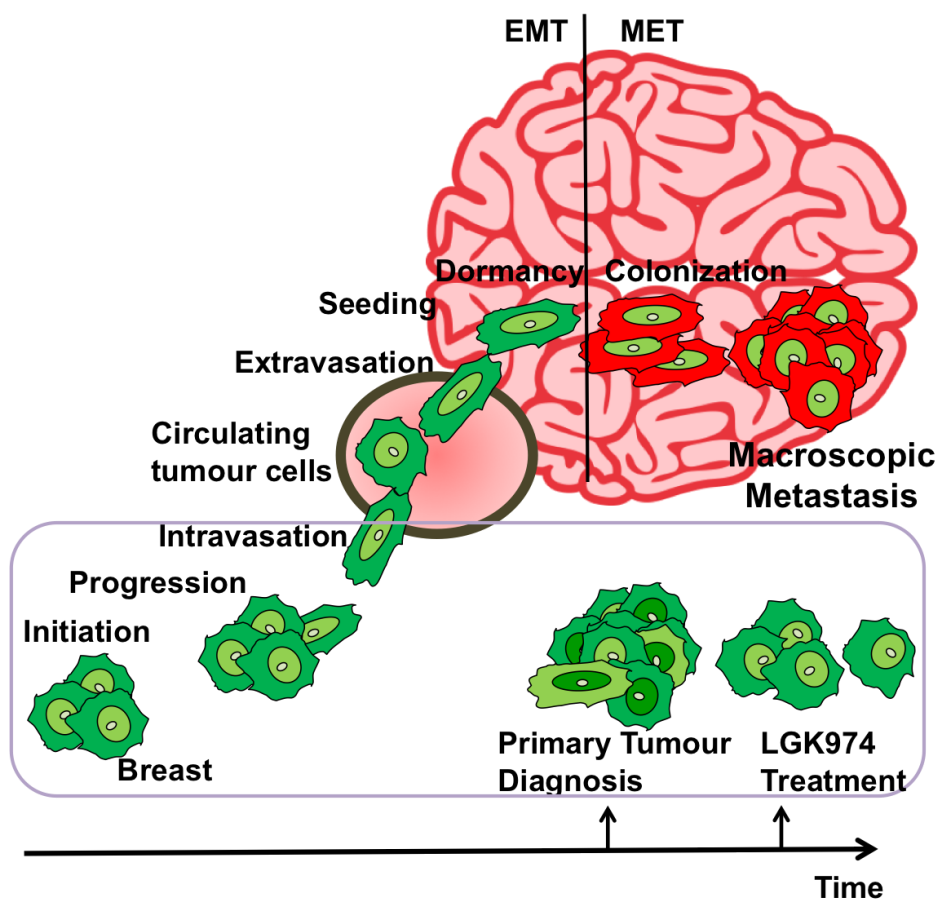
Fig 38: Effect of LGK974 on primary tumour and colonized tumour cell.
Treatment of LGK974 on primary tumour was successful but not on colonized tumour cells in a cerebral metastasis model. Most important, this biological treatment strategy could lead to progression of already seeded breast cancer cells in the distant organ while the primary tumour respond to the therapy and regress. Now, if seeding is really an early event in the process of metastasis, before diagnosis of the primary tumour, this finding have significant impact on all further treatment strategies affecting stem cell factors or EMT.

Remarkably, the injection of the cancer cell line E0771LG in combination with LGK974 had no effect on survival. The reason for this might be Wnt dependent differences in the colonization capacity of tumour cells from cancer cell line E0771LG compared to 4T1. Cancer cells undergoing EMT and MET are capable of invasion, migration and proliferation and therefore promote tumour cell colonization. Recently, it was shown, that Wnt signalling induces EMT and MET (Qi et al., 2014),(Bo et al., 2013). The activity of β-catenin as a cadherin-binding protein leads to a break of cell-to-cell adhesions built by β-catenin and E-cadherin. An overexpression of E-cadherin and the reduction of mesenchymal markers leads to the downregulating of Wnt signalling (Schäfer et al., 2014b). These findings also might explain our results: after injection of the cancer cell line 410.4 metastasis development was much slower and subsequent demonstrated better OS compared to the injection of cancer cell line 4T1 or E0771G. Moreover, E-cadherin was highly expressed in metastasis developed from 410.4 compared to the other cancer cell lines used in this study, leading to suggest that high levels of E-cadherin in metastasis and corresponding cancer cell lines might give a better prognosis for survival. In contrast, loss of E-cadherin expression contributes to metastasis (Kalluri and Weinberg, 2009). Clearly, these circumstances need to be further analysed by investigating the interdependencies of Wnt signalling, EMT and MET by confirming that Wnt signalling is involved in tumour cell colonization and that Wnt can promote EMT and MET. To investigate the role of EMT and MET on tumour cell colonization in our model, transcription markers, e.g. Snail, Slug, ZEB1, ZEB2, Twist1 or Twist2, which are regulating EMT and MET, need to be investigated and analysed (Kalluri and Weinberg, 2009).

Interestingly, Louie et al. (2013) found in the human breast cancer cell line MCF7, low levels of E-cadherin at the cell membrane and high levels of the transcription factor Snail in the nucleus, however, breast cancer cell lines selective to the brain showed low levels of E-cadherin and high levels of Snail, indicating that these cells underwent EMT (Louie et al., 2013). Furthermore, Wnt3a was found to promote the expression of the key transcription factor for EMT, Snail. Besides, Wnt3a increases metastasis (Qi et al., 2014). Hence, the microenvironment is important for the outcome of Wnt signalling and for EMT and MET. Consequently, we suggest, that LGK974 may lead to EMT and MET and therefore to tumour cell colonization and development of metastasis depending on the presence of activated, specific Wnt molecules in the microenvironment. The hypothesis that LGK974 impacts on Wnt signalling and that Wnt signalling could induce

transcriptional changes in order to drive EMT and MET should be followed up. In order to do this, the transcription factors Twist1, Twist2, ZEB1, ZEB2 and Snail need to be investigated. First *in vitro* experiments on this showed that cancer cell lines expressed different levels of transcription factors for EMT after stimulation of LGK974. Twist, was demonstrated to be upregulated in highly metastatic 4T1 cells but downregulated in non-metastatic cells. Furthermore, Twist increased breast cancer metastasis by promoting EMT (Yang et al., 2004). The expression of the EMT and MET transcription marker Twist2 was significantly changed after treatment with LGK974 compared to the untreated control. Twist2 gene expression was increased after the stimulation with LGK974 leading to suggest, that LGK974 is increasing Twist2 expression and therefore EMT and MET. In order to prove this hypothesis, more experiments, with higher N numbers, need to be performed and confirmed on protein level. Further, developed metastasis of the cancer cell line 4T1 need to be analysed for their Twist2 expression patterns, to identify metastasis that are responsive to LGK974.

The microenvironment was frequently investigated to play an important role in survival and growth of metastatic cells and the formation of metastasis (Quail and Joyce, 2013). Moreover, microglia cells were shown to be involved in tumour cell invasion (Lorger and Felding-Habermann, 2010). However, very little is known about the interaction between the brain environment and colonizing tumour cells. Interestingly, microglia activation was decreased in breast cancer cell lines selected from brain metastasis with a MET-like phenotype. By inducing an EMT-like phenotype in these cells, the number of activated microglia cells was increased (Louie et al., 2013). These findings underline close relationships between the immune response and metastatic formation by EMT. Moreover, it was shown that microglia cells in brain metastasis of breast cancers promote tumour cell colonization in human patients (Fitzgerald et al., 2008b). The therapeutic manipulation of the cytoprotective or cytotoxic response of microglia cells requires new targets and strategies to successfully interfere with tumour cell colonization in the brain.

4.3 Immune response trigger by LPS and effects on cancer cell

To investigate and manipulate the local defence system in the CNS and see the effects on tumour cell colonization, the established cerebral metastasis mouse model of the

EO771LG was used. In this study we have performed treatments with lipopolysaccharides (LPS) to stimulate locally the microglia response.

However, before we started the intervention studies, we first proved by qRT-PCR that the glial cells and immune cells were activated after colonization of the cancer cell line E0771LG to the brain using the microglia markers CSF1 and CSFR1 and the astrocytes marker GFAP. Interestingly, CSF1 was significantly increased on the side that had been injected with cancer cells, compared to the non- injected side. This result indicates that microglia either reacted to the injection or to the presence of cancer cells. Furthermore, all markers were expressed in the control group where we injected only ECM. This result proved the presence of glia cells. However, control samples, showed no activated gene expression, especially, CSF1 and CSFR1 were not up-regulated despite the fact that mice underwent the same surgery as the cancer cell injected group. However, microglia and astrocytes staining clearly showed the absence of microglia and astrocytes in the control samples, but the presence and localisation in the cancer cell injected group. Nevertheless, we could not detect significant differences between control group and the cancer cell injected group in all analysed genes. Two reasons might explain this: In case of GFAP, due to the high expression levels of GFAP in these analyses it is possible that small differences could not be discerned. Secondly, only three control samples and seven samples with cancer cell injection were used until now. A higher N number of control samples need to be performed. Nevertheless, mice were sacrificed up to three weeks after the intracranial injection. The results showed expressions of all these genes, demonstrating the activation of glia cells in the presence of induced metastasis, while this glial activation might possibly be the cause of the injury during the injection (Loane and Byrnes, 2010). However, microglia and astrocytes staining clearly showed the presence and localisation of microglia cells and astrocytes in correlation with the injected side and the interaction with colonized tumour cells, which points to a colonized tumour cells-immune reaction. In comparison, the non- injected side of these brains showed a strong reduction of activated microglia cells and astrocytes.

In summary, these results strongly suggest, that the observed glial activation is not merely triggered by the injury of the surgery. Thus, another advantage of our model is the presence of a non-injected control side that will prove helpful to address these questions during metastatic progression, as I have pointed out here. We could also quantify colonized tumour cells in the cancer cells injected brains with CK8. Furthermore, we can prove the

presence of microglia cells and astrocytes here. Therefore, this model can be used for further experiments addressing metastasis-immune related questions.

LPS was recently shown to induce an immune response, which leads to the activation of microglia cells and astrocytes in the CNS (He et al., 2006b). Moreover, LPS-induced cytotoxicity on metastatic cancer cells were executed by microglia cells. This effect is dependent on time and concentration of LPS application. It was shown, that when using lower levels of LPS, cancer cells are insensitive to the microglial cytotoxicity. Therefore, apoptosis of cancer cells induced by microglia cells is dependent on the effect of LPS. Here, we wanted to investigate the role of LPS on tumour cell colonization as a potential trigger for the activation of glia cells in our newly established cerebral metastasis model.

After the injection of cancer cells locally pre-treated with LPS into mice, their survival was highly significantly increased in comparison to the non LPS-treated group. These first preliminary results on survival indicate that LPS might have a protective effect, by giving an additional boost to the activation of microglia, and confirmed preliminary findings by Han-Ning Chuang (http://hdl.handle.net/11858/00-1735-0000-000D-F01F-7). She showed that LPS hindered microglia induced invasion of cancer cells, which was also confirming the study of He et al (2006). Furthermore, Wnt5a was shown to play an important role in tumour invasion (Pukrop et al., 2006). Han-Ning confirmed that Wnt5a expressed from microglia cells is essential for tumour cells to invade and colonize the brain parenchyma effectively. More experiments need to be performed for a better understanding of the colonizing behaviour of tumour cells and the role of microglia in this context. In order to do this, further analyses of the prepared brain tissue from the LPS experiment of our syngeneic cerebral metastasis mouse model can be performed. Immunstainings using, e.g. antibodies against GFAP and IBA might be useful to investigate the role of microglia in tumour cell colonization. Moreover, gene expression analyses can be performed to further test the role of Wnt in this context. In order to do this, brain metastasis tissue should be analysed for all established markers on the Wnt profile, shown here, as well as CSF1, CSF1R and GFAP.

LPS was identified to activate microglia and cytokine induction by activating the Toll-like receptor (TLR) pathway, where TLR4 is responding to LPS (Regen et al., 2011). TLR4 is using the myeloid differentiation primary response gene 88 (MyD88) to drive inflammatory response. Another adapter is necessary for transferring TLR4 signalling, the

TIR-domain- containing protein (TRIF) (Kawai and Akira, 2009). The differences in the LPS response have been described as an early MyD88 depending response, which leads to the activation of nuclear factor-κB (NF-κB). Additionally, a later TRIF response to LPS leads to the late activation of NF-κB and to the induction of cytokines, chemokines, and other transcription factors (Mogensen, 2009). These findings demonstrate the different response of MyD88 or TRIF to LPS.

Interestingly, MyD88 was shown to play a role in promoting metastasis (Hagemann et al., 2008). Therefore, LPS activates TLR4 and signals in a MyD88- and TRIF-dependent way. This indicates that two adaptors in TLR signalling, MyD88 and TRIF, which are responding differently to LPS, may regulate tumour cell colonization via different mechanisms. By using microglia from Myd88 deficient mice, Han-Ning showed a reduction of microglia-induced invasion of cancer cells in her brain slices model. It can therefore be hypothesised that the adaptor MyD88 is required for tumour cell colonization, whereas the adapter TRIF causes the protective effects of TLR4 activation. Moreover, TRIF- and MyD88-deficient microglia can change the effects of LPS also on Wnt related genes, which also underlies the impact of MyD88 and TRIF on tumour cell colonization (http://hdl.handle.net/11858/00-1735-0000-000D-F01F-7).

In order to further elaborate on these results and interpretations, the involved pathways in tumour cell colonization need to be investigated in more detail. Therefore, gene expression levels of MyD88 and TRIF need to be tested by using the prepared brain tissue from the LPS experiment. We suggest that high expression of MyD88 leading in tumour cell colonization and metastasis and high level of TRIF leading suppressing of tumour cell colonization. Moreover, there are several mouse strains available, e.g. MyD88 knockout or TRIF knockout mice and both models have a background strain of C57BL/6. These mice are ideal to address these questions in combination with the syngeneic mouse model by using the methods established here. In order to do this, the established cerebral metastasis mouse model of C57BL/6 should be used in combination with the cancer cell line E0771LG, which is derived from C57BL/6 mice. Interestingly, first own experiments showed that the application of LPS has no protective effect in a TRIF knockout mouse model, which is in support of the hypothesis stated above. TRIF knockout mice injected with the cancer cell line E0771LG with LPS treatment did not survive longer than TRIF knockout mice injected with the cancer cell line E0771LG without LPS treatment. This strongly indicates the importance of TRIF on the protective effect of LPS in tumour cell

colonization. In contrast, in the case of MyD88 knockout mice, we were not able to detect differences between MyD88 knockout mice injected with E0771LG without LPS treatment and MyD88 knockout mice injected with E0771LG with LPS treatment. However, in WT mice with induced metastasis in the absence of LPS survived a mean of 19days, while mice of the LPS treatment group survived almost a week longer. Thus, two independent metastasis mouse models with a disrupted TLR4-signalling pathway died earlier than WT-controls, strongly suggesting that the protective effect of LPS requires intact TLR4 signalling, in particular in microglia.

This result demonstrates that TRIF and MyD88 are indeed necessary for the protective effect of LPS. Moreover, LPS application without intact MyD88 or TRIF-signalling even seems to have a detrimental effect on survival. We were able to address our established syngeneic cerebral metastasis mouse model to a different experimental design and could prove the protective effect of LPS in the WT mouse model. We supported *in vivo* the protective effect of LPS on breast cancer metastasis to the brain.

In this study syngeneic cerebral metastasis mouse models were successfully established, which can be used to better understanding the role of the brain microenvironment on tumour cell colonization during different infiltration patterns. Furthermore, therapeutic treatment strategies claiming at the treatment of metastatic breast cancer can be applied using these different models.

5 Summary

We characterised four murine cancer cells and investigated typical markers, which were similar to human cancer cells. We established syngeneic cerebral metastasis mouse models, methods to quantify the metastatic cancer cells in the brain parenchyma´s well as the metastatic capacity of these colonized tumour cells. We investigated the colonization behaviour of these cancer cell lines *in vivo* and demonstrated differences in tumour cell colonization and the reaction of the glia cells. Importantly, our results are consistent with human studies. Interestingly, we demonstrate that colonized tumour cells were able to further disseminate in the brain as source for new metastatic lesions.

The Wnt profiles of the cancer cell lines were investigated and Wnt5a and Wnt7b were identified and provide the basis for targeting Wnt signalling for further experiments in the respective models.

Furthermore, we investigate an effective dose of the Porcupine Inhibitor LGK974 in cell culture and prove the inhibitory effect of the LGK974 on Wnt secretion and functional effects on tumour invasion *in vitro* and could confirm previous findings of LGK974 on primary tumours. Moreover, we observed another effect of LGK974 and demonstrated that LGK974 appears to worsen the colonization in the 4T1 colonization model but not EO771LG. Therefore, the treatment of LGK974 on primary tumours seems to be a good treatment strategy, but not for metastatic cells. Also, the effects seem to be dependent on specific Wnt profiles.

Additionally, we were able to address our established syngeneic cerebral metastasis mouse model to a different experimental design to investigate the role of microglia in tumour cell colonization. So far we could trigger an immune response with LPS and could prove the protective effect of LPS in the WT mouse model.

6 Bibliography

Abbott, N.J., Rönnbäck, L., and Hansson, E. (2006). Astrocyte-endothelial interactions at the blood-brain barrier. Nat. Rev. Neurosci. 7, 41–53.

Aslakson, C.J., and Miller, F.R. (1992a). Selective events in the metastatic process defined by analysis of the sequential dissemination of subpopulations of a mouse mammary tumor. Cancer Res. 52, 1399–1405.

Aslakson, C.J., and Miller, F.R. (1992b). Selective events in the metastatic process defined by analysis of the sequential dissemination of subpopulations of a mouse mammary tumor. Cancer Res. 52, 1399–1405.

Barron, K.D. (1995). The microglial cell. A historical review. J. Neurol. Sci. 134, 57–68.

Berridge, M.V., and Tan, A.S. (1992). The protein kinase C inhibitor, calphostin C, inhibits succinate-dependent mitochondrial reduction of MTT by a mechanism that does not involve protein kinase C. Biochem. Biophys. Res. Commun. 185, 806–811.

Bhowmick, N.A., Neilson, E.G., and Moses, H.L. (2004). Stromal fibroblasts in cancer initiation and progression. Nature 432, 332–337.

Bingham, D., John, C.M., Panter, S.S., and Jarvis, G.A. (2011). Post-injury treatment with lipopolysaccharide or lipooligosaccharide protects rat neuronal and glial cell cultures. Brain Res. Bull. 85, 403–409.

Bo, H., Zhang, S., Gao, L., Chen, Y., Zhang, J., Chang, X., and Zhu, M. (2013). Upregulation of Wnt5a promotes epithelial-to-mesenchymal transition and metastasis of pancreatic cancer cells. BMC Cancer 13, 496.

Bos, P.D., Zhang, X.H.-F., Nadal, C., Shu, W., Gomis, R.R., Nguyen, D.X., Minn, A.J., Van de Vijver, M., Gerald, W., Foekens, J.A., et al. (2009). Genes that mediate breast cancer metastasis to the brain. Nature 459, 1005–1009.

Carbonell, W.S., Ansorge, O., Sibson, N., and Muschel, R. (2009). The Vascular Basement Membrane as "Soil" in Brain Metastasis. PLoS ONE 4, e5857.

Chambers, A.F., MacDonald, I.C., Schmidt, E.E., Morris, V.L., and Groom, A.C. (2000). Clinical targets for anti-metastasis therapy. Adv. Cancer Res. 79, 91–121.

Chambers, A.F., Groom, A.C., and MacDonald, I.C. (2002). Dissemination and growth of cancer cells in metastatic sites. Nat. Rev. Cancer 2, 563–572.

Chen, B., Dodge, M.E., Tang, W., Lu, J., Ma, Z., Fan, C.-W., Wei, S., Hao, W., Kilgore, J., Williams, N.S., et al. (2009). Small molecule-mediated disruption of Wnt-dependent signaling in tissue regeneration and cancer. Nat. Chem. Biol. 5, 100–107.

Chen, J.J.W., Lin, Y.-C., Yao, P.-L., Yuan, A., Chen, H.-Y., Shun, C.-T., Tsai, M.-F., Chen, C.-H., and Yang, P.-C. (2005). Tumor-Associated Macrophages: The Double-Edged Sword in Cancer Progression. J. Clin. Oncol. 23, 953–964.

Chuang, H.-N., van Rossum, D., Sieger, D., Siam, L., Klemm, F., Bleckmann, A., Bayerlová, M., Farhat, K., Scheffel, J., Schulz, M., et al. (2013). Carcinoma cells misuse the host tissue damage response to invade the brain. Glia 61, 1331–1346.

Clevers, H., and Nusse, R. (2012). Wnt/β-Catenin Signaling and Disease. Cell 149, 1192–1205.

Clevers, H., and van de Wetering, M. (1997). TCF/LEF factor earn their wings. Trends

Genet. TIG 13, 485–489.

Dodge, M.E., Moon, J., Tuladhar, R., Lu, J., Jacob, L.S., Zhang, L., Shi, H., Wang, X., Moro, E., Mongera, A., et al. (2012). Diverse chemical scaffolds support direct inhibition of the membrane-bound O-acyltransferase porcupine. J. Biol. Chem. 287, 23246–23254.

Eichler, A.F., Chung, E., Kodack, D.P., Loeffler, J.S., Fukumura, D., and Jain, R.K. (2011a). The biology of brain metastases—translation to new therapies. Nat. Rev. Clin. Oncol. 8, 344–356.

Eichler, A.F., Chung, E., Kodack, D.P., Loeffler, J.S., Fukumura, D., and Jain, R.K. (2011b). The biology of brain metastases—translation to new therapies. Nat. Rev. Clin. Oncol. 8, 344–356.

Ewens, A., Mihich, E., and Ehrke, M.J. (2005). Distant metastasis from subcutaneously grown E0771 medullary breast adenocarcinoma. Anticancer Res. 25, 3905–3915.

Fidler, I.J. (2011). The role of the organ microenvironment in brain metastasis. Semin. Cancer Biol. 21, 107–112.

Fidler, I.J., and Kripke, M.L. (1977). Metastasis results from preexisting variant cells within a malignant tumor. Science 197, 893–895.

Fitzgerald, D.P., Palmieri, D., Hua, E., Hargrave, E., Steeg, P.S., Herring, J.M., Qian, Y., Vega-Valle, E., Weil, R.J., Stark, A.M., et al. (2008a). Reactive glia are recruited by highly proliferative brain metastases of breast cancer and promote tumor cell colonization. Clin. Exp. Metastasis 25, 799–810.

Fitzgerald, D.P., Palmieri, D., Hua, E., Hargrave, E., Steeg, P.S., Herring, J.M., Qian, Y., Vega-Valle, E., Weil, R.J., Stark, A.M., et al. (2008b). Reactive glia are recruited by highly proliferative brain metastases of breast cancer and promote tumor cell colonization. Clin. Exp. Metastasis 25, 799–810.

Giulian, D. (1993). Reactive glia as rivals in regulating neuronal survival. Glia 7, 102–110.

Hagemann, T., Robinson, S.C., Schulz, M., Trümper, L., Balkwill, F.R., and Binder, C. (2004). Enhanced invasiveness of breast cancer cell lines upon co-cultivation with macrophages is due to TNF-alpha dependent up-regulation of matrix metalloproteases. Carcinogenesis 25, 1543–1549.

Hagemann, T., Lawrence, T., McNeish, I., Charles, K.A., Kulbe, H., Thompson, R.G., Robinson, S.C., and Balkwill, F.R. (2008). "Re-educating" tumor-associated macrophages by targeting NF-κB. J. Exp. Med. 205, 1261–1268.

Halleskog, C., and Schulte, G. (2013). WNT-3A and WNT-5A counteract lipopolysaccharide-induced pro-inflammatory changes in mouse primary microglia. J. Neurochem. 125, 803–808.

Hanisch, U.-K., and Kettenmann, H. (2007). Microglia: active sensor and versatile effector cells in the normal and pathologic brain. Nat. Neurosci. 10, 1387–1394.

He, B.P., Wang, J.J., Zhang, X., Wu, Y., Wang, M., Bay, B.-H., and Chang, A.Y.-C. (2006a). Differential Reactions of Microglia to Brain Metastasis of Lung Cancer. Mol. Med. 12, 161–170.

He, B.P., Wang, J.J., Zhang, X., Wu, Y., Wang, M., Bay, B.-H., and Chang, A.Y.-C. (2006b). Differential Reactions of Microglia to Brain Metastasis of Lung Cancer. Mol. Med. 12, 161–170.

Huguet, E.L., McMahon, J.A., McMahon, A.P., Bicknell, R., and Harris, A.L. (1994a). Differential Expression of Human Wnt Genes 2, 3, 4, and 7B in Human Breast Cell Lines and Normal and Disease States of Human Breast Tissue. Cancer Res. 54,

2615–2621.

Huguet, E.L., McMahon, J.A., McMahon, A.P., Bicknell, R., and Harris, A.L. (1994b). Differential Expression of Human Wnt Genes 2, 3, 4, and 7B in Human Breast Cell Lines and Normal and Disease States of Human Breast Tissue. Cancer Res. 54, 2615–2621.

Joyce, J.A., and Pollard, J.W. (2009). Microenvironmental regulation of metastasis. Nat. Rev. Cancer 9, 239–252.

Kalluri, R., and Weinberg, R.A. (2009). The basics of epithelial-mesenchymal transition. J. Clin. Invest. 119, 1420–1428.

Kamino, K., and Mohr, U. (1993). Intracranial metastases of induced lung carcinomas in rats. Int. J. Exp. Pathol. 74, 181–186.

Karrison, T.G., Ferguson, D.J., and Meier, P. (1999). Dormancy of Mammary Carcinoma After Mastectomy. J. Natl. Cancer Inst. 91, 80–85.

Kawai, T., and Akira, S. (2009). The roles of TLRs, RLRs and NLRs in pathogen recognition. Int. Immunol. 21, 317–337.

Kaye, A.H., Morstyn, G., Gardner, I., and Pyke, K. (1986). Development of a Xenograft Glioma Model in Mouse Brain. Cancer Res. 46, 1367–1373.

Kennedy, P.G., Lisak, R.P., and Raff, M.C. (1980). Cell type-specific markers for human glial and neuronal cells in culture. Lab. Investig. J. Tech. Methods Pathol. 43, 342–351.

Kirikoshi, H., and Katoh, M. (2002). Expression of WNT7A in human normal tissues and cancer, and regulation of WNT7A and WNT7B in human cancer. Int. J. Oncol. 21, 895–900.

Klemm, F., Bleckmann, A., Siam, L., Chuang, H.N., Rietkötter, E., Behme, D., Schulz, M., Schaffrinski, M., Schindler, S., Trümper, L., et al. (2011). β-catenin-independent WNT signaling in basal-like breast cancer and brain metastasis. Carcinogenesis 32, 434–442.

Kühl, M., Geis, K., Sheldahl, L.C., Pukrop, T., Moon, R.T., and Wedlich, D. (2001). Antagonistic regulation of convergent extension movements in Xenopus by Wnt/beta-catenin and Wnt/Ca2+ signaling. Mech. Dev. 106, 61–76.

Kurayoshi, M., Yamamoto, H., Izumi, S., and Kikuchi, A. (2007). Post-translational palmitoylation and glycosylation of Wnt-5a are necessary for its signalling. Biochem. J. 402, 515–523.

Laemmli, U.K. (1970). Cleavage of structural proteins during the assembly of the head of bacteriophage T4. Nature 227, 680–685.

Lancaster, M., Rouse, J., and Hunter, K.W. (2005). Modifiers of mammary tumor progression and metastasis on mouse chromosomes 7, 9, and 17. Mamm. Genome Off. J. Int. Mamm. Genome Soc. 16, 120–126.

Langley, R.R., Fan, D., Guo, L., Zhang, C., Lin, Q., Brantley, E.C., McCarty, J.H., and Fidler, I.J. (2009). Generation of an Immortalized Astrocyte Cell Line from H-2Kb-tsA58 Mice to Study the Role of Astrocytes in Brain Metastasis. Int. J. Oncol. 35, 665–672.

Liu, J., Pan, S., Hsieh, M.H., Ng, N., Sun, F., Wang, T., Kasibhatla, S., Schuller, A.G., Li, A.G., Cheng, D., et al. (2013a). Targeting Wnt-driven cancer through the inhibition of Porcupine by LGK974. Proc. Natl. Acad. Sci. 110, 20224–20229.

Liu, J., Pan, S., Hsieh, M.H., Ng, N., Sun, F., Wang, T., Kasibhatla, S., Schuller, A.G., Li, A.G., Cheng, D., et al. (2013b). Targeting Wnt-driven cancer through the inhibition

of Porcupine by LGK974. Proc. Natl. Acad. Sci. U. S. A. 110, 20224–20229.

Livak, K.J., and Schmittgen, T.D. (2001). Analysis of relative gene expression data using real-time quantitative PCR and the 2(-Delta Delta C(T)) Method. Methods San Diego Calif 25, 402–408.

Loane, D.J., and Byrnes, K.R. (2010). Role of Microglia in Neurotrauma. Neurother. J. Am. Soc. Exp. Neurother. 7, 366–377.

Lorger, M., and Felding-Habermann, B. (2010). Capturing Changes in the Brain Microenvironment during Initial Steps of Breast Cancer Brain Metastasis. Am. J. Pathol. 176, 2958–2971.

Lorger, M., Lee, H., Forsyth, J.S., and Felding-Habermann, B. (2011). Comparison of in vitro and in vivo approaches to studying brain colonization by breast cancer cells. J. Neurooncol. 104, 689–696.

Louie, E., Chen, X., Coomes, A., Ji, K., Tsirka, S., and Chen, E. (2013). Neurotrophin-3 modulates breast cancer cells and the microenvironment to promote the growth of breast cancer brain metastasis. Oncogene 32, 4064–4077.

Lowry, O.H., Rosebrough, N.J., Farr, A.L., and Randall, R.J. (1951). Protein measurement with the Folin phenol reagent. J. Biol. Chem. 193, 265–275.

Luo, J., Elwood, F., Britschgi, M., Villeda, S., Zhang, H., Ding, Z., Zhu, L., Alabsi, H., Getachew, R., Narasimhan, R., et al. (2013). Colony-stimulating factor 1 receptor (CSF1R) signaling in injured neurons facilitates protection and survival. J. Exp. Med. 210, 157–172.

Mani, S.A., Guo, W., Liao, M.-J., Eaton, E.N., Ayyanan, A., Zhou, A.Y., Brooks, M., Reinhard, F., Zhang, C.C., Shipitsin, M., et al. (2008). The epithelial-mesenchymal transition generates cells with properties of stem cells. Cell 133, 704–715.

Marchand, E.R., and Riley, J.N. (1979). Self-centering head holder system for small animal stereotaxy. Brain Res. Bull. 4, 141–143.

Marshall, O.J. (2004). PerlPrimer: cross-platform, graphical primer design for standard, bisulphite and real-time PCR. Bioinforma. Oxf. Engl. 20, 2471–2472.

Mikels, A.J., and Nusse, R. (2006). Wnts as ligands: processing, secretion and reception. Oncogene 25, 7461–7468.

Miller, F.R. (1983). Tumor subpopulation interactions in metastasis. Invasion Metastasis 3, 234–242.

MO, M.-L., LI, M.-R., CHEN, Z., LIU, X.-W., SHENG, Q., and ZHOU, H.-M. (2013). Inhibition of the Wnt palmitoyltransferase porcupine suppresses cell growth and downregulates the Wnt/β-catenin pathway in gastric cancer. Oncol. Lett. 5, 1719–1723.

Mogensen, T.H. (2009). Pathogen Recognition and Inflammatory Signaling in Innate Immune Defenses. Clin. Microbiol. Rev. 22, 240–273.

Morton, C.L., and Houghton, P.J. (2007). Establishment of human tumor xenografts in immunodeficient mice. Nat. Protoc. 2, 247–250.

Mosmann, T. (1983). Rapid colorimetric assay for cellular growth and survival: application to proliferation and cytotoxicity assays. J. Immunol. Methods 65, 55–63.

Murphy, J.B. (1913). TRANSPLANTABILITY OF TISSUES TO THE EMBRYO OF FOREIGN SPECIES : ITS BEARING ON QUESTIONS OF TISSUE SPECIFICITY AND TUMOR IMMUNITY. J. Exp. Med. 17, 482–493.

Nakamura, Y. (2002). Regulating factors for microglial activation. Biol. Pharm. Bull. 25, 945–953.

Nguyen, D.X., Bos, P.D., and Massagué, J. (2009). Metastasis: from dissemination to organ-specific colonization. Nat. Rev. Cancer 9, 274–284.

Nusse, R. (2005). Wnt signaling in disease and in development. Cell Res. 15, 28–32.

Paget, S. (1989). The distribution of secondary growths in cancer of the breast. 1889. Cancer Metastasis Rev. 8, 98–101.

Perou, C.M., Sørlie, T., Eisen, M.B., van de Rijn, M., Jeffrey, S.S., Rees, C.A., Pollack, J.R., Ross, D.T., Johnsen, H., Akslen, L.A., et al. (2000). Molecular portraits of human breast tumours. Nature 406, 747–752.

Proffitt, K.D., Madan, B., Ke, Z., Pendharkar, V., Ding, L., Lee, M.A., Hannoush, R.N., and Virshup, D.M. (2013). Pharmacological Inhibition of the Wnt Acyltransferase PORCN Prevents Growth of WNT-Driven Mammary Cancer. Cancer Res. 73, 502–507.

Pukrop, T., and Binder, C. (2008). The complex pathways of Wnt 5a in cancer progression. J. Mol. Med. Berl. Ger. 86, 259–266.

Pukrop, T., Klemm, F., Hagemann, T., Gradl, D., Schulz, M., Siemes, S., Trümper, L., and Binder, C. (2006). Wnt 5a signaling is critical for macrophage-induced invasion of breast cancer cell lines. Proc. Natl. Acad. Sci. U. S. A. 103, 5454–5459.

Pukrop, T., Dehghani, F., Chuang, H.-N., Lohaus, R., Bayanga, K., Heermann, S., Regen, T., Van Rossum, D., Klemm, F., Schulz, M., et al. (2010a). Microglia promote colonization of brain tissue by breast cancer cells in a Wnt-dependent way. Glia 58, 1477–1489.

Pukrop, T., Dehghani, F., Chuang, H.-N., Lohaus, R., Bayanga, K., Heermann, S., Regen, T., Rossum, D.V., Klemm, F., Schulz, M., et al. (2010b). Microglia promote colonization of brain tissue by breast cancer cells in a Wnt-dependent way. Glia 58, 1477–1489.

Qi, L., Sun, B., Liu, Z., Cheng, R., Li, Y., and Zhao, X. (2014). Wnt3a expression is associated with epithelial-mesenchymal transition and promotes colon cancer progression. J. Exp. Clin. Cancer Res. CR 33.

Quail, D., and Joyce, J. (2013). Microenvironmental regulation of tumor progression and metastasis. Nat. Med. 19, 1423–1437.

Ramakrishna, R., and Rostomily, R. (2013). Seed, soil, and beyond: The basic biology of brain metastasis. Surg. Neurol. Int. 4, S256–S264.

Regen, T., van Rossum, D., Scheffel, J., Kastriti, M.-E., Revelo, N.H., Prinz, M., Brück, W., and Hanisch, U.-K. (2011). CD14 and TRIF govern distinct responsiveness and responses in mouse microglial TLR4 challenges by structural variants of LPS. Brain. Behav. Immun. 25, 957–970.

Ribatti, D., Mangialardi, G., and Vacca, A. (2006). Stephen Paget and the "seed and soil" theory of metastatic dissemination. Clin. Exp. Med. 6, 145–149.

Saijo, K., and Glass, C.K. (2011). Microglial cell origin and phenotypes in health and disease. Nat. Rev. Immunol. 11, 775–787.

Schäfer, G., Narasimha, M., Vogelsang, E., and Leptin, M. (2014a). Cadherin switching during the formation and differentiation of the Drosophila mesoderm – implications for epithelial-to-mesenchymal transitions. J. Cell Sci. 127, 1511–1522.

Schäfer, G., Narasimha, M., Vogelsang, E., and Leptin, M. (2014b). Cadherin switching during the formation and differentiation of the Drosophila mesoderm – implications

for epithelial-to-mesenchymal transitions. J. Cell Sci. 127, 1511–1522.

Semënov, M.V., Zhang, X., and He, X. (2008). DKK1 Antagonizes Wnt Signaling without Promotion of LRP6 Internalization and Degradation. J. Biol. Chem. 283, 21427–21432.

Siegfried, E., Wilder, E.L., and Perrimon, N. (1994). Components of wingless signalling in Drosophila. Nature 367, 76–80.

Da Silva, B.B., Lopes-Costa, P.V., dos Santos, A.R., de Sousa-Júnior, E.C., Alencar, A.P., Pires, C.G., and Rosal, M.A. (2009). Comparison of three vascular endothelial markers in the evaluation of microvessel density in breast cancer. Eur. J. Gynaecol. Oncol. 30, 285–288.

Smid, M., Wang, Y., Zhang, Y., Sieuwerts, A.M., Yu, J., Klijn, J.G.M., Foekens, J.A., and Martens, J.W.M. (2008). Subtypes of Breast Cancer Show Preferential Site of Relapse. Cancer Res. 68, 3108–3114.

Steeg, P.S., Camphausen, K.A., and Smith, Q.R. (2011). Brain metastases as preventive and therapeutic targets. Nat. Rev. Cancer 11, 352–363.

Taghian, A., Budach, W., Zietman, A., Freeman, J., Gioioso, D., and Suit, H.D. (1993). Quantitative Comparison between the Transplantability of Human and Murine Tumors into the Brain of NCr/Sed-nu/nu Nude and Severe Combined Immunodeficient Mice. Cancer Res. 53, 5018–5021.

Thiery, J.P. (2002). Epithelial–mesenchymal transitions in tumour progression. Nat. Rev. Cancer 2, 442–454.

Towbin, H., Staehelin, T., and Gordon, J. (1979). Electrophoretic transfer of proteins from polyacrylamide gels to nitrocellulose sheets: procedure and some applications. Proc. Natl. Acad. Sci. U. S. A. 76, 4350–4354.

Valastyan, S., and Weinberg, R.A. (2011). Tumor metastasis: molecular insights and evolving paradigms. Cell 147, 275–292.

Van de Vijver, M.J., He, Y.D., van't Veer, L.J., Dai, H., Hart, A.A.M., Voskuil, D.W., Schreiber, G.J., Peterse, J.L., Roberts, C., Marton, M.J., et al. (2002). A gene-expression signature as a predictor of survival in breast cancer. N. Engl. J. Med. 347, 1999–2009.

Watanabe, O., Imamura, H., Shimizu, T., Kinoshita, J., Okabe, T., Hirano, A., Yoshimatsu, K., Konno, S., Aiba, M., and Ogawa, K. (2004). Expression of Twist and Wnt in Human Breast Cancer. Anticancer Res. 24, 3851–3856.

Weigelt, B., Peterse, J.L., and van't Veer, L.J. (2005). Breast cancer metastasis: markers and models. Nat. Rev. Cancer 5, 591–602.

Weil, R.J., Palmieri, D.C., Bronder, J.L., Stark, A.M., and Steeg, P.S. (2005). Breast cancer metastasis to the central nervous system. Am. J. Pathol. 167, 913–920.

Willipinski-Stapelfeldt, B., Riethdorf, S., Assmann, V., Woelfle, U., Rau, T., Sauter, G., Heukeshoven, J., and Pantel, K. (2005). Changes in Cytoskeletal Protein Composition Indicative of an Epithelial-Mesenchymal Transition in Human Micrometastatic and Primary Breast Carcinoma Cells. Clin. Cancer Res. 11, 8006–8014.

Wu, C., Orozco, C., Boyer, J., Leglise, M., Goodale, J., Batalov, S., Hodge, C.L., Haase, J., Janes, J., Huss, J.W., et al. (2009). BioGPS: an extensible and customizable portal for querying and organizing gene annotation resources. Genome Biol. 10, R130.

Wu, Y., Ginther, C., Kim, J., Mosher, N., Chung, S., Slamon, D., and Vadgama, J.V.

(2012). Expression of Wnt3 activates Wnt/β-catenin pathway and promotes EMT-like phenotype in trastuzumab resistant HER2-overexpressing breast cancer cells. Mol. Cancer Res. MCR 10, 1597–1606.

Yamanaka, H., Moriguchi, T., Masuyama, N., Kusakabe, M., Hanafusa, H., Takada, R., Takada, S., and Nishida, E. (2002). JNK functions in the non-canonical Wnt pathway to regulate convergent extension movements in vertebrates. EMBO Rep. 3, 69–75.

Yang, J., Mani, S.A., Donaher, J.L., Ramaswamy, S., Itzykson, R.A., Come, C., Savagner, P., Gitelman, I., Richardson, A., and Weinberg, R.A. (2004). Twist, a master regulator of morphogenesis, plays an essential role in tumor metastasis. Cell 117, 927–939.

Yook, J.I., Li, X.-Y., Ota, I., Fearon, E.R., and Weiss, S.J. (2005). Wnt-dependent regulation of the E-cadherin repressor snail. J. Biol. Chem. 280, 11740–11748.

Zhang, M., and Olsson, Y. (1997). Hematogenous metastases of the human brain--characteristics of peritumoral brain changes: a review. J. Neurooncol. 35, 81–89.